27648

NAME OF AUTHOR NOM DE L'AUTEUR __LESLIE GAMMIE__

TITLE OF THESIS TITRE DE LA THÈSE __THE   PHOTOLYSIS   OF   TETRIMETHYLDISILANE__

__AND THE   REACTIONS OF   TRIMETHYLSILYL__

__RADICALS__

UNIVERSITY UNIVERSITÉ __UNIVERSITY   OF   ALBERTA__

DEGREE FOR WHICH THESIS WAS PRESENTED
GRADE POUR LEQUEL CETTE THÈSE FUT PRÉSENTÉE __Ph D__

YEAR THIS DEGREE CONFERRED ANNÉE D'OBTENTION DE CE GRADE __1976__

NAME OF SUPERVISOR NOM DU DIRECTEUR DE THÈSE __Dr O P STRAUSZ__

DATED DATÉ __Dec 3rd 1975__ SIGNED SIGNÉ __Leslie Gammie__

PERMANENT ADDRESS RÉSIDENCE FIXE __9043 90 St__

__EDMONTON, ALBERTA__

THE UNIVERSITY OF ALBERTA

THE PHOTOLYSIS OF TETRAMETHYLSILANE

AND THE REACTIONS OF TRIMETHYLSILYL RADICALS

by

LESLIE GAMMIE Ⓒ

A THESIS

SUBMITTED TO THE FACULTY OF GRADUATE STUDIES AND RESEARCH

IN PARTIAL FULFILMENT OF THE REQUIREMENTS FOR THE DEGREE

OF DOCTOR OF PHILOSOPHY

DEPARTMENT OF CHEMISTRY

UNIVERSITY OF ALBERTA

EDMONTON, CANADA

SPRING, 1976

THE UNIVERSITY OF ALBERTA

FACULTY OF GRADUATE STUDIES AND RESEARCH

The undersigned certify that they have read, and recommend to the Faculty of Graduate Studies and Research, for acceptance, a thesis entitled

THE PHOTOLYSIS OF TETRAMETHYLSILANE
AND THE REACTIONS OF TRIMETHYLSILYL RADICALS

submitted by

LESLIE GAMMIE

in partial fulfilment of the requirements for the degree of Doctor of Philosophy.

....
O. P. Strausz - Supervisor

....
H. E. Gunning

....
G. R. Freeman

....
W. A. G. Graham

....
D. B. Robinson - Chemical Engineering

....
D. J. Le Roy - External Examiner

Date .. November. 24 ......1975.

ABSTRACT

The gas phase xenon resonance lamp photolysis of tetra-
methylsilane and the medium pressure mercury lamp photolysis of
bis(trimethylsilyl)mercury have been investigated in detail. The
resulting product distribution was accounted for in both studies and
mechanisms were proposed. The reactions of the trimethylsilyl radical
were examined and the findings used to help explain the mechanisms
in the photolysis studies.

The 147 nm photolysis of tetramethylsilane yielded ten
measurable products and a polymer deposit on the cell window. The
mechanism was deduced from the effect of pressure, exposure time,
nitric oxide scavenging and isotopic labelling. The photolysis was
shown to proceed by a minimum of six primary steps, with C-Si bond
cleavage being the predominant ($\sim$77%) mode of decomposition. The
quantum yield of fluorescence was found to be less than 10^{-5}.

The occurrence of the trimethylsilyl radical as one of the
major primary products and the lack of knowledge of its properties, led
to the photolysis of bis(trimethylsilyl)mercury at wavelengths greater
than 300 nm as a simpler source of the radical. The mechanism was
determined by pressure studies, time studies and radical scavenging
with nitric oxide, ethylene and oxygen, and found to be a clean source
of trimethylsilyl radicals.

From the data a disproportionation-combination rate constant
ratio of 0.046 for trimethylsilyl radicals was obtained. The existence
of disproportionation clearly demonstrates a preference for formation
of a silaethylene-type structure. The relative stabilities of singlet

and triplet silaethylene were found to be almost equivalent in an ab initio molecular orbital calculation.

The mercurial was also photolyzed in the presence of other added silanes to obtain relative rates of hydrogen abstraction by the trimethylsilyl radical. Arrhenius parameters for the abstraction reactions were calculated by the BEBO method and from the available evidence a value was estimated for the trimethylsilyl radical recombination rate constant.

It was also possible to demonstrate the existence of cross-disproportionation and combination reactions between trimethylsilyl radicals and other silyl radicals and to estimate corresponding k_d/k_c ratios.

ACKNOWLEDGMENTS

TABLE OF CONTENTS

TABLE OF CONTENTS (cont'd)

TABLE OF CONTENTS (cont'd)

LIST OF TABLES

LIST OF TABLES (cont'd)

LIST OF FIGURES (cont'd)

CHAPTER I

INTRODUCTION

The photochemistry of silicon compounds and the reactions of
silicon radicals are still relatively new fields and are of increasing
interest as shown by the recent reviews surveying the general chemistry
of silicon[1-6], silicon radical chemistry[7,8], and the chemistry of sily-
lenes[9]. Most of the earlier photochemical work on silanes was essen-
tially preparatory,[10] and it is only recently that the kinetic-mechanistic
aspects have been investigated. In addition, our knowledge of free
radical chemistry[11,12] is based almost wholly on alkyl and aryl radicals,
a condition that could be improved if we expanded the field by studying
the reactions of radicals containing elements other than carbon.

A   Silicon Chemistry

1.   Comparison of Some Silicon and Carbon Properties

Silicon is the second member of the Main Group IV elements
but there are important differences between it and carbon along with the
similarities that might be expected from having the same $ns^2 np^2$
electronic structure. Silicon is a larger atom than carbon and tends
to form weaker bonds to itself, to carbon and to hydrogen than does
carbon, but stronger bonds to more electronegative atoms such as the
halogens, oxygen and nitrogen, either because of bonding, with silicon's
3d orbitals or because of its low electronegativity.

According to the Pauling scale of electronegativity[13],
silicon (1.8) is significantly different from carbon (2.5) and

1

hydrogen (2.1), such that whereas in alkanes the C-H bond is slightly polar with the δ^- charge on carbon, in silicon hydrides the bond polarity is in the opposite sense with the δ^+ charge on silicon. Thus the susceptibility of silicon hydrides to nucleophilic attack is an example of the difference in reactivity of silicon and carbon.

Silicon does not form long chain molecules as carbon does, the largest known being 10 silicon atoms long[14], but does form large molecules with alternating silicon and oxygen atoms, the industrially important siloxanes.

Since the main mode of bonding for both carbon and silicon is sp^3 hybridization similar types of compounds exist, such as hydrides, alkyl hydrides, halides, and ethers, but silicon can increase its normal coordination number of four to five or six by using its vacant d-orbitals to form sp^3d or sp^3d^2 hybrids[15,16]. The vacant d-orbitals on silicon lie about 130 kcals/mole[17] above the highest occupied orbitals whereas in carbon this gap is 220 kcals/mole[17] so that the silicon orbitals are much more readily available[18]. Thus silicon can enter into a d_π - p_π interaction[19-24] with electron donor groups such as phenyl, vinyl, oxygen or halogen to form a partial π bond. The contentious issue of silicon p_π - p_π bonding will be discussed later.

2. Thermodynamic Properties

Thermodynamic properties are very useful in relating radical reactivities and energetics of radical reactions and help to contribute to the fundamental understanding of the processes involved. Unfortunately the literature is full of mutually inconsistent and conflicting values for the heats of formation and bond dissociation energies of

silicon compounds and few measurements or estimates of silicon entropies have been made.

Many bond energies[25,26] have been obtained from first-order non-chain thermolyses of compounds where the observed activation energy may be equated with the energy of the bond being broken[27], e.g. $D(Si-Si)$ from thermolysis of hexamethyldisilane[28].

$$(CH_3)_3SiSi(CH_3)_3 \underset{k_{reverse}}{\overset{k_{forward}}{\rightleftharpoons}} 2(CH_3)_3Si .$$

This assumes that the activation energy for the reverse process is zero and that the interpretation of the kinetic data is correctly assigned to the actual initial dissociation. Many pyrolyses are complicated by the fact that the observed activation energy may not be directly related to any single bond dissociation.

Other bond energies have been calculated from electron impact measurements by mass spectrometry[29] where the appearance potential of a fragment ion can be related to the ionization potential of the ion and the dissociation energy of the bond broken:

$$R_1 - R_2 \rightarrow R_1^+ + R_2 + e^-$$
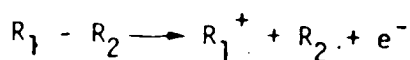
$$\text{Thus, } A(R_1^+) = D(R_1 - R_2) + I.P. (R_1).$$

Usually, $D(R_1 - R_2)$ is supplied from a kinetic measurement and the ionization potential of R_1 so obtained can then be applied to a series of compounds containing the group R_1 to find $D(R_1 - R_3)$. In addition heats of formation can be related to appearance potentials and further bond energy values can be calculated. A set of available bond energies is given in Table I-1.

TABLE I-1

Selected Bond Energies of Silicon Compounds (kcals/mole)

Compound	D(Bond)	Reference
H_3Si-H	94	30
H_5Si_2-H	90	31
CH_3SiH_2-H	≲94	32
$(CH_3)_3Si-H$	81	7
	85	33
	88	34
	90	35
CH_3-SiH_3	86	36
$CH_3-Si(CH_3)_3$	76	37
	85	29
$H_3Si-SiH_3$	81	30
$(CH_3)_3Si-Si(CH_3)_3$	67	38
	81	28
	86	29
$(CH_3)_3SiCH_2-H$	97	39

Heats of formation, usually obtained through heats of combustion from calorimetry[40], are subject to large errors with silicon compounds due to the involatility of silica, formation of surface films and a tendency to detonate, so that many earlier results are of doubtful reliability. Later techniques such as deriving heats of formation from heats of hydrolysis[41] may give more consistent results. The spread in results for some chosen silanes is demonstrated in Table I-2.

B. Radical Reactions

1. Alkyl Radical Reactions

Since the main body of information on radical properties has been gathered from alkyl radical reactions it would be helpful to summarize the known reactions and sources of these radicals before noting the differences applicable to silicon radical chemistry.

An alkyl free radical is an alkane molecule in which one of the carbon atoms has a free valence with one unpaired electron. A di-radical is a species with two free valence sites on different carbon atoms, and a carbene has two free sites on the same carbon atom.

Methyl radicals have been shown to be planar[47] and other evidence points to other alkyl radicals also being planar with sp^2 hydridization around the radical site.

Alkyl radicals are stable up to high temperatures but are also very reactive[12]. The fastest reactions that they undergo are combination and disproportionation. Combination is an exothermic process which involves pairing of the free electrons on two radicals to form a new bond, e.g.

$$CH_3 + CH_3 \longrightarrow CH_3\text{-}CH_3{}^*$$
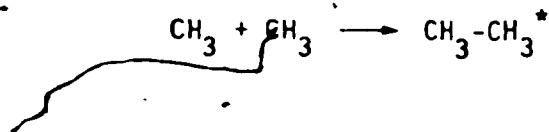
TABLE I-2

Selected Heats of Formation of Silicon Compounds

Compound	ΔH°_f (298°) kcals/mole	Reference
SiH_4	8.2	42
	8.7	43
Si_2H_6	17.1	40
	19.0	43
CH_3SiH_3	-4.0	44
	-11.8	43
	1.0	45
$(CH_3)_2SiH_2$	-7.8	45
	-15.2	44
	-29.8	43
$(CH_3)_3SiH$	-18.1	45
	-28	44
	-44.5	43
	-55	37
$(CH_3)_4Si$	-33	45
	-42.2	44
	-55.5	43
	-68	37
$(CH_3)_3SiSi(CH_3)_3$	-50	45
	-52	46
	-118	37
	-126	29

This appears to take place at a rate close to the collision frequency for methyl radicals but it is not clear whether larger alkyl radicals combine as fast or whether the rates are orders of magnitude slower. The process apparently does not involve an activation energy though one might expect, at least in the larger radicals, an activation energy approximately equivalent to the rotational barrier up to about 5 kcals/mole.

The "hot" molecule formed will decompose to radicals again if the released energy is not dissipated. Collision with other gas molecules is an effective method of stabilization and 10 torr total pressure is sufficient to obtain stabilization of $C_2H_6^*$ with unit probability in any collision. Current values for some alkyl radical recombination rate constants are shown in Table I-3.

The rate of disproportionation[59] is of the same order of magnitude as combination for most alkyl radicals. This reaction involves abstraction of a hydrogen atom from a carbon atom adjacent to the radical site.

$$CH_3CH_2 + CH_3CH_2 \longrightarrow CH_3CH_3 + CH_2=CH_2$$

This also involves no activation energy, so that there is a characteristic ratio of rate constants for combination and disproportionation for each alkyl radical which is nearly independent of temperature.

Note that disproportionation involves the cleavage of a C-H bond and the formation of two new bonds, one of which is a C-C π bond.

Abstraction by a radical from a molecule involves simultaneous formation of one bond and cleavage of another to form a new radical:

$$CH_3 + H-CR_3 \longrightarrow CH_3---H---CR_3 \longrightarrow CH_4 + CR_3.$$
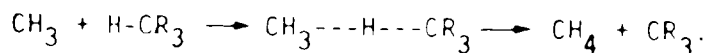
TABLE I-3

Selected Alkyl Radical Recombination Rate Constants

Radical	$\log k_r$ $(cc.mole^{-1}sec^{-1})$	Reference
CH_3	13.4	48,49
	13.5	50
C_2H_5	13.4	51
	11.6	52
	11.4	53
i-C_3H_7	13.8	54
	11.6	55
t-C_4H_9	12.5	56
	8.4	57
	8.6	58

, This process involves measurable activation energies usually between 5 and 20 kcals/mole[12].

Another process which requires an activation energy is the addition of a radical to a double bond to form a new radical:

$$CH_3 + CH_2=CH_2 \longrightarrow CH_3-CH_2-CH_2$$

Activation energies are of the order of 5 - 10 kcals/mole.

Radicals can also rearrange and decompose, but both of these processes normally require very high activation energies and are usually found only in high temperature pyrolysis studies[12].

Carbenes undergo two main types of reaction[60]; insertion into a single bond

$$CH_2 + CR_3CR_3 \longrightarrow R-CH_2-CR_2CR_3^*$$

and addition across a double bond

$$CH_2 + CR_2=CR_2 \longrightarrow CR_2 \overset{CH_2^*}{\underset{\triangle}{}} CR_2$$
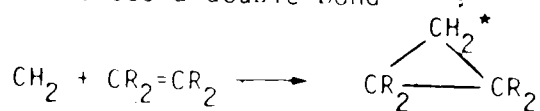
Both of these processes are highly exothermic and can lead to decomposition of the excited product, the amount of decomposition decreasing with the increase in the number of vibrational degrees of freedom of the molecule formed. Insertion into different C-H bonds seems to be relatively indiscriminate if the effect of abstraction[61] by the carbene is subtracted.

Carbene insertion into silanes seems to show a preference for Si-H bonds over C-H bonds[62] in the order tertiary · secondary · primary[63] and there is no dependence on excess carbene energy[64].

2. Silicon Radicals

Silicon radicals undergo types of reactions similar to those of alkyl radicals but to different extents and with different results.

Silyl radicals have been shown to be pyramidal[65,66] rather than planar and are stable up to high temperatures, but few values are available for their rates of reaction.

Formation of a :   n polymer is almost always associated with the presence of silyl radicals mainly due to reactions of reactive silicon diradicals, the analogues of alkenes.

Very little information is available on the combination/disproportionation reactions of silyl radicals and no hydrogen abstraction studies have been done in the gas phase. The efficient addition of silicon radicals to double bonds[67] has been widely studied and is one of the principal reactions employed in the synthesis of organosilicon compounds.

Silyl radicals are expected to react more slowly than alkyl radicals in abstraction from saturated compounds since the Si-H bond energies are lower than the corresponding C-H bond energies. The empirical Polanyi equation[68] shows a linear relationship between the enthalpy change for an abstraction reaction and the observed activation energy for a homologous series.

Silylenes, the analogues of carbenes, have been studied in some detail[9,69]. Arrhenius parameters or relative rates have been obtained for insertion reactions of silylene and methylsilylenes into various silanes[70,71]. The silylenes were obtained by pyrolysis of a suitable silane and were found to insert into Si-H bonds but not into Si-C, C-C, or C-H bonds. It is possible that they may insert into Si-Si bonds. Information on abstraction by silylenes is sparse and in

the absence of other reagents silylenes polymerize.

3. Sources of Radicals

Radicals are produced in the thermolysis of almost any compound, but this type of system poses difficulties for the study of radical reactions since the high temperatures required for thermolysis also lead to decomposition of the radicals themselves[72], and in addition there are experimental difficulties associated with conditioning of the reactor walls[73].

Photolysis[74] has the advantage of exciting the molecule with a known energy. If this leads to homolysis of a bond or bonds, the resulting fragments will be at room temperature or within 200°C of it and any further decomposition will be a function of the excess energy they contain. In addition, any products formed will be stable and will not undergo photolytic decomposition if conversion is kept below a few percent.

Mercury photosensitization is another source of radicals which has the advantage that the bond cleavage is selective and less energy is introduced into the system than is usual in direct photolysis.

4. Reactions of Alkyl Radicals with Silanes

A large body of information has accumulated on the hydrogen abstraction reactions by alkyl radicals from a variety of silanes, and it has been shown that A-factors are similar to those for abstraction from alkanes but that activation energies are lower because of the greater reactivity of silanes. The decrease in activation energies agrees with the observation that Si-H bond energies are lower

than C-H bond energies but the trend in the experimental activation energies for abstraction from different Si-H bonds does not agree with the observed trend in Si-H bond energies (Table I-1).

Table I-4 shows the Arrhenius parameters for a representative set of abstractions by alkyl radicals from silanes.

C. Photochemistry

1. Vacuum Ultraviolet Spectroscopy

Monosilanes absorb in the vacuum ultraviolet and their spectra[77,78] are similar to those of the alkanes[79] both in structure and extinction coefficient except that the silanes are red-shifted some 10 to 20 nm compared to the corresponding alkane.

The spectra all show a continuum and have some fine structure around 140 nm. Tetramethylsilane has a window around 150 nm that is absent in the other partially methylated silanes, indicating that the Si-H bond is probably the main absorber in this region.

Interpretation of the spectra is best attempted by comparison with the methods that have been used to understand the photochemical decomposition of alkanes in the vacuum ultraviolet.

It has been suggested that there are two types of σ,σ^* transitions in the alkanes[80]. The longer wavelength region corresponds to a $(C-C)\sigma$ electron promotion to an upper state while the shorter wavelength region corresponds to promotion of a $(C-H)\sigma$ electron. Other interpretations[81] show that there may be quite a number of allowable transitions from the valence molecular orbitals of the system to Rydberg-type 3p orbitals.

Photolysis of the carbon analogue of tetramethylsilane,

TABLE I-4

Arrhenius Parameters for Hydrogen Abstraction by

Alkyl Radicals from Silanes

Radical	Reactant	log A $cc.mole^{-1}sec^{-1}$	E_a $kcal\ mole^{-1}$	Reference
CH_3	SiH_4	12.26	7.47	75
	CH_3SiH_3	12.28	8.13	76
	$(CH_3)_2SiH_2$	12.07	8.30	76
	$(CH_3)_3SiH$	11.69	8.31	76
	$(CH_3)_4Si$	11.34	9.66	76
	Si_2H_6	11.96	5.65	31
C_2H_5	SiH_4	11.73	7.25	75
	Si_2H_6	11.75	5.65	75
$n-C_3H_7$	SiH_4	11.52	6.91	75
$i-C_3H_7$	SiH_4	11.84	8.63	75

neo-pentane[82], has been undertaken by Ausloos _et al_. and their results serve as a convenient model to illustrate the similarities and differences between silicon and carbon compounds.

The main fragmentation processes were:

$$neo\text{-}C_5H_{12} + h\upsilon \xrightarrow{1} CH_4 + iso\text{-}C_4H_8$$

$$\xrightarrow{2} CH_3 + H + iso\text{-}C_4H_8.$$

$$\xrightarrow{3} 2CH_3 + C_3H_6.$$
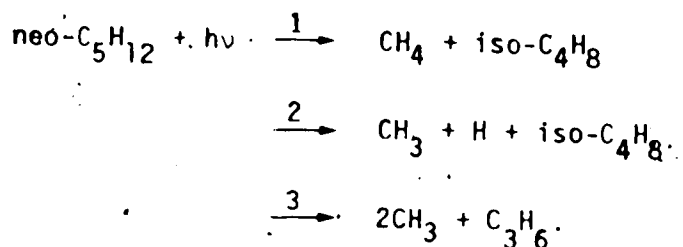
The main conclusions were:

i) Isobutene was the major primary product, being formed in two of the primary steps, and this together with the production of propylene in step 3 meant that alkenes were the major result of photolysis.

ii) Approximately 75% of the methane was formed in a molecular elimination step.

iii) Elimination of a hydrogen molecule, a process which is of major importance in the simpler alkanes, is of little importance in the photolysis of neo-pentane.

iv) Approximately 80% of the bond cleavage is in the C-C bonds.

The absorption spectrum of neo-pentane shows a continuum below 172 nm, and Raymonda and Simpson argue that the region from 172 to 123 nm is due to C-C electron transitions and that the C-H transitions occur near the methane band centre, from 124 to 120 nm.

Under these circumstances photolysis at 147 nm (195 kcals/mole)

should give exclusively C-C cleavage. Although the experimental results show that C-C cleavage predominates, the existence of other decomposition paths shows that absorption in one moiety can lead to rupture of other bonds. Thus the excited state would appear to have strongly delocalized orbitals.

One would then expect tetramethylsilane to photolyze in a similar fashion mainly via Si-C cleavage although the non-existence of stable silicon-carbon double bonds could change the type of primary decomposition. Prediction of such features as molecular elimination is also complicated by the present lack of understanding of the theoretical aspects of absorption spectra.

2. Actinometric Photochemistry

Both carbon dioxide and to a lesser extent nitrous oxide have been used as chemical actinometers for 147 nm radiation since it is generally believed that for CO_2 photolysis at 147 nm, $\phi CO = 1.0$ and for N_2O photolysis at 147 nm, $\phi N_2 = 1.44$.

Carbon dioxide has been studied in some detail because of its general use as an actinometer and its role in planetary atmospheres[83].

Early work[84] established that the initial step was dissociation of the excited molecule to form carbon monoxide and an oxygen atom. Below 165 nm the oxygen atom is formed in the ^1D state and below 128 nm it is formed in the ^1S state as well. The fate of these excited atoms is thought to be very rapid relaxation to the ^3P state by interaction with CO_2 molecules.

The oxygen atoms can then combine and provide a source of molecular oxygen which can account for the formation of ozone. However,

the predicted O_2/CO ratio of 0.5 is not attained in many cases. The quantum yield of O_2 is often variable and this is attributed to adsorption and heterogeneous reactions of oxygen atoms on the walls of the reaction vessel. Recent work by Cvetanovic[85] has shown that the photolysis of water acts as a catalyst for the decomposition of ozone.

Not all the results yield $\phi_{CO} = 1.0$ but it is difficult to explain lower values since there seems to be no fluorescence following photon absorption[86] and the dissociation yield seems to be invariant with pressure[87].

Slanger et al.[88] found that the dissociation quantum yield varies with wavelength from 121 nm to 149 nm with the highest yield at 123.6 nm and they expressed their yields relative to Inn's value[89] of 0.75 at 147 nm. The estimated error limits for both values, 1.00 and 0.75, are almost large enough to include the other value. The question of whether there are stable excited states of CO_2 is unresolved at this point but since most researchers have adopted $\phi_{CO} = 1.0$, this value has been used in our calculations.

Nitrous oxide photolysis has also been used as a vacuum ultraviolet actinometer; $\phi_{N_2} = 1.44$[90-92].

The major step in dissociation at 147 nm appears to be

$$N_2O + h\nu \longrightarrow N_2(^1\Sigma^+) + O(^1D)$$
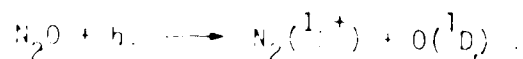
but the simultaneous occurrence of other steps is also possible. The yield of N_2 above unity presumably results from the reaction

$$O(^1D) + N_2O \longrightarrow O_2 + N_2.$$

The mechanisms involved are quite complex and the yields of other products

may vary depending on conditions.

3. Photolysis of Silanes

Direct gas phase photolysis studies have been carried out in this laboratory on monomethylsilane[93], dimethylsilane[94] and disilane[95] while Ring et al. have studied monosilane[96].

Comparison of the salient features of the decomposition of the above silanes with the decomposition of their carbon analogues has revealed important facets of th photochemistry of silanes.

Vacuum ultraviolet photolysis of monomethylsilane with a xenon resonance lamp (147 nm) gave products which could be explained by invoking six primary steps (Table I-5) with the loss of hydrogen accounting for 67 of the total primary quantum yield. The primary steps, their quantum yields and the mechanisms of the processes were established from the nature of the products, their dependence on conversion, pressure, addition of radical scavengers such as nitric oxide and ethylene, and the use of deuterium labelling.

The effect of wavelength was also examined by photolyzing with a krypton resonance lamp (123.6 nm). The increased photonic energy (231 kcals/mole) gave the same types of primary steps but there was increased polyfragmentation.

Hydrogen and methane were both formed by molecular elimination and by abstraction reactions. The silylenes formed inserted quantitatively into the Si-H bonds of the substrate, while the 1,2-diradical formed in step 3 contributes to polymer formation and the silylmethylene diradical formed in step 4 undergoes unimolecular isomerization to give a 1,2-diradical which also is lost as polymer.

TABLE I-5

Primary Steps in the 147 nm Photolysis
of Monomethylsilane

			ϕ
$CH_3SiH_3 + h\nu$	$\xrightarrow{1}$	$CH_3SiH + H_2$	0.32
	$\xrightarrow{2}$	$CH_3SiH + 2H$	0.05
	$\xrightarrow{3}$	$CH_2SiH_2 + H_2$	0.23
	$\xrightarrow{4}$	$CHSiH_3 + H_2$	0.07
	$\xrightarrow{5}$	$CH_4 + SiH_2$	0.09
	$\xrightarrow{6}$	$CH_3 + H + SiH_2$	0.26
			1.02

Photolysis of the ca[...]e[97-99], shows almost exclusive hydrogen loss with molecular elimination predominating. The molecular elimination along with simultaneous loss of two hydrogen atoms accounts for over 90% of the decomposition.

Elimination of methane and C-C bond cleavage are very minor processes.

Monomethylsilane photolysis is thus noticeably different as it shows appreciable amounts of Si-C bond cleavage with formation of methane and methyl radicals accounting for some 35% of the primary yield, although most of the remainder is molecular hydrogen elimination (62%).

Photolysis of dimethylsilane-d_2 with a Xe resonance lamp was also carried out and the primary steps (Table I-6) derived in the same manner as before. The decomposition involves twelve primary steps leading to many different silicon fragments. Methane and hydrogen were formed by both molecular elimination and radical formation and Si-C cleavage accounts for 28% of the bonds broken.

The silylenes formed inserted quantitatively into Si-H bonds and approximately half of the silicon fragments terminated in the polymer. Because of this loss of silicon residues it was impossible to unambiguously define certain reaction paths and maintain a strict material balance.

Photolysis of propane[100-102], the carbon analogue, is somewhat simpler in that only five primary steps are involved and there is less polyfragmentation than in the dimethylsilane case, where simultaneous loss of two methyl groups, two hydrogen molecules, or a

TABLE I-6

Primary Steps in the 147 nm Photolysis
of Dimethylsilane-d_2

			ϕ
$(CH_3)_2SiD_2 + h$	1	$CH_3SiD + CH_3D$	0.15
	2	$CH_3SiD + CH_3 + D$	0.20
	3	$SiD_2 + 2CH_3$	0.08
	4	$CH_2SiD_2 + CH_4$	0.05
	5	$CH_3SiD_2H + CH_2$	0.04
	6	$(CH_3)_2Si + D_2$	0.07
	7	$CHSiD_2 + CH_3 + H_2$	0.04
	8	$CHCH_3Si + D_2 + H_2$	0.07
	9	$CH_2CH_3Si + HD + D$	0.09
	10	$CHCH_3SiD + HD + H$	0.05
	11	$CH_2CH_3SiD_2 + H$	0.05
	12	$CH_2CH_3SiD + HD$	0.12
			1.01

hydrogen molecule and a hydrogen atom are postulated. This perhaps indicates that the carbon fragments are more readily stabilized than their silicon counterparts.

Disilane photolysis was carried out with a low pressure mercury lamp since its absorption spectrum extends to 210 nm. The photolysis was again studied as a function of time, pressure, deuterium labelling, and the addition of radical scavengers, from which five primary steps were postulated (Table I-7), the two major ones being the molecular elimination of monosilane and hydrogen.

Since silicon-silicon bond rupture and a single hydrogen loss together accounted for less than 10 of the primary yield there must be efficient energy randomization because absorption at 210 nm is associated with the silicon-silicon bond. Molecular hydrogen elimination gave a 1,2-diradical which contributed to polymer formation while the silylene formed inserted into the substrate.

Again we see that photolysis of disilane gives quite different results than both monosilylsilane and ethane in that molecular elimination of monosilane accounts for some 41 of the primary yield, and most of the remainder is molecular hydrogen formation. Thus it seems that increasing silicon substitution gives increasing amounts of silylene and correspondingly smaller amounts of hydrogen. However, it is not clear at this point whether this is due to the much

TABLE I-7

Primary Steps in the Photolysis of Disilane

Using a Low Pressure Mercury Arc

		Relative Yield
$Si_2H_6 + h\nu$ $\xrightarrow{1}$	$H + Si_2H_5$	3%
$\xrightarrow{2}$	$SiH_3 + SiH_3$	6
$\xrightarrow{3}$	$H_2 + SiH_3SiH$	3%
$\xrightarrow{4}$	$H_2 + SiH_2SiH_2$	47
$\xrightarrow{5}$	$SiH_4 + SiH_2$	41%

decomposition:

$$SiH_4 \xrightarrow{h\nu} SiH_2 + H_2$$
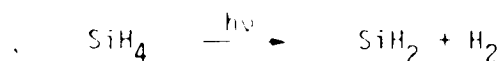
This was inferred partly from the fact that photolysis of mixtures of SiH_4/SiD_4 produced no SiH_3SiD_3. Since it has been shown, however, that monosilyl radicals disproportionate rather than combine[103] this conclusion must be considered tentative.

A point that has to be taken into account in the photolysis of silicon compounds is that the photolysis of the polymer formed can also give products. Siegel and Stewart[104] showed that the vacuum ultraviolet photolysis of polydimethylsilane gave gaseous hydrogen, methane and ethane as products with a total quantum yield of 0.06.

4. Hg Photosensitization of Silanes

It has been shown that when alkylsilanes containing at least one Si-H bond are subjected to Hg photosensitization there is selective bond cleavage giving H atoms and silyl radicals[105]. The main products are then H_2 and the silyl radical dimer. A minor step is the formation of molecular hydrogen and a silylene. Thus Hg photosensitization of alkylsilanes is a good source of substituted silyl radicals.

The Hg photosensitization of monosilane[106] is more complex in that five primary steps have to be postulated and the reaction appears to be very inefficient. Disilane[107] however behaves more like the methylsilanes in that there is one primary step producing H atoms and disilyl radicals. The subsequent reactions are more complex and include disproportionation/combination and displacement reactions. If the disilyl radicals combine they give chemically activated tetrasilane

which can decompose or be pressure stabilized. The decomposition proceeds exclusively by 1,2-diradical elimination which leads to polymer formation.

5. Photolysis of Bis(trimethylsilyl)mercury

There are few clean sources of silyl radicals but one that has been investigated in solution chemistry is the photolysis and thermolysis of disilyl mercury compounds.

These compounds are prepared relatively simply by shaking the halogen derivative of the desired silyl radicals with Na amalgam in cyclohexane solution[107]. The partially methylated silyl mercury compounds could not be isolated because of their instability but bis(trimethylsilyl)mercury more stable than the corresponding carbon compound and will sublime undecomposed at 60°C. The mercurial is a yellow solid at room temperature and melts with decomposition at 102°C where its vapour pressure is 1 torr. Eaborn and co-workers have shown that photolysis of bis(trimethylsilyl)mercury appears to produce trimethylsilyl radicals which can be trapped by olefins or will add to benzene or toluene to give the normal products of homolytic aromatic substitution[108,109].

Photolysis was found to be a better source than thermolysis[110-113] since the latter was found to involve mainly bimolecular reactions with solvent with unimolecular homolysis being unimportant.

No values of the Si-H bond energy in these mercury compounds have been measured but estimates have been made of 47.8 kcals/mole[111] and 13.6 kcals/mole[113]. In any case it is appreciably less than the C-H or Si-C bond energies. Absorption spectra have been recorded and maxima noted at 243 nm, 330 nm and 360 nm[116] so that photolysis is

easily accomplished by use of a medium pressure mercury lamp and appropriate filters can vary the input energy.

D. Tetramethylsilane Decomposition

   1. Radiolysis

Decomposition of tetramethylsilane has been accomplished by radiolysis with 50-pkeV X-rays[114]. In this case the major products were hydrogen, methane, ethane and ethyltrimethylsilane. Reaction mechanisms were deduced from deuterium labelling experiments, and addition of nitric oxide and ethylene as radical scavengers. The hydrogen and methane were produced by molecular eliminations, atomic reactions and to a lesser extent by "hot" intermediates. The ethane was formed almost exclusively by methyl radical combination. The principal carbosilane products all seemed to arise from reactions of CH_3, $(CH_3)_3Si$ and $(CH_3)_3SiCH_2$ radicals.

The authors estimate that 12 of the H_2 and 40 of the methane are formed by molecular elimination and in addition that 25% of the methane is formed from unscavengeable "hot" methyl radical abstraction reactions.

Although to a large extent the reactions in this type of radiation system can be explained by free radical mechanisms the possibility of other reactive species such as ions, excited and superexcited molecules, and atoms, cannot be ignored[115]. Usually molecules close to the particle tracks will be ionized while others further away will just be raised to an excited state.

It seemed necessary to carry out the decomposition with a define energy input.

2. Pyrolysis

The pyrolysis of tetramethylsilane has been investigated recently in a flow system[116] at 810-980°K and the decomposition was found to be first order in a seasoned reaction vessel.

The major products were methane, ethane, trimethylsilane, 1,1,3,3-tetramethyl-1,3-disilacyclobutane, hexamethyldisilane, and 2,2,4,4-tetramethyl-2,4-disilapentane.

The decomposition could be represented by the expression:

$$\log k = (14.30 \pm 0.23) - (67600 \pm 800)/(2.303RT)$$

The activation energy (67.6 kcals/mole) is smaller than the reported $D((CH_3)_3Si-CH_3)$ of 76 kcals/mole so the presence of a chain mechanism could not be ruled out.

A π-stabilized diradical, $(CH_3)_2SiCH_2$, was postulated as an intermediate because of the composition of the polymer formed, the existence of the disilacyclobutane dimerization product and the possibility of radical decomposition lowering the experimental activation energy:

$$(CH_3)_3SiCH_2 \longrightarrow (CH_3)_2Si=CH_2 + CH_3$$

Disproportionation of trimethylsilyl radicals and cross-disproportionation of trimethylsilyl and methyl radicals were also postulated as sources of the intermediate.

Decomposition of some of the radical intermediates and the doubtful stability of some of the products make definition of a mechanism very difficult.

E. Silicon-Carbon Double Bonds

No stable compound has been isolated which contains a $Si=C$ or $Si=Si$ double bond but a lot of evidence[117,118] points to the probability that the Si-C diradical has a certain degree of stability which might be termed a quasi double bond.

It is not clear why a stable double bond to silicon does not exist. It has been suggested that p_π - p_π overlap is poorer for higher row elements[119] but quantum mechanical calculations do not support this postulate..

Most of the recent work has been concentrated on determining the character of a reaction intermediate of the type $R_2Si=CH_2$ which could also be written as

$$R_2\dot{S}i-\dot{C}H_2 \quad \text{or} \quad \overset{+}{R_2Si}-\overset{-}{C}H_2$$
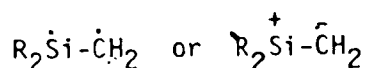
Experimental data from the thermolysis of silacyclobutanes have shown that some intermediate, which will add to olefins and is trapped by alcohols, ketones and aldehydes, exists.

Gusel'nikov and co-workers[120] postulated dimerization of the intermediate:
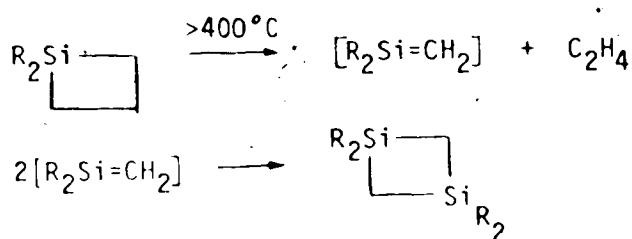
while at lower pressures the intermediate seems to polymerize to give $(-R_2SiCH_2-)_n$.

The rate constant for decomposition of the silacyclobutane compared very closely with the value for the decomposition of the carbon

analogue and the similarity of the Arrhenius parameters suggests, that the same mechanism is occurring, i.e. breaking of one bond to form a biradical as the rate-determining step followed by spontaneous decomposition to the intermediate and ethylene[121].

Sommer and co-workers[122-126] have used alcohols, ketones, aldehydes and olefins to trap the intermediate. Alcohols add across the "double bond"

$$[Me_2Si=CH_2] + MeOH \longrightarrow Me_2Si \begin{array}{c} OMe \\ \\ Me \end{array}$$
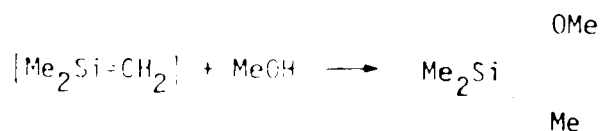
With aldehydes and ketones the intermediate is probably best described as $(Me_2\overset{\delta+}{Si}=\overset{\delta-}{CH_2})$ which behaves as an electrophile

$$R_2Si=CH_2 \longrightarrow \begin{array}{c} R_2Si \\ \parallel \\ O \end{array} + \begin{array}{c} CH_2 \\ \mid \\ C \end{array} \longrightarrow (R_2SiO)_3, (R_2SiO)_4$$
$$+ \qquad\qquad R_1 \quad R_2 \qquad\qquad + polymer$$
$$O=CR_1R_2$$
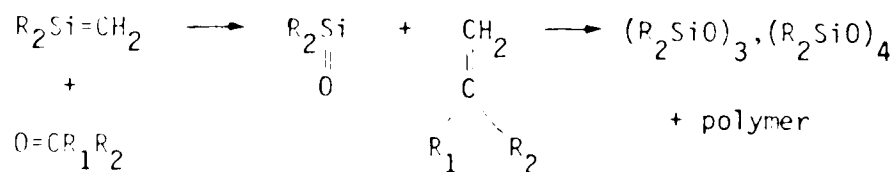
Poark and Peddle[127] have also postulated $[Me_2Si=SiMe_2]$ as a stabilized intermediate which could be captured by anthracene and naphthalene.

A few theoretical calculations have been carried out on this problem with differing results.

Curtis[128] has studied silaethylene $(H_2Si=CH_2)$ and disilaethylene $(H_2Si=SiH_2)$ using EHMO and CNDO calculations and has postulated that energy mismatching of carbon and silicon p-orbitals was responsible for a weak π-bond in silaethylene (<10 kcals/mole) but obtained a strong π-bond for disilaethylene and predicted it should be quite stable. He found the diradical H_2Si-CH_2 to be only ~35 kcals/mole less stable than

the olefin analogue.

Silaethylene was also studied by Damrauer and Williams[129] using CNDO calculations and they obtained a strong π-bond, suggesting that there was theoretical justification for the existence of a stable silicon-carbon double bonded species.

Both sets of calculations found that the C=Si bond was very polar ($\overset{+}{Si}-\overset{-}{C}$) which could make it very reactive and perhaps explain its apparent reactivity.

Walsh[130] used kinetic and thermodynamic data to set limits on the π-bond energy in methylenedimethylsilane (($CH_3)_2Si=CH_2$) of 30-42 kcals/mole thus making it about half as strong as the olefin π-bond.

Dewar and co-workers[43] used MINDO calculations to calculate heats of formation, molecular geometries and ionization potentials for numerous silanes. Then, on the assumption that the ability of an unsaturated compound to undergo addition at a double bond would depend on the strength of that bond, they used the calculated heats of formation to obtain heats of hydrogenation from which π-bond strengths could be estimated. They estimated the π bond energies in C=Si to be 42 kcal/mole and in Si=Si to be 23 kcal/mole.

Most of the results would seem to lead to the conclusion that the "double-bonded" species have a certain degree of stability but that the bonds are very polar and in consequence very reactive.

F. Present Investigation

Photolyses of monomethylsilane, dimethylsilane and disilane have been undertaken previously in this laboratory. Photolysis of tetramethylsilane was therefore undertaken to extend the range of the

research and examine any mechanistic differences caused by the lack
of Si-H bonds. It was hoped that this would help establish any trends
in reactivity in the alkylsilane series and that these could then be
compared and contrasted with the results from the photolysis of simple
alkanes.

During this study it was found that the trimethylsilyl radical
was a major primary product and so the photolysis of bis(trimethylsilyl)-
mercury was undertaken in a search for a simple gas-phase source of this
radical. It then appeared desirable to examine the reactivity of this
radical with other silanes to see if absolute rate constants for abstrac-
tion could be derived so that Arrhenius parameters could be obtained
and compared with the values for alkyl radicals.

CHAPTER II

EXPERIMENTAL

1. Vacuum Systems

Two vacuum systems were utilized, one for photolysis and distillation, and the other, a mercury-free system, for manufacturing the xenon resonance lamps.

i) The photolysis system was a conventional vacuum assembly[131] (Figure II-1) equipped with Delmar mercury float valves, Hoke TY440 or Hoke 425106Y-316-SS valves, or stopcocks lubricated with high-vacuum grease. The system was pumped by a two-stage mercury diffusion pump, backed by a Welch Duo-Seal oil rotary pump. This was capable of achieving pressures of 10^{-6} torr of foreign gas although the vapour pressure of mercury in the system was approximately 10^{-3} torr. Pressures were measured with a mercury manometer or a McLeod gauge.

A distillation line consisting of u-traps, a spiral trap, a solid nitrogen trap, and a Toepler pump, was used for purification of reactants and separation of products.

Gas transfers and distillations were monitored on a Pirani Vacuum Gauge (Consolidated Vacuum Corporation type GP-140) using Pirani tubes (type GP-001) as the sensing heads.

Samples could be introduced to a gas chromatograph via the Toepler pump and gas burette assembly.

A low-pressure line was used to operate the mercury float valves, the manometer and the Toepler pump.

ii) The second vacuum system was mercury free and pumped by a
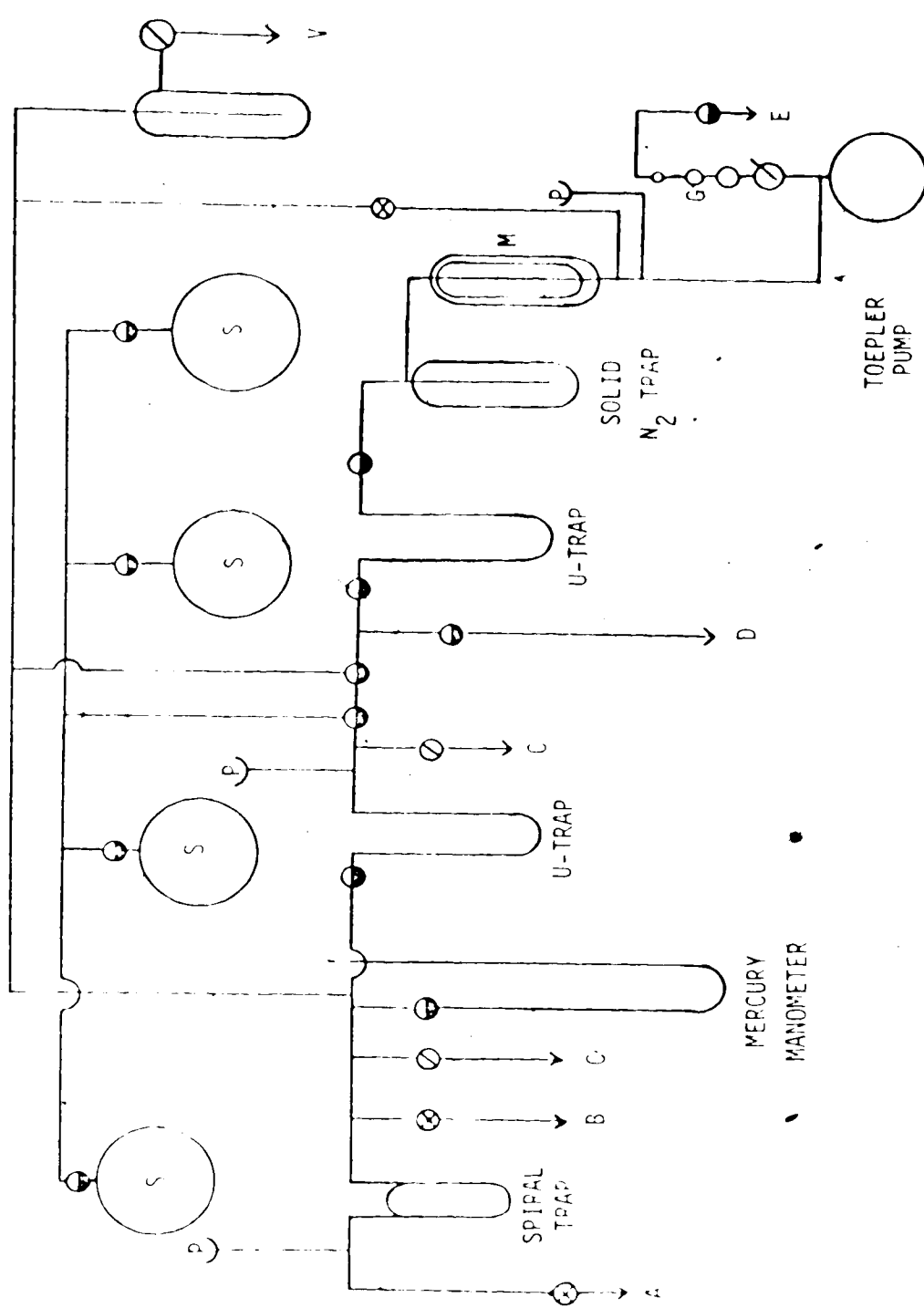
FIGURE II-1. HIGH VACUUM SYSTEM. A, to photolysis cell. B, ampoule with silicone seal. C, to atmosphere. D, to McLeod gauge. E, to thermal conductivity analytical system. P, Pirani type. M, one-stage mercury diffusion pump. S, storage bulbs. G, gas burette. V, to vacuum line. ⊗ - Hoke valve. ⊘ - glass stopcock. ● - mercury float valve.

three-stage oil diffusion pump (Octoil S oil), backed by a Welch Duo-Seal oil rotary pump.

Greased stopcocks (Apiezon N grease) and Hoke 425106Y-916-SS valves were used.

A Pirani vacuum gauge and tubes along with an oil manometer (silicon oil DC 200) were used to monitor pressure.

The lamp filler gases (xenon and neon) were stored in pyrex bulbs fitted with Hoke valves.

2. Ultraviolet Techniques

a) Light sources - xenon, mercury lamps

i) The lamp used for the vacuum ultraviolet photolyses was a xenon resonance lamp. These lamps have been shown[132,133] to be the best sources of light in this wavelength region because of their high intensity ($10^{15} - 10^{16}$ quanta/sec) and their monochromatic purity (Table II-1), which makes it possible to define how much energy is being absorbed, to select quenchers or scavengers which will not photolyze and to eliminate ionization interference if desired. Their relative ease of manufacture and operation also commends their use.

The main emission line of the xenon lamp is at 147 nm, with the line at 129.5 nm contributing about 2%. The lamps can be used at room temperature if a getter material (Ba-Al-Ni alloy) is used, or, in the absence of a getter, liquid oxygen can be used as a refrigerant to remove the impurities which would destroy the spectral purity of the lamp.

ii) Other sources of radiation were a low-pressure mercury lamp (Hanovia 687A45) and a medium-pressure mercury arc (Hanovia 42569 type

TABLE II-1

Emission Lines of Rare Gas Resonance Lamps[a]

Gas	Lines (nm)	Relative Abundance
Xenon	147.0	100
	129.5	2
Krypton	123.6	100
	116.5	28
Argon	106.7	
	104.8	
Neon	74.4	
	73.6	
Helium	58.4	

[a] J. G. Calvert and J. N. Pitts,"Photochemistry",
John Wiley and Sons, Inc., New York, 1967.

SH) (Table II-2).

The low-pressure lamp was used as a source of 254 nm radiation and the medium-pressure lamp was used at various wavelengths from 200 to 400 nm by including appropriate wavelength filters.

b) Xenon lamp manufacture

i) The xenon lamps were cylindrical Pyrex tubes, 22 mm in diameter and 170-200 mm in length, fitted with a single lithium fluoride window, 20 mm × 2 mm, attached to a flat ground surface with black wax (Apiezon W).

A subsidiary volume was attached to the main body of the lamp and in this one to four barium (Ba-Al-Ni alloy) getters (Kemet Division, Union Carbide) were placed imbedded in 14 mm Pyrex tubing (Figure II-2).

The lamp was connected to the mercury-free vacuum system and evacuated for several days during which time it was frequently baked with a hand torch. The lamp was tested by filling with 5 - 10 torr of Neon and then discharging with a 2450-Mc/sec Hg 198 Microwave Exciter (Baird Atomic Inc.) operated at 40 - 50 power through a V-shaped antenna which was placed parallel to and from 1 to 10 mm away from the lamp surface. In this way adsorbed impurities (oxygen and water) on the lamp surface could be monitored. If significant amounts of impurity were present the neon either would not discharge at all or would discharge only for a few minutes, the initial scarlet colour becoming pink and then quickly extinguished. If this occurred the lamp had to be re-evacuated and baked again until it could hold a discharge of bright scarlet without flickering for more than one hour. The Barium getters were used to form a barium mirror on the walls of the lamp to

TABLE II-2

Emission Lines of Mercury Lamps

Lamp	Wavelength (nm)	Relative Intensity
Low-pressure mercury[a]	184.9	20
	253.7	100
Medium-pressure mercury[b]	222	14
	232-248	38
	254	16
	265	15
	270-289	22
	297	16
	302-303	24
	313	50
	365-366	100
	404-408	42
	436	77
	546	93
	577-579	76

a B. T. Barnes, J. Applied Phys., 31, 852 (1960).

b J. G. Calvert and J. N. Pitts, "Photochemistry", John Wiley and Sons, Inc., New York, 1967.
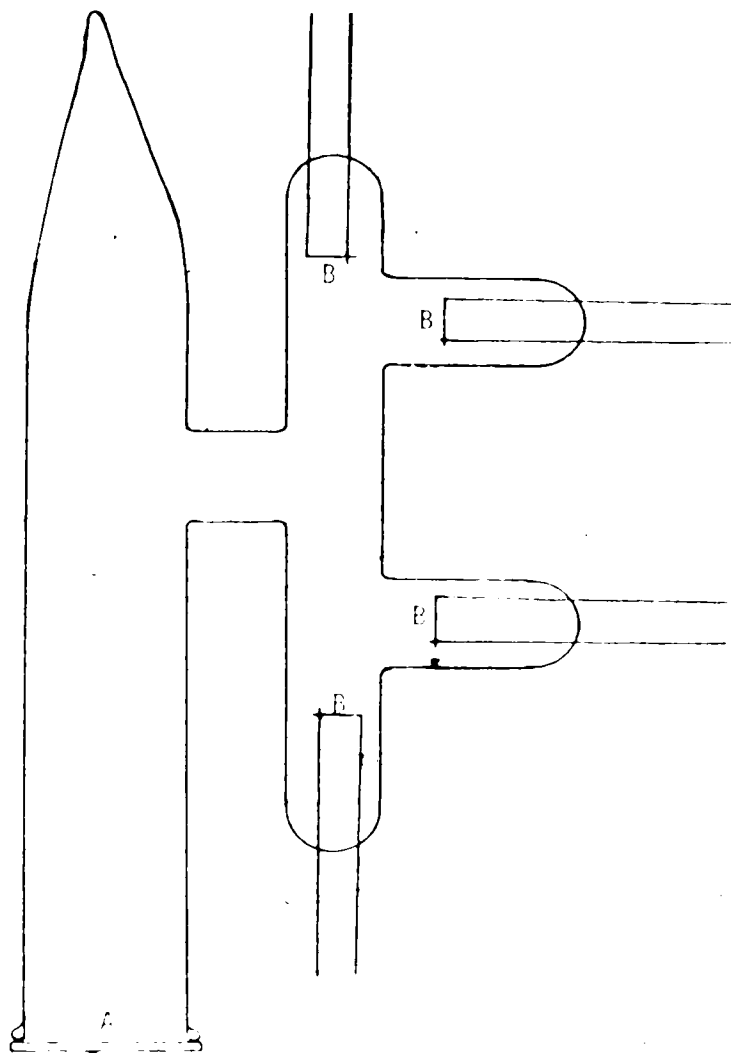
FIG. II-1. Xenon Resonance Lamp. A, lithium fluoride window. B, Fe-Al-Ni getter.

adsorb impurities generated during the lamp's use. The getter was heated by a current controlled by a rheostat, firstly to degas (1-2 volts), then the current was increased until the getter was a bright red (4-5 volts) and a black mirror formed on the walls of the getter tube. When more than one getter was incorporated in the lamp they could be used in turn to prolong the life of the lamp when it was seen to deteriorate. One getter was usually discharged just before or just after filling the lamp with xenon. The operating lamp was filled with 0.2 - 0.3 torr of xenon and 1.5 - 2.0 torr of neon as carrier gas. The lamp was tested with the microwave generator at this point and then sealed off with a hand torch if it performed satisfactorily.

The lamps tended to deteriorate with usage and several lamps were used in this study. All the lamps required the use of a Tesla coil (Electro-Technic Products) to initiate the discharge.

ii) The lamps used in the condensed phase studies were similar to the gas phase lamps except that they incorporated a male 40/50 ground glass joint and the lithium fluoride window was attached with epoxy resin (Armstrong Products Co., Inc.). Black wax (Apiezon W) could not be used in this case since the lack of cooling inside the photolysis cell allowed the black wax to heat up to such an extent that the window could be detached from the lamp.

c) Windows

The most commonly used window materials in the ultraviolet and vacuum ultraviolet regions are shown on Table II-3.

i) In the vacuum ultraviolet quartz is the most suitable material for wavelengths down to 170 nm, followed by suprasil down to

TABLE II-3

Window Materials[a]

Material	Thickness (mm)	Wavelength (nm) for 10% Transmission
LiF	1	105
CaF_2 (synthetic)	3	122
Sapphire (synthetic)	0.5	142
Suprasil	1	155
Quartz, clear fused	10	172
Quartz, crystal	10	186
Vycor 791	1	212
Vycor 790	2	254
Corex D	1	250
Pyrex (Corning 774)	1	280
Window glass (standard)	1	307

[a] J. G. Calvert and J. N. Pitts, Jr., Photochemistry, John Wiley and Sons, Inc., New York, 1966, p. 748.

155 nm. These are convenient in that they can be joined directly to a quartz reaction vessel, or through a graded seal to a pyrex vessel, and they can be heated quite strongly.

Sapphire is good to 142 nm which means that it can transmit the 147 nm xenon line while selectively screening out the 129.5 nm line.

Synthetic calcium fluoride is transparent to 122 nm and lithium fluoride has the shortest wavelength cut-off of readily available materials at 105 nm. These windows are more fragile and the most convenient way of affixing the windows to the cell is by using black wax (Apiezon W).

The low wavelength transmittance cut-offs shift to the red with increasing temperature[134]. This does, however, restrict their use to room temperature studies.

ii) Near Ultraviolet Region - At wavelengths greater than 300 nm there are a large number of glass and chemical filters for the isolation of desired wavebands but between 200 and 300 nm the range is more limited. The simplest solution to eliminating higher energy radiation is provided by the range of glass filters from Vycor to window glass shown on Table II-3.

There are some chemical filters in this region. The 254 nm mercury line can be isolated by using aqueous solutions of $NiSO_4$ or $CoSO_4$ with a 5 cm path length. However in general the percentage transmission is less with the chemical filters and their use is associated with fairly stringent operating conditions (e.g. the $NiSO_4$, $CoSO_4$ solutions should be pre-irradiated for ca. 4 hours to obtain a constant transmittance which lasts for several days.)

3. Photolysis Systems

Four different cells were used in various experiments, all of which were carried out under static conditions.

i) A cylindrical Pyrex cell 25 mm in diameter and 175 mm in length with a volume of 132 ml including cold finger and valve attachment was used in the vacuum ultraviolet photolysis of tetramethylsilane. The cell had a single lithium fluoride window, 28 mm in diameter and 2 mm thick, which was attached to the ground glass surface at one end of the cell body with Black Wax (Apiezon W). The window was removed and polished after each photolysis with Cerium Oxide (Optical Equipment Company) to remove polymer formed on the inside surface. The cell window was placed against the lamp window, and both were surrounded by a glass cylinder through which nitrogen flowed during photolysis to remove oxygen which would strongly absorb the emitted radiation.

ii) Photolysis of bis(trimethylsilyl)mercury was carried out in a cylindrical quartz cell 48 mm in diameter and 150 mm in length with a volume of 177 ml including cold finger and valve attachment. This cell had 2 mm thick quartz windows.

iii) The third cell was used in the search for fluorescence from tetramethylsilane. This was a quartz cell 38 mm in diameter and 148 mm in length with a volume of 170 ml including cold finger and valve attachment. It has a 2 mm thick quartz window, and at ninety degrees to it, a 2 mm thick lithium fluoride window.

iv) In the condensed phase studies a pyrex cell wa   ed with a female 40/50 ground glass joint so that the lamp could be   ated

within the cell, which was 120 mm in length and 45 mm in diameter. The lamp was sealed into the cell with black wax (Apiezon W) (Figure II-3).

4. Analytical System.

The main analytical method employed was gas chromatography with detection by flame ionization or thermal conductivity.

i) The thermal conductivity gas chromatograph (Gow-Mac TR-11-B) was coupled directly to the high vacuum system. The power supply was a Gow-Mac 9999C and the results were read out on a Sargent recorder. This system was used for gases which are non-condensable at liquid nitrogen temperatures (H_2, CH_4, O_2, CO). The power supply unit was operated at 150 ma when helium was the carrier gas (for CO, O_2 analysis) and 110 ma when argon was the carrier (H_2, CH_4 analysis). The chromatograph was operated at 142°C and the gas flow was controlled by an Edwards needle valve. The pressure of the product gases was measured in a gas burette in the high vacuum system and the gases were then introduced to an evacuated loop through which the carrier gas flow of the gas chromatograph could be diverted by means of three switch-type Hoke valves. The stream then flowed to a 13X molecular sieves column and thence to the detector. Response factors were measured and used to calculated relative amounts of products.

ii) The flame ionization gas chromatographs used were a Perkin-Elmer 801 and a Hewlett-Packard 5750, the former being used in the initial stages for the condensed phase studies and the latter for the remainder of the work since it was ten times more sensitive. Both used helium as carrier gas through a dual column arrangement, with the Perkin-Elmer using spiral glass columns and the Hewlett-Packard aluminum or stainless
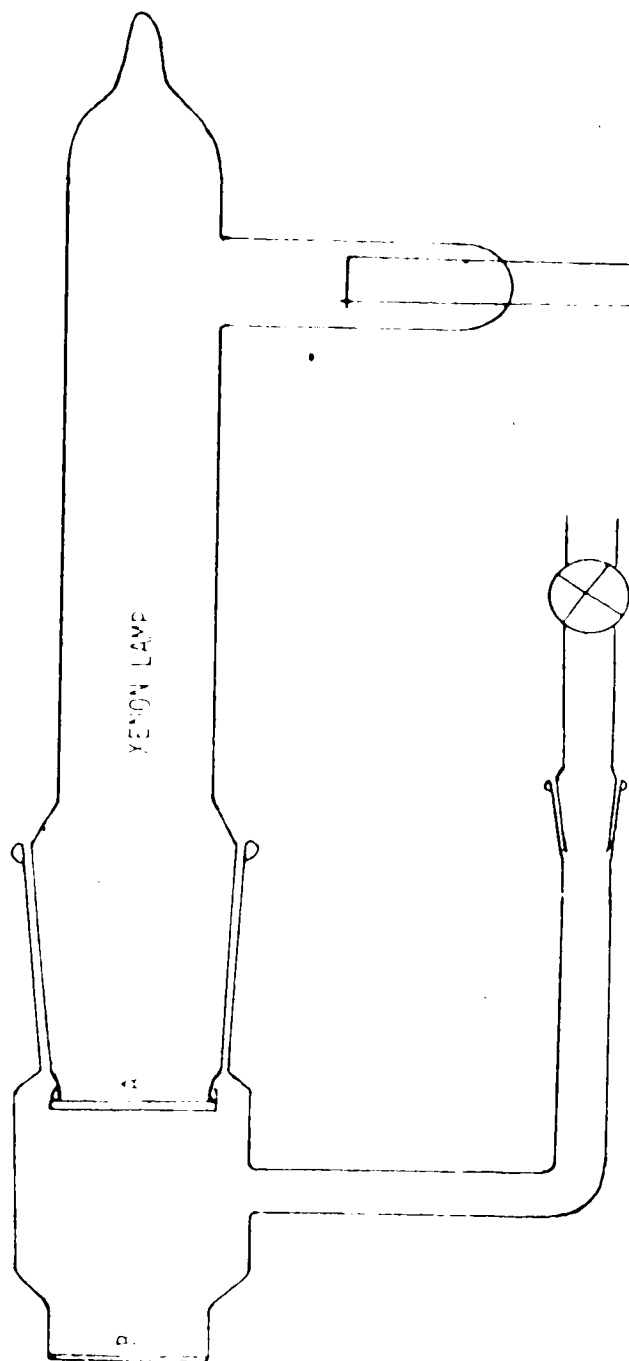
FIGURE II-3. Condensed Phase Photolysis System. A, lithium fluoride window.
B, quartz window.

steel columns. Sample introduction was by gas syringe injection and the results were displayed on a Sargent RS recorder. Response factors were determined for as many of the products as possible and used to calculate relative product yields. Absolute yields could be found by including a calibrated internal standard.

The columns used, their construction, and their operating conditions are summarized in Tables II-4 and II-5.

5. Procedure

i) Photolysis of Tetramethylsilane

Reactants were introduced into the photolysis cell and the xenon resonance lamp was initiated with a Tesla coil. All studies were done at ambient temperature and the lamp was operated at 15% - 90% power from the microwave generator. The space between the cell and lamp windows was flushed with nitrogen during photolysis to remove oxygen which strongly absorbs the 147 nm radiation. Formation of a polymer on the inside of the cell window during photolysis necessitated actinometry runs before and after each photolysis. Carbon dioxide was used as the actinometer taking :(CO) = 1.00. Pressures of 100 torr and photolysis times of 5 minutes were generally employed. The polymer formed was removed after each determination by removing the cell window and polishing it with a paste of cerium oxide and 95% ethanol.

After photolysis the reaction mixture was frozen down (-196°C) and the non-condensable gases pumped off with a one-stage mercury diffusion pump and a Toepler pump to the gas burette where their absolute yield was measured. The non-condensable gases were then

TABLE II-4

Thermal Conductivity GC Columns and Operating Conditions

Column	Flow Rate	Temperature	Construction	Compounds Analyzed
Molecular Sieves 13x, 30-60 mesh	65 cc/min Argon	Room Temperature	8 ft. × 6 mm glass	H_2, CH_4
Molecular Sieves 13x, 30-60 mesh	50 cc/min Helium	Room Temperature	8 ft. × 6 mm glass	CO, CO_2 H_2, NO

TABLE II-5

Flame Ionization GC Columns and Operating Conditions

A. Perkin-Elmer 881

Column	Flow Rate	Temperature	Construction	Compounds Analyzed
Porapak Q	30 ml/min Helium	75 - 150°C	5 ft. x 1/5 in. glass	Ethane, Ethylene, Propane, Monomethylsilane, Dimethylsilane
Silicone Oil DC 200 10% on Chromosorb WAW 60-80 mesh	30 ml/min Helium	60 - 100°C	25 ft. x 1/5 in. glass	Monomethylsilane, Dimethylsilane, Trimethylsilane, Tetramethylsilane, Disilanes

B. Hewlett Packard 5750

Column	Flow Rate	Temperature	Construction	Compounds Analyzed
Porapak Q	60 ml/min Helium	100 - 200°C	5 ft. x 1/4 in. aluminum	Methane, Ethane, Ethylene, Propane, Monomethylsilane, Dimethylsilane, Trimethylsilane, Tetramethylsilane

TABLE II-5 (cont'd)

Column	Flow Rate	Temperature	Construction	Compounds Analyzed
Silicone Oil DC 200 10% on Chromosorb WAW 60-80 mesh	60 ml/min Helium	60 - 150°C	16 ft.x1/4 in. aluminum	Monosilane Disilane Monoethylsilane Dimethylsilane Triethylsilane Tetraethylsilane Ethyldiethylsilane Ethyltrimethylsilane Hexamethyldisilane Hexamethyldisiloxane Tetraethyldisilapentane Dimethyldisilahexane Trisilane Tetrasilane
Silica Gel Medium Activity	60 ml/min Helium	80 - 130°C	12 ft.x1/4 in. stainless steel	Trimethylsilane Isobutane Hexamethyldisilane
Tri-cresyl Phosphate 10% on Chromosorb W 30-60 mesh	60 ml/min Helium	50 - 150°C	22 ft.x1/4 in. stainless steel	Similar to Silicone Oil column but different separations.

introduced to the thermal conductivity gas chromatograph for analysis.

The condensable products were then transferred along with the substrate to an ampoule fitted with a Burrell Silicone rubber seal. The mixture was allowed to warm up and was raised to atmospheric pressure by introducing helium with a gas syringe. The ampoule contents were mixed by pumping with the gas syringe and a suitably sized sample (1 - 2 ml) was then withdrawn for injection onto the appropriate column of the flame ionization gas chromatograph.

ii) Photolysis of Bis(trimethylsilyl)mercury.

The mercury lamps used in these studies were warmed up for fifteen minutes before use and were placed 10 50 mm from the cell window with the selected filter in place. The mercurial was degassed before each run and then a known amount was frozen into the photolysis cell cold finger which was covered with aluminum foil to prevent photolysis of the solid mercurial. Any other reactant was then measured out in an adjacent volume and frozen into the cell. The mixture was allowed to warm up and then photolyzed. The whole reaction mixture was then transferred to the ampoule fitted with the silicone rubber seal and the procedure continued as for the tetramethylsilane photolysis.

iii) Fluorescence from Tetramethylsilane

The 170 ml cell was enclosed in a black box with two apertures aligned with the cell windows. A xenon resonance lamp was used to photolyze the gas through the lithium fluoride window and an IP 28 photomultiplier was placed against the other aperture. Nitrogen was used to flush the air from in front of the xenon lamp and a 210 nm

interference filter was fitted between the cell and the photomultiplier to eliminate visible and unwanted radiation (Figure II-4). Photomultiplier readings were recorded with the cell empty and with 10 - 100 torr of gas present. All measurements were taken in a darkened room. The light intensity from a low-pressure lamp was calibrated by using nitrous oxide ($\phi(N_2)$ = 1.44) as an actinometer and this was then used to give a reference signal on the photomultiplier.

iv) Photolysis in the Condensed Phase

Reactants were introduced into the cell in the gas phase and then solidified or liquefied onto the flat surface at the bottom of the cell by using an appropriate low-temperature bath on the outside of the cell. Photolyses were done in sequence by irradiating for a certain period of time, then pumping off any non-condensable products, freezing down another layer of reactant and then repeating the process up to ten times. Carbon dioxide in the gas phase was used as the actinometer. After photolysis the products were treated in the same way as in the gas phase photolysis.

6. Other Equipment

i) Mass spectra were determined on Associated Electronics Industries instruments, models MS9 and MS12.

ii) Hydrogen, methane and ethane isotope ratios were determined on a Consolidated Electrodynamics Industries, Model MS10 mass spectrometer.

7. Materials

A list of the materials used in this study is given in Table II-1.
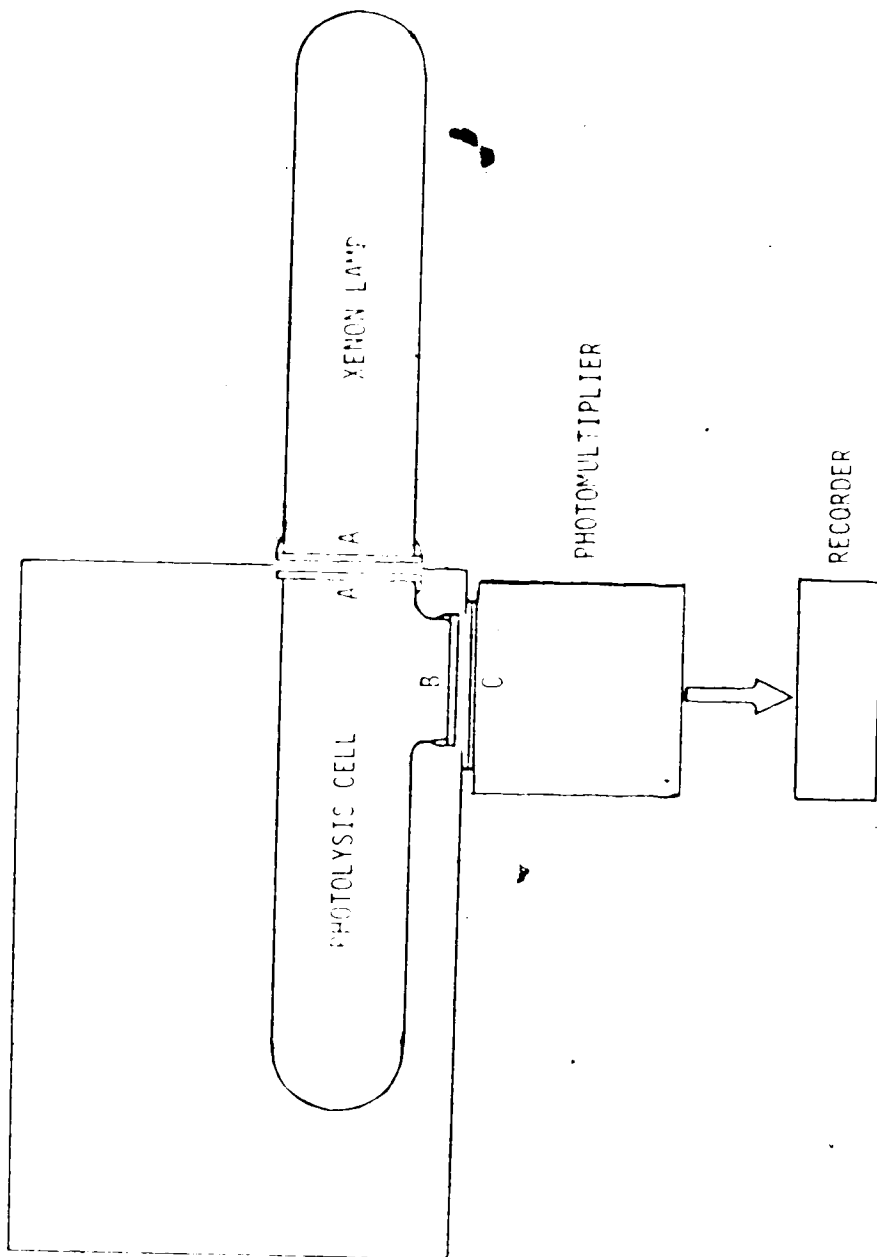
FIGURE II-4. Fluorescence System. A, lithium fluoride windows. B, quartz window. C, interference filter.

TABLE II-6

Materials Used

Material	Supplier	Purification
Helium	Canadian Liquid Air (for G.C.)	Passed through a column of molecular sieves at ambient temperature.
Neon	Airco	Assayed Reagent
Argon	Liquid Carbonic Canada (for G.C.)	Passed through columns of molecular sieves and drierite at ambient temperature.
Xenon	Airco	Assayed Reagent.
Hydrogen	Airco	Assayed Reagent.
Hydrogen	Canadian Liquid Air (for G.C.)	None.
Deuterium	Matheson	Passed through column of molecular sieves.
Deuterium hydride	ICN Canada Ltd.	Passed through column of molecular sieves.
Nitrogen	Airco	Assayed Reagent.
Nitrogen	Liquid Carbonic Canada (for flushing cell window)	None.

TABLE II-6 (cont'd)

Material	Supplier	Purification
Oxygen	Airco	Assayed Reagent.
Carbon monoxide	Airco	Assayed Reagent.
Carbon dioxide	Airco	Assayed Reagent.
Methane	Matheson	None.
Methane-d_4	Merck, Sharp, Dohme	None.
Ethane	Phillips Petroleum Co.	Degassed at $-196°C$.
Propane	Phillips Petroleum Co.	Degassed at $-196°C$.
n-Butane	Phillips Petroleum Co.	Degassed at $-196°C$.
i-Butane	Phillips Petroleum Co.	Degassed at $-196°C$.
Ethylene	Phillips Petroleum Co.	Degassed at $-196°C$.
Neopentane	Phillips Petroleum Co.	Degassed at $-196°C$.
Nitric Oxide	Matheson	Passed through soda lime trap at $-78°C$ and P_2O_5 column at ambient temperature. Degassed at $-196°C$, Distilled at $-186°C$.
Nitrous oxide	Matheson	Degassed at $-196°C$. Distilled at $-130°C$.

TABLE II-6 (cont'd)

Material	Supplier	Purification
Compressed Air	Canadian Liquid Air (for G.C.)	None.
Monosilane	Merck, Sharp, and Dohme	Degassed at -196°C. Distilled at -160°C.
Monosilane-d_4	Merck, Sharp, and Dohme	Degassed at -196°C. Distilled at -160°C.
Disilane	Merck, Sharp, and Dohme	Degassed at -160°C. Distilled at -130°C.
Disilane-d_6	Merck, Sharp, and Dohme	Degassed at -160°C. Distilled at -130°C.
Monomethylsilane	Merck, Sharp, and Dohme	Degassed at -196°C. Distilled at -130°C.
Monomethylsilane-d_3	Merck, Sharp, and Dohme	Degassed at -196°C. Distilled at -130°C.
Dimethylsilane	Peninsular Chem. Research	Degassed at -196°C. Distilled at -130°C.
Dimethylsilane-d_2	Merck, Sharp, and Dohme	Degassed at -196°C. Distilled at -130°C.

TABLE II-6 (cont'd)

Material	Supplier	Purification
Trimethylsilane	Chemical Procurement Labs	Degassed at -196°C. Distilled at -130°C.
Trimethylsilane-d	Merck, Sharp, and Dohme	Degassed at -196°C. Distilled at -130°C.
Tetramethylsilane	Aldrich Chemical Co.	Degassed at -130°C. Distilled at -98°C.
Tetramethylsilane-d$_{12}$	Merck, Sharp, and Dohme	Degassed at -130°C. Distilled at -98°C.
Hexamethyldisilane	City Chem. Corp.	Degassed at -130°C. Distilled at -98°C.
Hexamethyldisiloxane	Pierce Chemical Co.	Degassed at -130°C. Distilled at -98°C.
Bis(trimethylsilyl)mercury	Dr. W. A. G. Graham University of Alberta	Degassed at room temperature.
Lithium fluoride	Harshaw Chem. Co.	None.

CHAPTER III

THE XENON RESONANCE LAMP PHOTOLYSIS
OF TETRAMETHYLSILANE

A. RESULTS

The direct gas-phase photolysis of tetramethylsilane (TMS) in a static system by a xenon resonance lamp was studied as a function of substrate pressure, exposure time, concentration of added free radical scavenger, and mole fraction of tetramethylsilane in mixtures of tetramethylsilane and per-deuterated tetramethylsilane. All experiments were done at room temperature.

1. Products

The products of photolysis are given in Table III-1 and are listed here in decreasing order of importance: ethane (C_2H_6), methane (CH_4), trimethylsilane (Tri-MS), hydrogen (H_2), hexamethyl-disilane (HMDS), ethyldimethylsilane (EDMS), ethyltrimethylsilane (ETMS), and three other disilanes tentatively identified by retention time and mass spectrometric analysis as 2,2,4-trimethyl-2,4-disila-pentane (Tri-MDSP), 2,2,4,4-tetramethyl-2,4-disilapentane (Tet-MDSP), and 1,4-dimethyl-2,5-disilahexane (DMDSH). In addition traces of ethylene, propane, propylene, dimethylsilane and two other unidentified disilanes were also found (all comprising 1% of total product yield). A solid polymeric substance also formed as a deposit on the inside of the reaction cell window.

TABLE III-1

Relative Yields of Products

(Pressure Stabilized)

Product	Relative Yield (%)
C_2H_6	30.0
CH_4	31.0
Tri-MS	12.0
H_2	9.0
HMDS	6.0
EDMS	3.0
ETMS	3.5
Tri-MDSP	2.0
Tet-MDSP	1.5
DMUSH	1.0

2. Effect of Substrate Pressure

The effect of substrate pressure from 5 to 400 torr on product yields was examined in 15 minute photolyses. The relative yields are listed in Table III-2 and shown graphically in Figures III-1, III-2 and III-3 where it can be seen that the yields of methane, trimethylsilane and hexamethyldisilane increase slightly with pressure indicating pressure stabilization of "hot" products. In a complimentary fashion the yields of ethane, hydrogen and ethyldimethyl-silane decrease with increasing pressure indicating that at lower pressures their yields are increased by fragmentation of "hot" products to produce more hydrogen, methane and methyl radicals. Other products are not noticeably dependent on pressure. Since yields are essentially constant above 100 torr, all subsequent experiments were carried out at pressures of 100 torr or higher to avoid interference from pressure-dependent fragmentations. The average relative yields of the pressure stabilized system are summarized in Table III-1.

3. Effect of Exposure Time

An exposure time study was carried out to determine the product quantum yields since the polymeric deposit on the cell window caused a decrease in the light intensity throughout the photolysis, making the absorbed light intensity a function of photolysis time. Carbon dioxide was used as the actinometer both before and after each photolysis using $\phi(CO) = 1.0$ (Chapter I, section I-2). The aim was to plot the post-actinometric light intensities vs. time and integrate to obtain the actual absorbed light. However it was found that the post actinometric runs were not dependable since the ratio of O_2 to CO

TABLE III-2(a)

Relative Yield (%) As A Function of Substrate Pressure

Pressure (torr)	CH_4	C_2H_6	Tri-MS	H_2	HMDS
5	21.3	38.1	8.6	6.9	3.6
5.5	24.3	28.0	5.4	14.8	5.4
9	29.3	29.7	7.8	11.5	3.4
9.5	21.5	31.2	6.9	12.2	5.8
10	27.4	31.0	8.6	8.6	4.1
16.5	26.2	35.0	7.8	8.4	4.7
19	25.6	32.9	8.1	6.9	6.2
20	24.5	31.2	10.1	10.4	4.7
23	28.5	35.6	8.3	7.1	5.6
30	25.3	29.5	10.8	7.6	5.0
34	31.0	27.9	12.3	8.1	5.1
50	23.2	36.3	8.9	5.8	7.1
53	23.9	29.0	8.5	11.6	8.6
56	29.6	26.4	6.8	15.5	4.6
100	28.4	32.0	12.2	6.8	5.5
138	27.6	29.9	10.3	8.3	9.7
170	31.2	29.8	9.5	9.0	9.1
200	34.7	31.1	13.4	7.5	2.2
275	33.2	33.2	11.3	10.8	4.1
400	35.9	25.2	16.4	9.6	4.4

TABLE III-2(b)

Relative Yield (%) As A Function of Substrate Pressure

Pressure (torr)	ETMS	EDMS	Tri-MDSP	Tet-MDSP	DMDSH
5	4.2	7.6	2.7	1.4	0.8
5.5	3.5	6.2	3.8	2.6	1.5
9	3.8	6.3	2.3	1.3	0.7
9.5	4.8	8.3	3.5	2.1	1.3
10	4.5	7.9	2.6	1.3	0.7
16.5	3.4	5.7	2.6	1.4	0.8
19	3.8	6.1	3.6	1.8	1.3
20	4.8	7.7	2.4	1.2	0.8
23	3.3	5.3	2.7	1.1	0.9
30	5.1	8.2	2.5	1.5	0.9
34	3.8	5.9	2.5	1.3	0.7
50	2.8	3.7	3.0	1.8	1.1
53	3.7	4.9	3.6	2.3	2.0
56	7.2	1.8	1.2	0.7	2.0
100	3.4	3.8	1.5	0.8	0.5
130	4.6	2.6	2.8	1.8	1.2
170	3.0	1.8	2.3	1.4	1.2
200	4.3	2.1	0.6	0.9	0.6
275	2.9	1.8	1.2	0.2	0.4
400	2.3	1.4	0.4	0.0	0.8
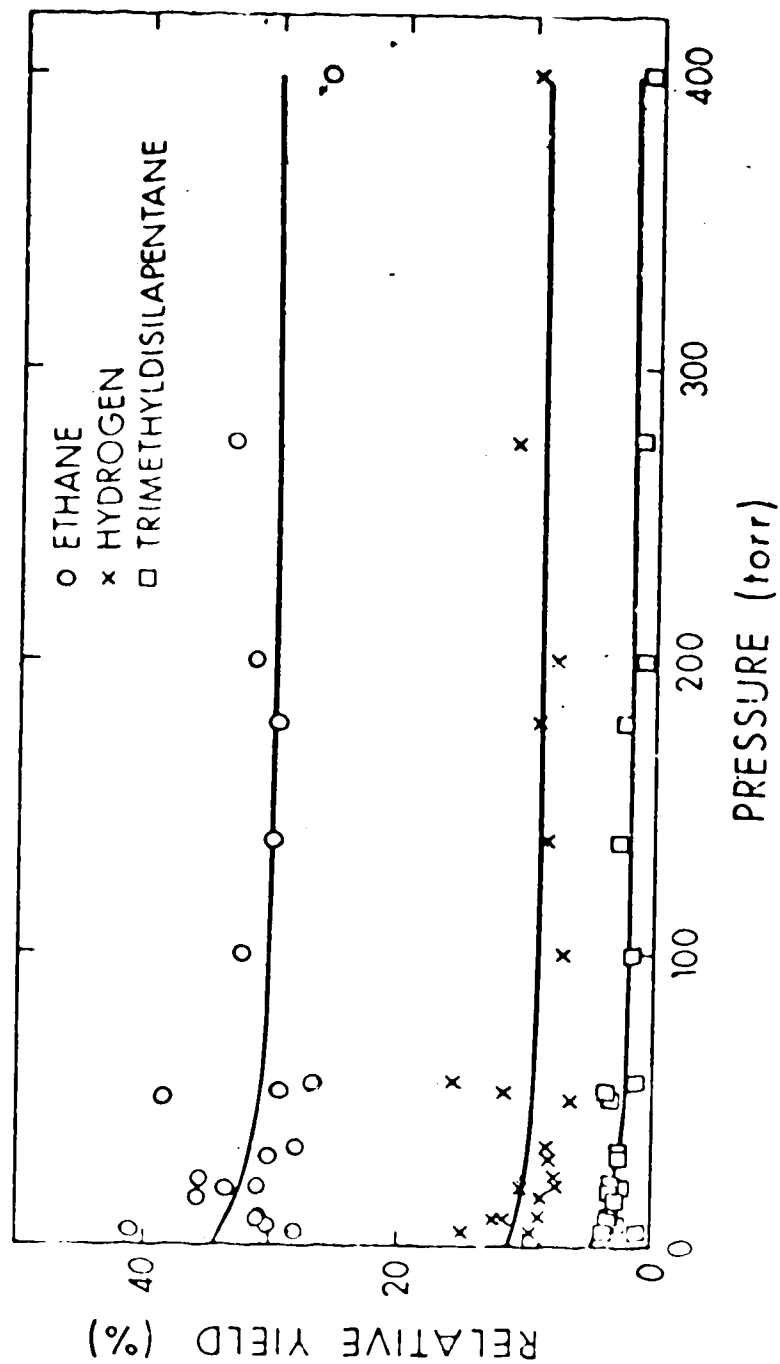
FIGURE III-1: Relative Yields of C_2H_6, H_2 and Tri-MDSP as a Function of Pressure from the Xenon Lamp Photolysis of Tetramethylsilane.
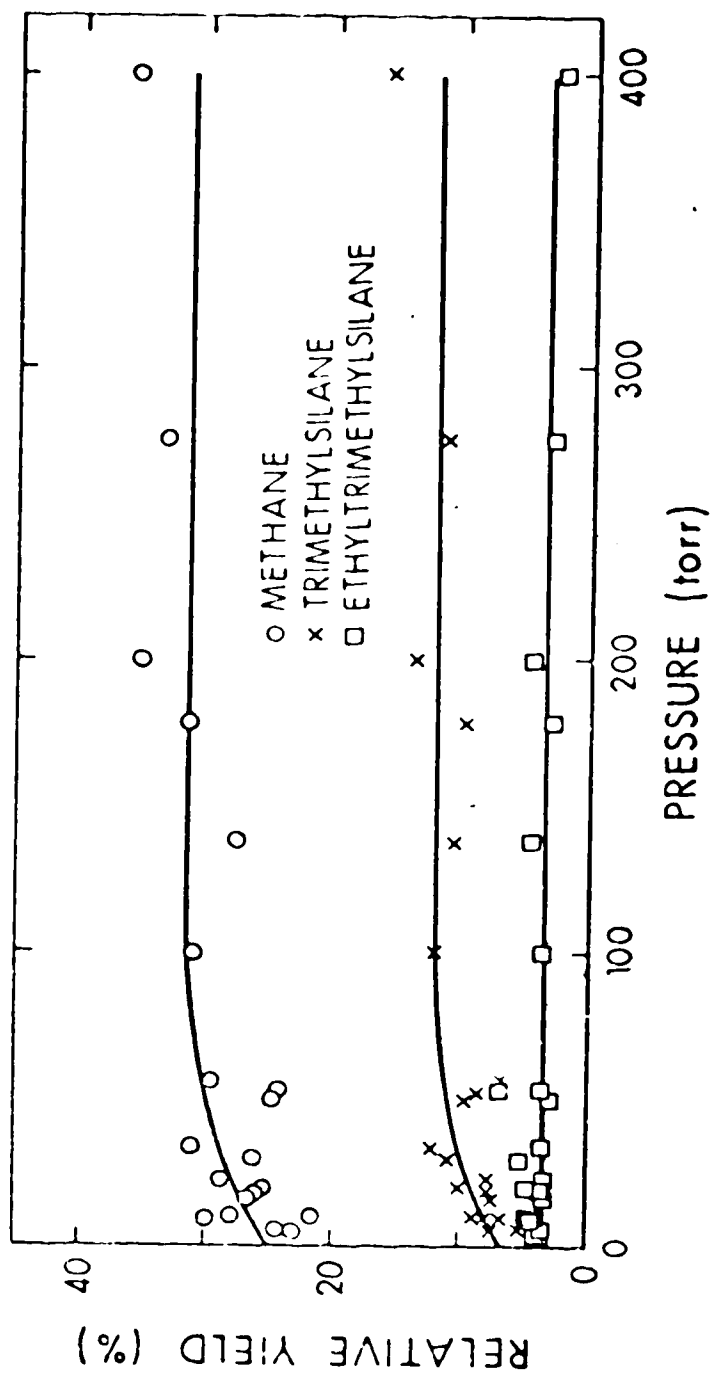
FIGURE III-2: Relative Yields of CH_4, Tri-MS and ETMS as a Function of Pressure from the Xenon Lamp Photolysis of Tetramethylsilane.
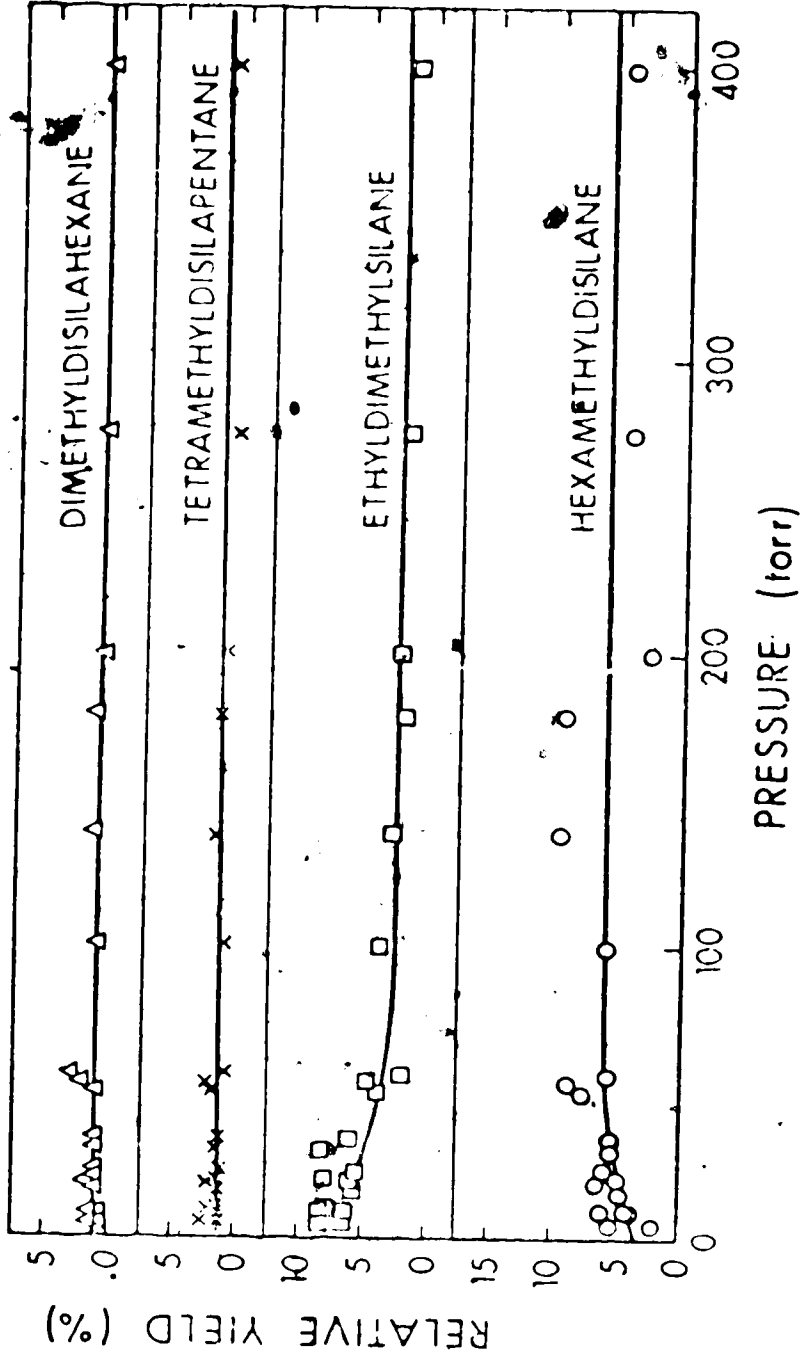
FIGURE III-3: Relative Yields of DMDSH, Tet-MDSP, EDMS and HMDS as a Function of Pressure from the Xenon Lamp Photolysis of Tetramethylsilane.

varied with the exposure time of the preceding silane photolysis
(Figure III-4). The pre-actinometric runs had an essentially constant
O_2/CO ratio of 0.50 whereas in the post-actinometric runs this ratio
decreased to as little as 0.06. This was interpreted as arising from a
reaction between oxygen and the deposited silicon polymer during acti-
nometer photolysis and leads to the possibility of complicating reactions.
This was not investigated further and quantum yields were determined by
using the pre-actinometry light intensities to obtain product quantum
yields which were plotted vs. exposure time. Exposure times varied from
30 seconds to 15 minutes and the results are shown in Table III-3 and
graphically on Figures III-5, III-6 and III-7. Extrapolation of these
plots to zero time should give correct product quantum yields since this
is equivalent to extrapolation to zero polymer formation. Since these
plots are exponential in nature the error in the extrapolated values
was minimized by using semi-log plots of : vs. time. The product
quantum yields so obtained are summarized in Table III-4.

The exposure time study was also used to decide if any of the
products were of secondary origin. As shown in Table III-5 and graphi-
cally on Figures III-8 and III-9 all the product yields are essentially
constant with time, consequently they are of primary origin.

4. Effect of Nitric Oxide as Scavenger

It has been shown previously that nitric oxide is an efficient
scavenger of monovalent alkyl and silyl radicals[93,105,135] while car-
benes and silylenes are unaffected. Thus photolysis in the presence of
a few torr of nitric oxide should enable us to differentiate between
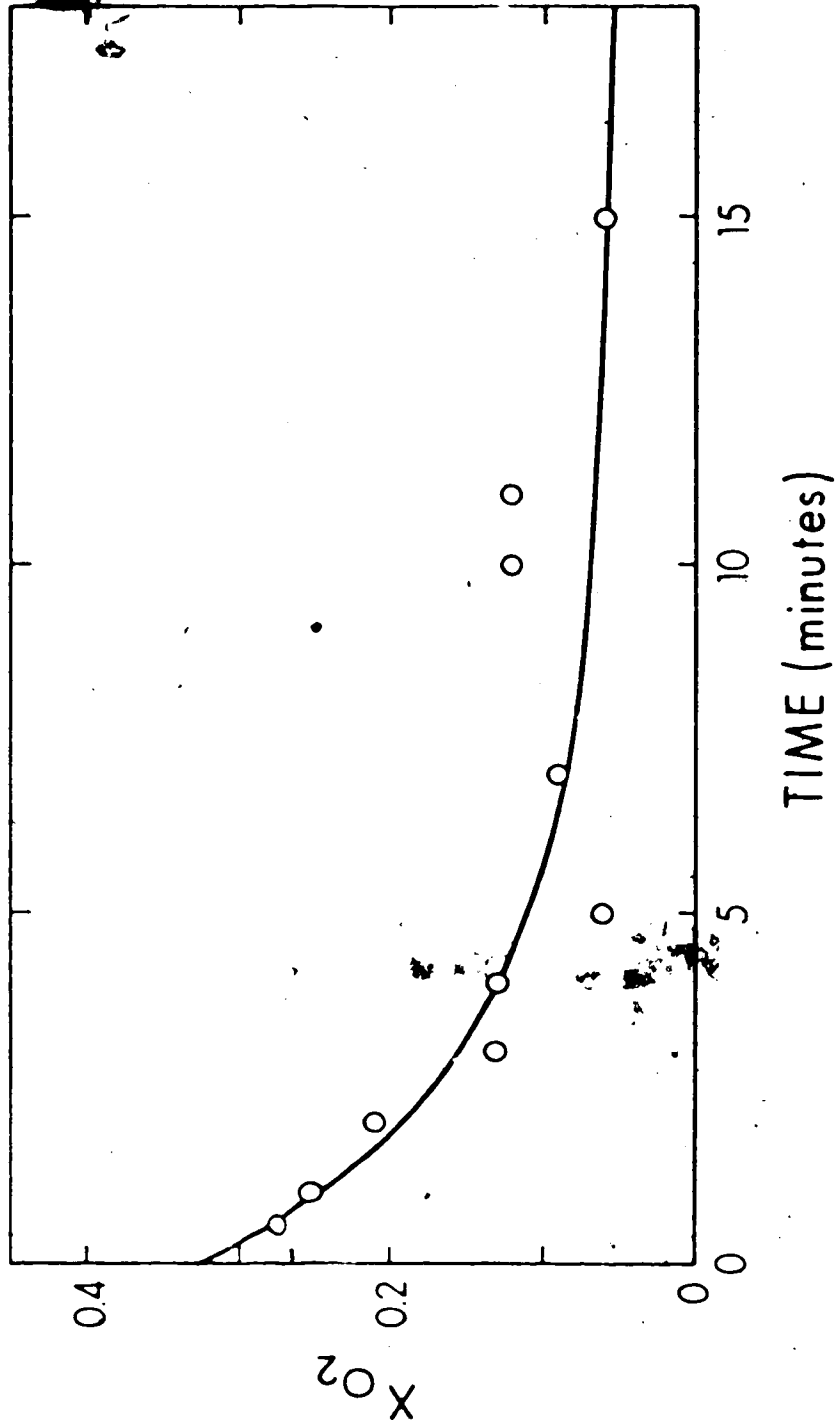
FIGURE III-4: Variation in Post-actinometric X_{O_2} with Tetramethylsilane Photolysis Time.

TABLE III-3(a)

Quantum Yield As A Function of Time

Time (mins)	CH$_4$	C$_2$H$_6$	Tri-MS	H$_2$	HMDS
1/2	0.215	0.249	0.098	0.078	0.069
1/2	0.225	0.239	0.096	0.096	0.074
1	0.186	0.143	0.072	0.053	0.042
2	0.135	0.148	0.056	0.048	0.038
3	0.128	0.107	0.048	0.044	0.029
4	0.106	0.105	0.042	0.037	0.026
5	0.097	0.068	0.035	0.032	0.019
7	0.089	0.075	0.029	0.030	0.020
10	0.065	0.066	0.025	0.023	0.018
12	0.067	0.057	0.023	0.028	0.015
15	0.050	0.035	0.018	0.020	0.013

TABLE III-3(b)

Quantum Yield As A Function of Time

Time (mins)	ETMS	EDMS	Tri-MDSP	Tet-MDSP	DMDSH
1/2	0.031	0.033	0.032	0.014	0.011
1/2	0.034	0.032	0.034	0.016	0.009
1	0.020	0.025	0.018	0.007	0.006
2	0.018	0.021	0.017	0.007	0.005
3	0.015	0.016	0.011	0.005	0.004
4	0.013	0.015	0.011	0.005	0.003
5	0.009	0.011	0.007	0.004	0.003
7	0.009	0.013	0.008	0.004	0.003
10	0.008	0.009	0.007	0.003	0.002
12	0.007	0.009	0.006	0.003	0.002
15	0.005	0.007	0.005	0.003	0.002
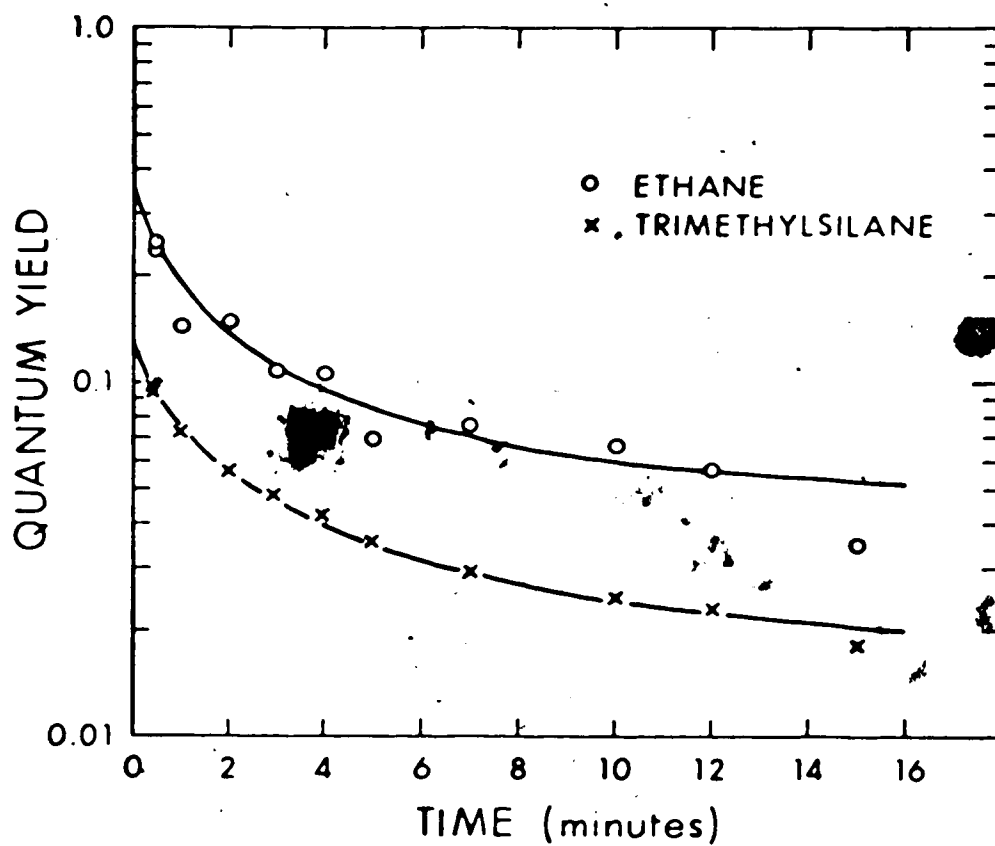
FIGURE III-5: Quantum Yields of C_2H_6 and Tri-MS as a Function of Time from the Xenon Lamp Photolysis of Tetramethylsilane.
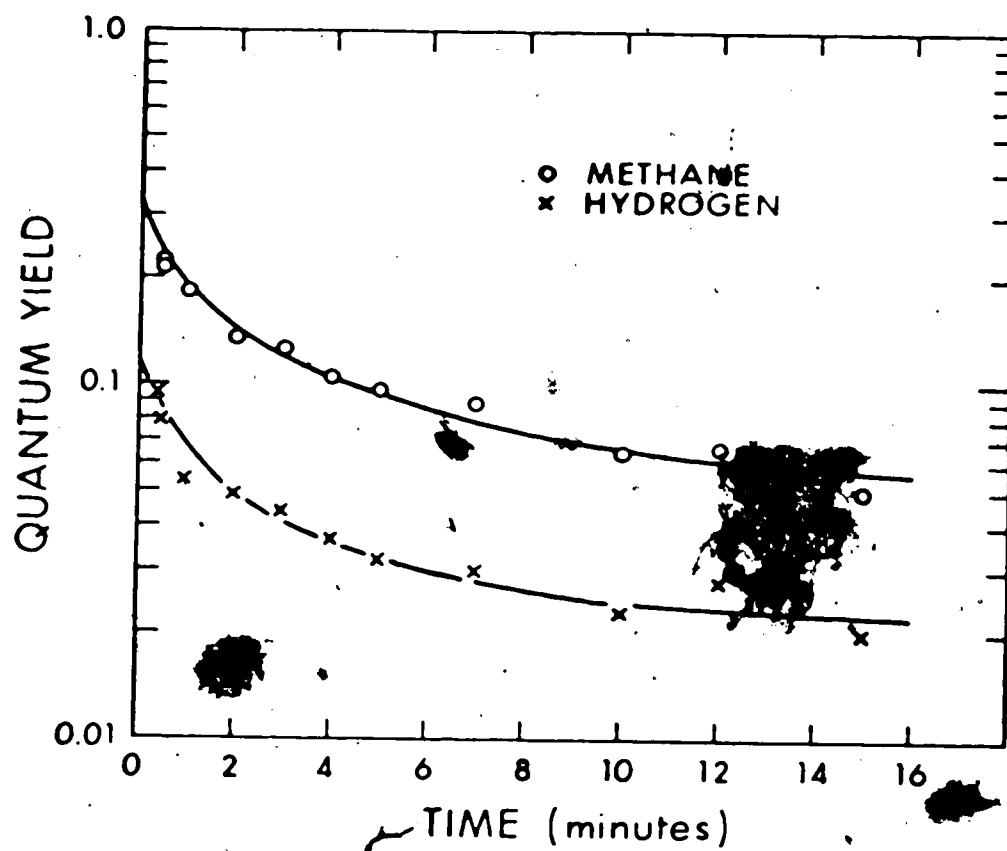
FIGURE III-6:   Quantum Yields of CH_4 and H_2 as a Function of Time from the Xenon Lamp Photolysis of Tetramethylsilane.
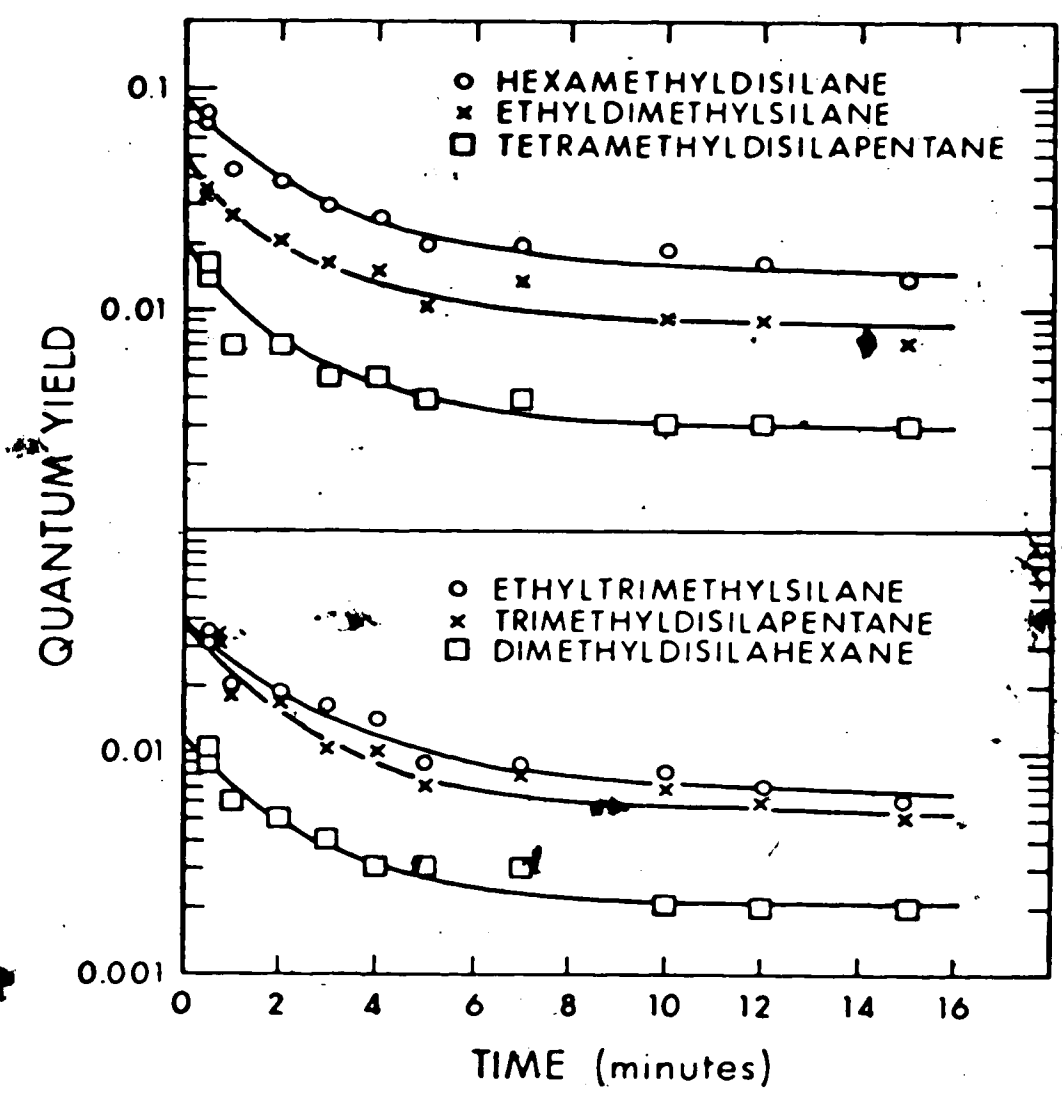
FIGURE III-7:   Quantum Yields of ETMS, Tri-MDSP, DMDSH, HMDS, EDMS

and Tet-MDSP as a Function of Time from the Xenon

Lamp Photolysis of Tetramethylsilane.

TABLE III-4

Quantum Yield of Products at Zero Time

Product	Quantum Yield :°
C_2H_6	0.35
CH_4	0.33
Tri-MS	0.13
H_2	0.12
HMDS	0.09
EDMS	0.05
ETMS	0.04
Tri-MDSP	0.04
Tet-MDSP	0.02
DMDSH	0.01

TABLE III-5(a)

Relative Yield (%) As A Function Of Time

Time (mins)	CH_4	C_2H_6	Tri-MS	H_2	HMDS
1/2	25.2	29.1	11.5	9.1	8.1
1/2	25.6	27.1	10.8	10.9	8.4
1	31.7	24.3	12.3	9.0	7.1
2	26.7	29.2	11.0	9.6	7.4
3	30.7	25.6	11.5	10.7	6.9
4	28.5	28.2	11.3	10.0	6.9
5	33.5	23.5	12.0	11.1	6.6
7	31.1	26.0	10.3	10.4	7.1
10	28.5	28.6	10.7	9.9	7.7
12	30.5	25.6	10.2	12.7	6.6
15	31.1	21.3	10.9	12.4	8.4

TABLE III-5(b)

Relative Yield (%) As A Function Of Time

Time (mins)	ETMS	FDMS	Tri-MDSP	Tet-MDSP	DMDSH
1/2	3.6	3.9	3.7	1.6	1.3
1/2	3.9	3.6	3.8	1.9	1.0
1	3.5	4.2	3.1	1.3	1.0
2	3.6	4.3	3.3	1.3	1.1
3	3.7	3.7	2.7	1.3	0.9
4	3.4	4.0	2.9	1.4	0.9
5	3.0	3.6	2.5	1.3	0.9
7	3.2	4.4	2.8	1.5	1.0
10	3.6	3.7	2.8	1.4	1.0
12	3.1	4.2	2.6	1.4	0.9
15	3.6	4.2	3.1	1.6	1.0

73
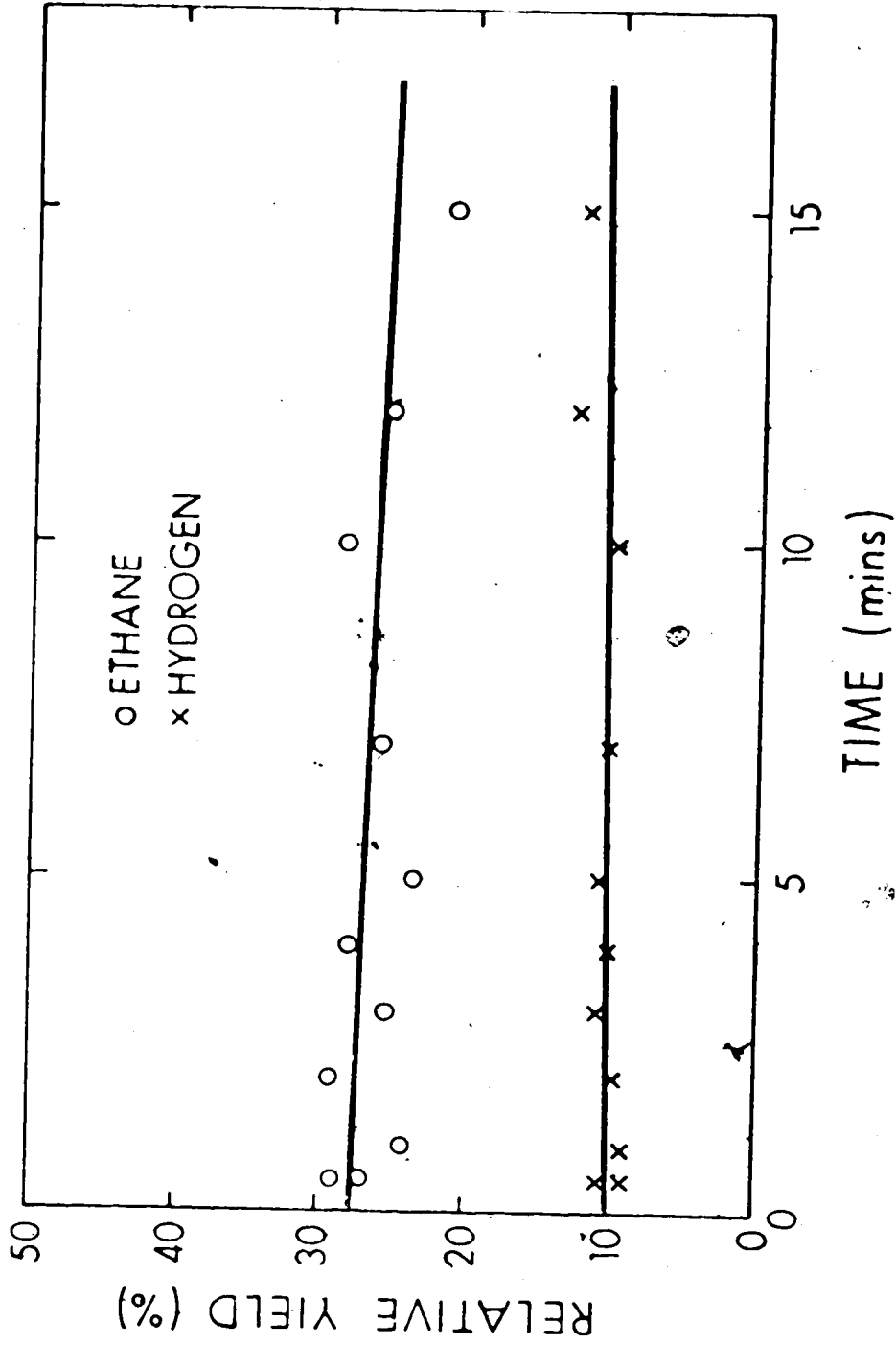
FIGURE III-8: Variation in Relative Yields of C_2H_6 and H_2 with Time from the Xenon Lamp Photolysis of Tetramethylsilane.
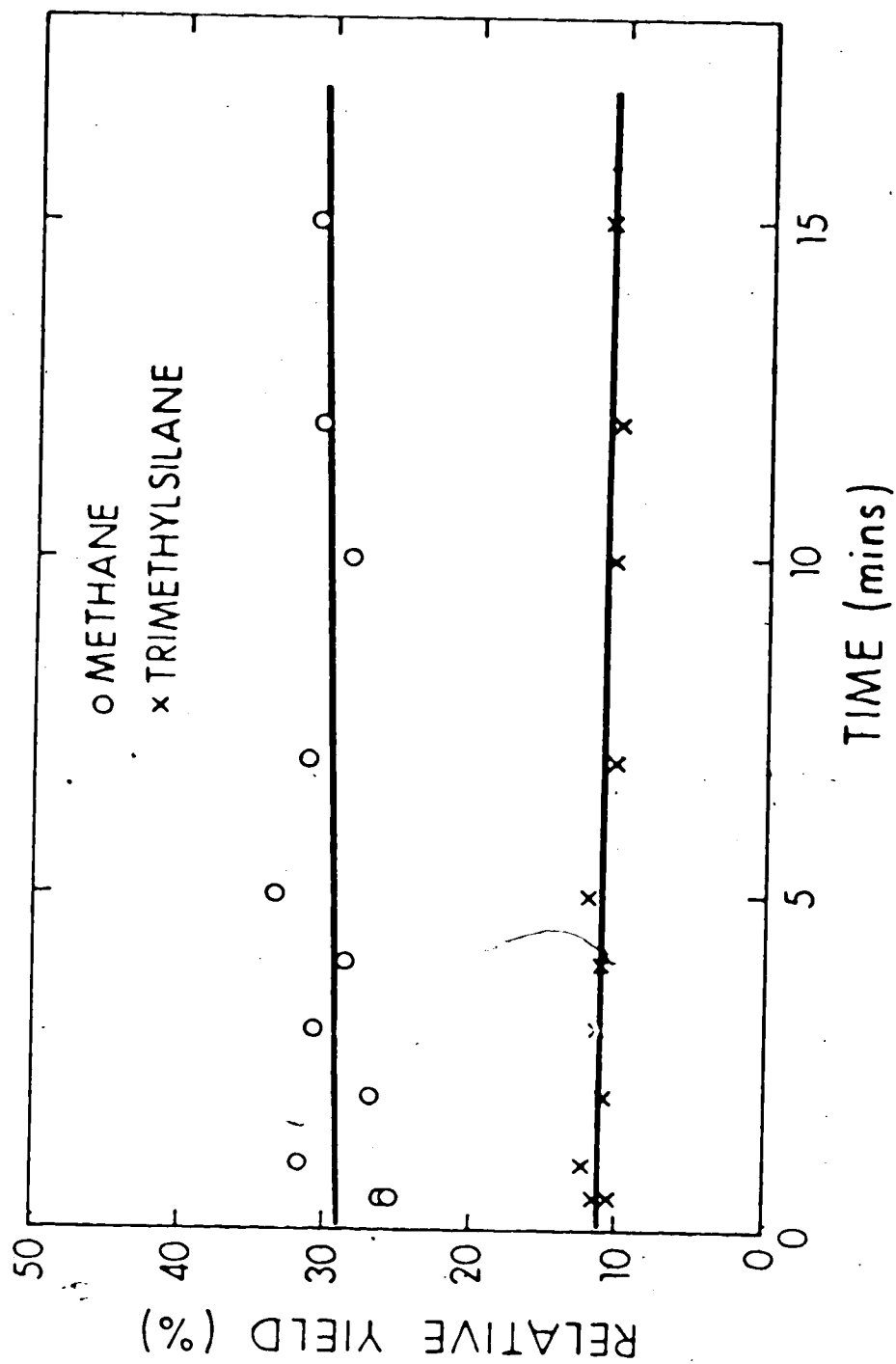
FIGURE III-9: Variation in Relative Yields of CH_4 and Tri-MS with Time from the Xenon Lamp Photolysis of Tetramethylsilane.

products formed by monoradical processes, and those formed by diradical or molecular processes, since nitric oxide will suppress formation of radical combination and abstraction products.

Experiments were carried out with up to 10ᵛ added nitric oxide and the results are shown in Table III-6 and Figure III-10.

Ethane, ethyldimethylsilane, hexamethyldisilane and the three other disilanes seem to be formed wholly by monoradical reactions since their yields are drastically suppressed by nitric oxide.

Trimethylsilane and ethyltrimethylsilane are both partially reduced from their original yields indicating that there are at least two modes of formation for each product, only one of which is scavengeable.

Similar mechanistic conclusions cannot be deduced from the changes in the yields of hydrogen and methane owing to the chain nature of the nitric oxide scavenging reaction. Similarly the yields of siloxanes produced indicate the presence of short chains in addition to demonstrating the presence of the radical $(CH_3)_3Si$.

5. Isotopic Labelling Studies

The non-deuterated and per-deuterated tetramethylsilanes were photolyzed in separate experiments at 100 torr to determine the relative yields of each product, since these could well be different. The total primary quantum yields should both be unity. Results are shown on Table III-7.

To determine the modes of formation of hydrogen and methane in the system photolyses were carried out using various mixtures of $(CH_3)_4Si$ and $(CD_3)_4Si$.

TABLE III-6

Effect of Nitric Oxide on Photolysis of Tetramethylsilane

| Product | μmoles product | | | |
| | % added Nitric Oxide | | | |
	0.0	2.5	5.0	10.0
C_2H_6	0.795	0.210	0.011	0.004
CH_4	1.136		a	
Tri-MS	0.405	0.100	0.091	0.138
H_2	0.375		a	
HMDS	0.222	0.001	0.000	0.000
EDMS	0.123	0.017	0.011	0.000
ETMS	0.101	0.059	0.050	0.032
Tri-MDSP	0.086	0.000	0.002	0.003
Tet-MDSP	0.044	0.000	0.000	0.000
DMDSH	0.031	0.003	0.000	0.004
A	-	-	[0.817]	[0.145]
B	-	[0.322]	[0.371]	[0.428]
HMDSO	0.022	0.288	0.328	0.985
C	-	[0.004]	[0.010]	[0.042]
D	-	[0.028]	[0.028]	[0.037]
N_2	-	0.450	1.780	2.200
N_2O	-		a	

a: not determined.

[ ]: response factors not known, taken same as for HMDS.
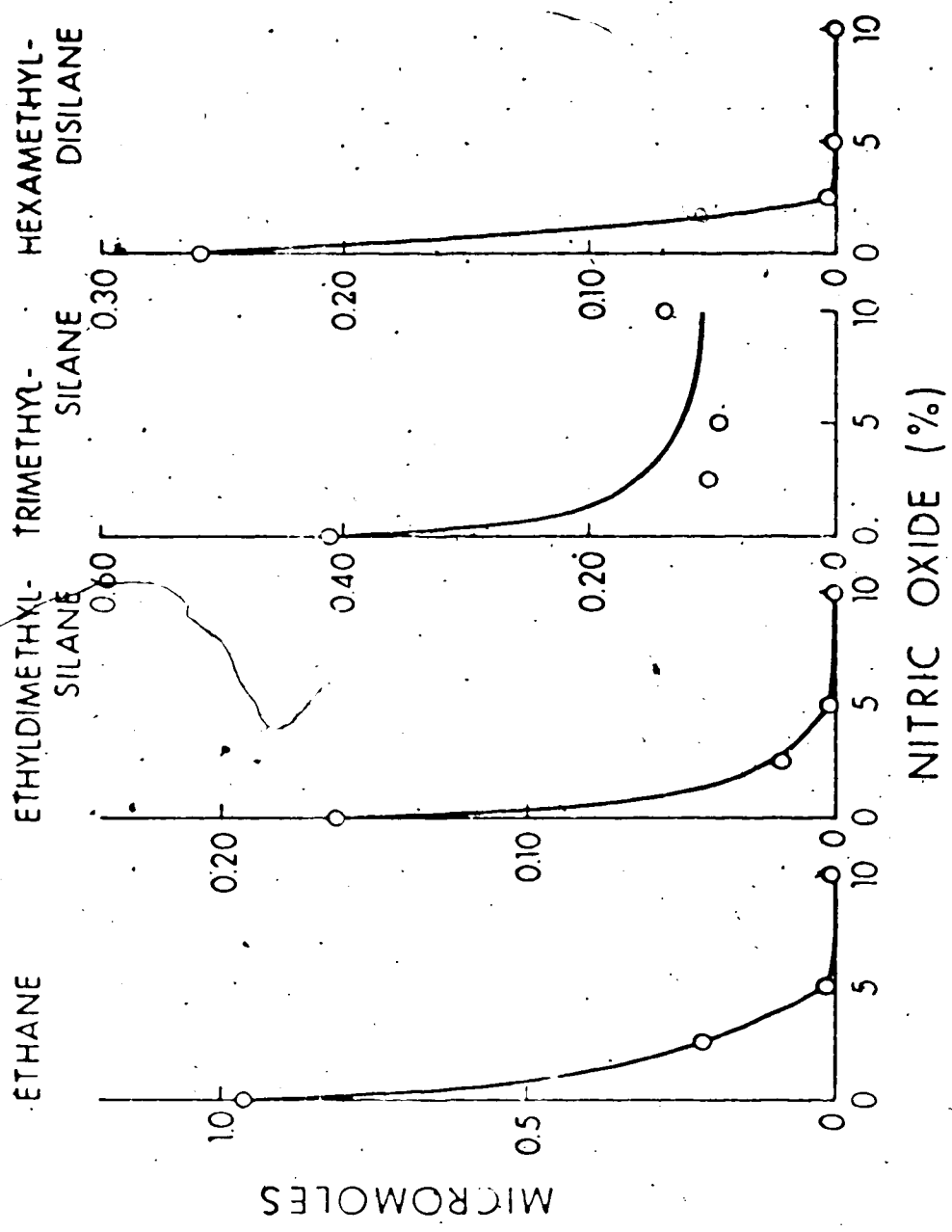
FIGURE III-10: Effect of Nitric Oxide on the Yields of C_2H_6, EDMS, Tri-MS and HMDS from the Xenon Lamp Photolysis of Tetramethylsilane.

TABLE III-7

Comparison of Relative Photolysis Yields for Tetramethylsilane

and Tetramethylsilane-d$_{12}$

Product	Relative Yield (%)		$\frac{\phi_{TMS}}{\phi_{TMS-d_{12}}}$
	TMS	TMS-d$_{12}$	
Ethane	30.0	31.7	
Methane	31.0	32.8	0.95
Tri-MS	12.0	9.9	
Hydrogen	9.0	10.2	0.88
HMDS	6.0	6.8	
EDMS	3.0	3.9	
ETMS	3.5	2.5	
Tri-MDSP	2.0	1.0	
Tet-MDSP	1.5	0.4	
DMDSH	1.0	0.7	

Analysis of the isotopic yields of the hydrogen, methane and ethane produced should indicate the relative contributions of molecular elimination and abstraction to the product yields. The isotopic composition of the products is listed in Table III-8 and shown graphically on Figures III-11, III-12 and III-13.

B. Auxiliary Studies.

1. Fluorescence Yield

A search was made for a fluorescence signal from tetramethylsilane and neo-pentane to determine if the quantum yield of decomposition was unity within experimental error.

No fluorescence was observed and a maximum value could be assigned to the fluorescence quantum yield from the error in the recorder baseline.

From nitrous oxide actinometry the output of the low-pressure Hg lamp in the region studied was 2×10^{13} quanta/sec. and this gave an output signal which was 10^3 times greater than the error in the baseline. Since the light intensity of the xenon lamp used to photolyze the tetramethylsilane was 2×10^{16} quanta/sec. the maximum value for the quantum yield of fluorescence is 10^{-6} for both tetramethylsilane and neo-pentane.

2. Condensed Phase Photolysis of Dimethylsilane

An auxiliary study was carried out on the condensed phase photolysis with a xenon lamp to investigate any differences in product distribution caused by the inhibition of secondary decomposition of internally excited fragments by the change in density as has been

TABLE III-8

Isotopic Composition of Hydrogen, Methane and Ethane from the Photolysis of Mixtures of Tetramethylsilane and Tetramethylsilane-d_{12}

Mole Fraction of Product	Mole Fraction of Tetramethylsilane						
	0.0	0.103	0.250	0.5	0.5	0.75	1.00
H_2	0.000	0.696	0.739	0.890	0.802	0.908	1.000
HD	0.000	0.238	0.221	0.102	0.191	0.084	0.000
D_2	1.000	0.066	0.040	0.008	0.007	0.008	0.000
CH_4	0.000	0.132	0.318	0.671	0.555	0.802	1.000
CH_3D	0.000	0.018	0.021	0.033	0.032	0.027	0.000
CD_3H	0.000	0.162	0.141	0.079	0.086	0.042	0.000
CD_4	1.000	0.688	0.520	0.217	0.327	0.129	0.000
C_2H_6	0.000	0.137	0.145	a	0.475	0.691	1.000
CH_3CD_3	0.000	0.200	0.364	a	0.342	0.278	0.000
C_2D_6	1.000	0.663	0.492	a	0.182	0.031	0.000

a: not determined.
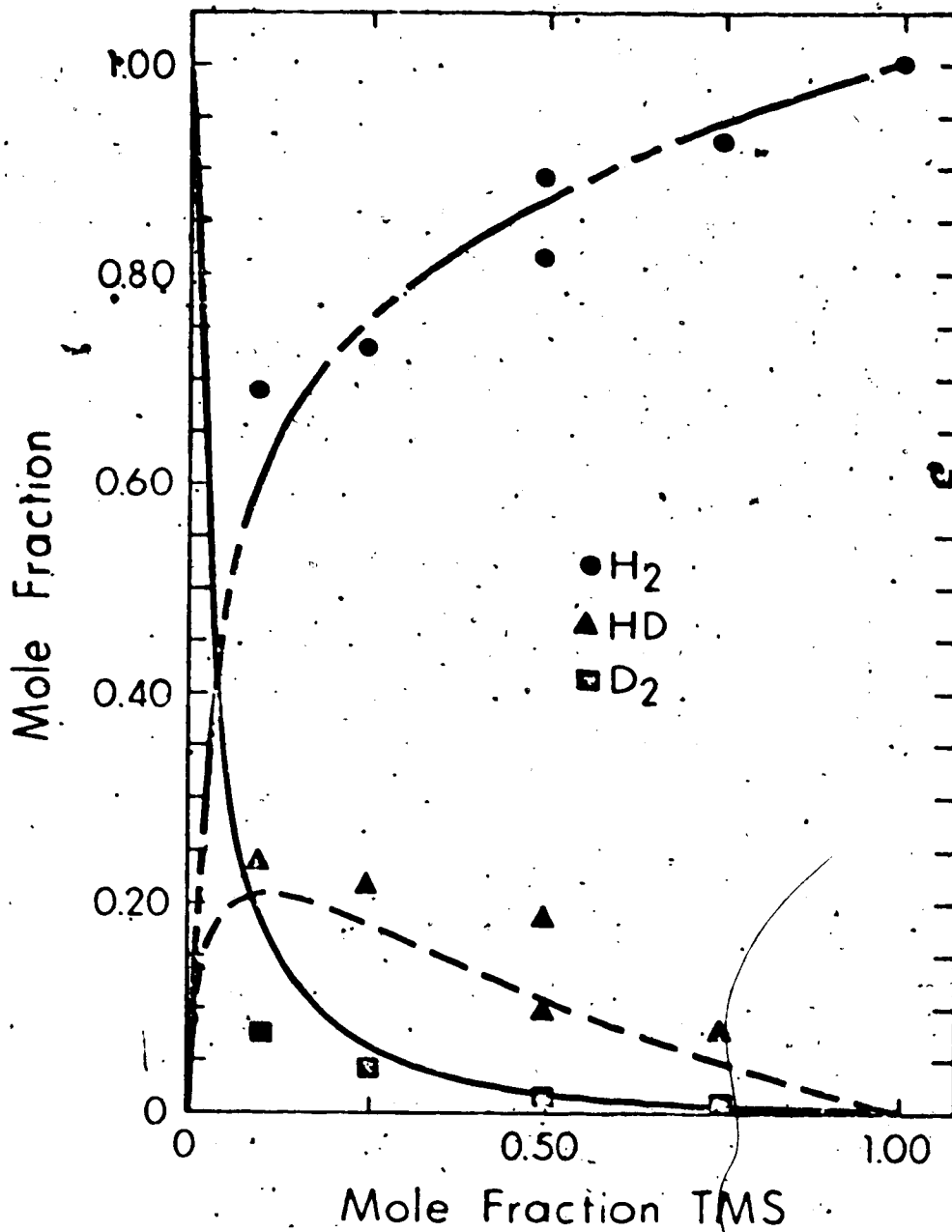
FIGURE III-11: Variation in Isotopic Hydrogen Yield As A Function of Relative Amounts of TMS and TMS-d$_{12}$.
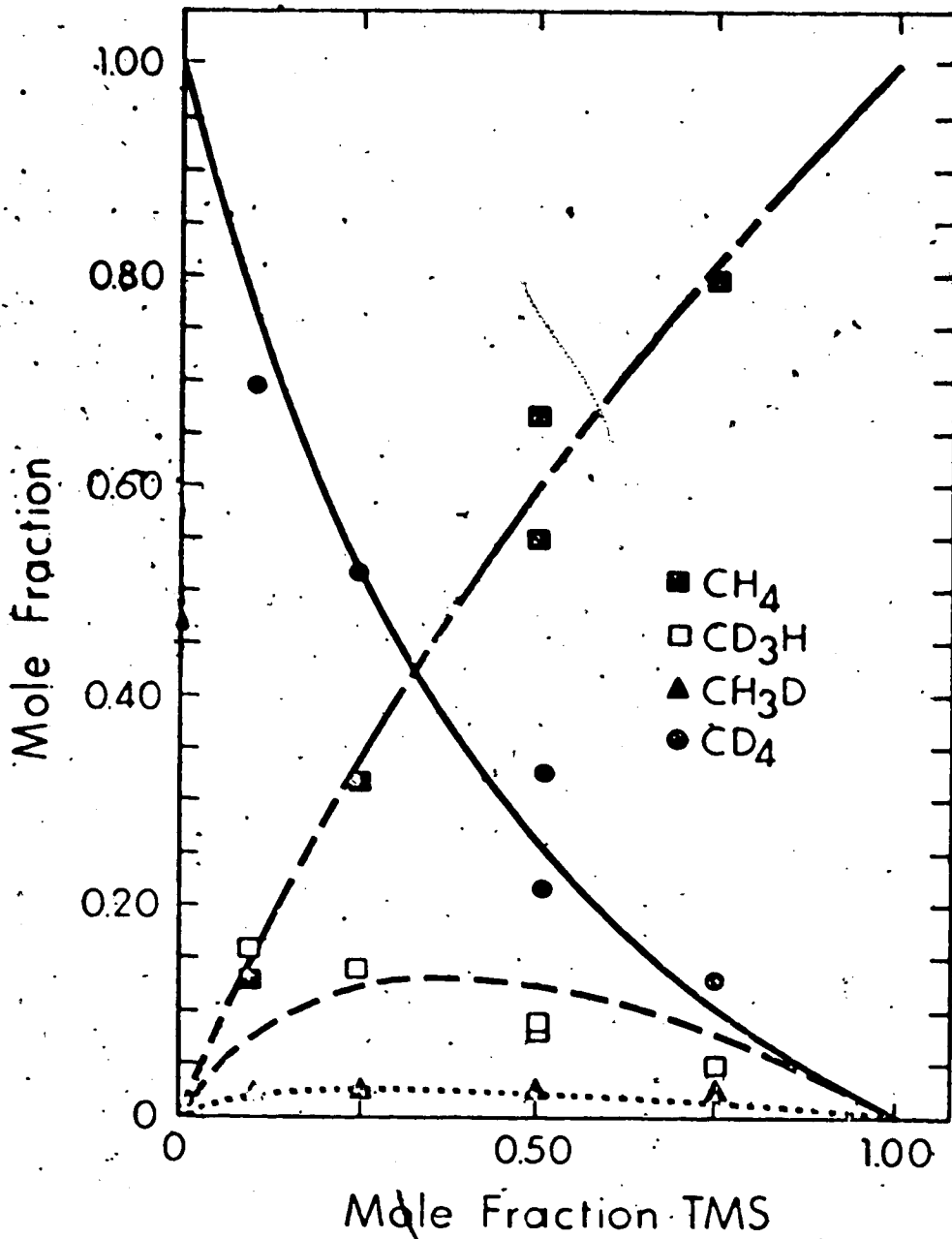
FIGURE III-12: Variation in Isotopic Methane Yield As A Function
Of Relative Amounts Of TMS and TMS-d_{12}.
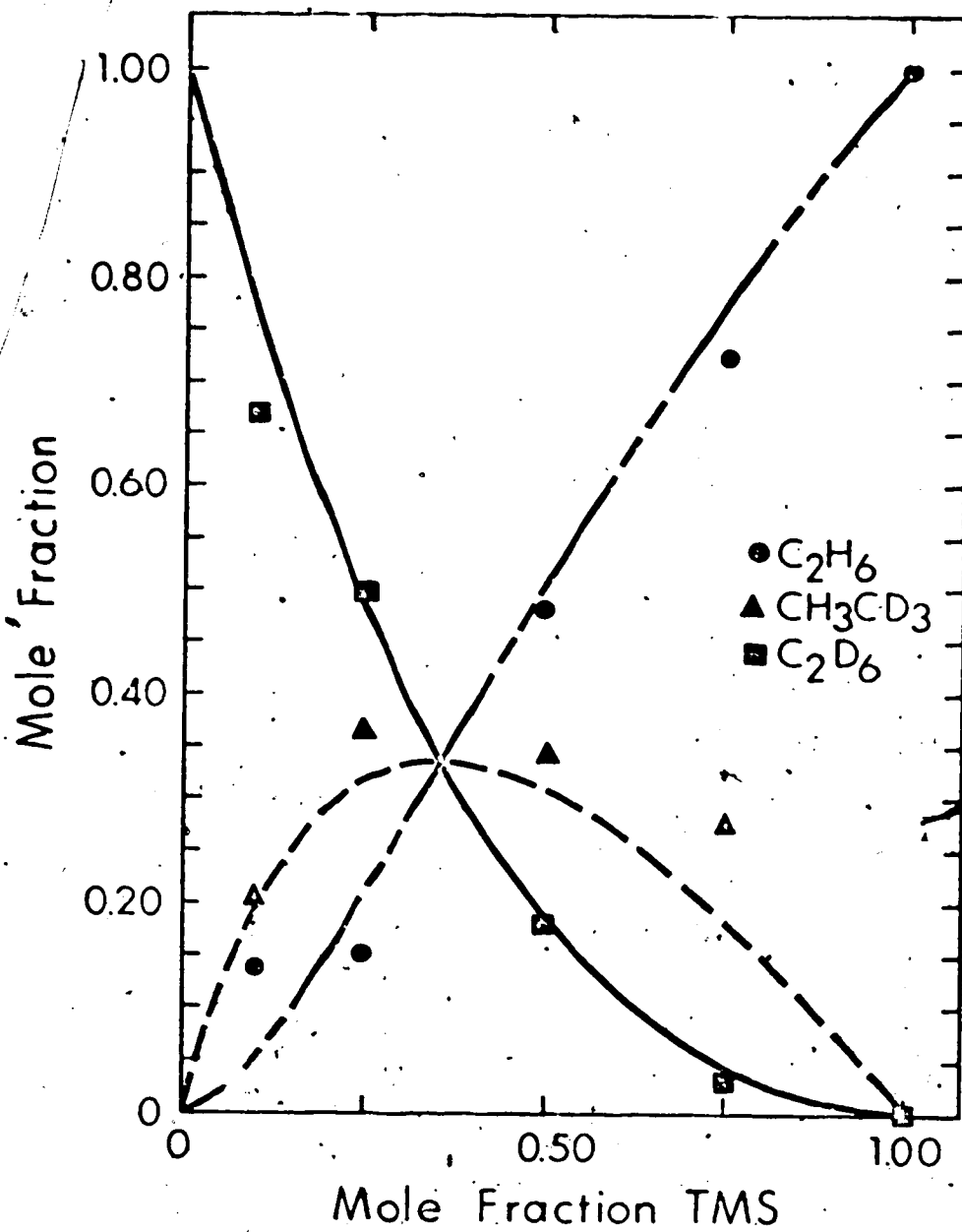
FIGURE III-13: Variation in Isotopic Ethane Yield As A Function
of Relative Amounts of TMS and TMS-d$_{12}$.

demonstrated for a number of saturated hydrocarbons[136-138].

This was carried out on dimethylsilane since the gas phase decomposition had been studied and the primary fragmentation processes elucidated[139].

The product yields were drastically reduced, with hydrogen and methane being measurable, and other products were obtained in such low yields that they were not readily identifiable on the gas chromatograph even with exposure times of two hours.

Different designs of cell and ░░░░░░ies were tried to optimize the yields and it is not clear at ░░░░░nt if the l░░░░ are due to geminate combination and disproportionation cage effects░░░ simple deactivation in the condensed phase or to differences in the absorption characteristics of the gas and condensed phases.

Results are shown in Table III-9 and Figure III-14 and extrapolated values give ϕ_{CH_4} = 0.045 and ϕ_{H_2} = 0.033 compared to gas phase values of ϕ_{CH_4} = 0.20 and ϕ_{H_2} = 0.90.

The project was discontinued at this point due to the experimental difficulties associated with measurement of products, percentage conversion and possible photolysis of products, and variation in lamp intensity over long periods of time.

C. Derivation of Mechanism

The photolysis of tetramethylsilane can proceed via a number of primary steps but with the preceding experimental evidence it is possible to deduce the most probable primary steps and calculate values for the primary quantum yields.

TABLE III-9

Quantum Yield as a Function of Exposure Time in the Condensed Phase Photolysis of Dimethylsilane

Time (mins)	ϕ_{H_2}	ϕ_{CH_4}	Phase
15	0.027	0.035	Solid
15	0.020	0.032	Solid
50	0.0	0.017	Liquid
60	0.008	0.015	Solid
90	0.007	0.001	Solid
120	0.007	0.013	Solid

Solid at -196°C

Liquid at -139°C
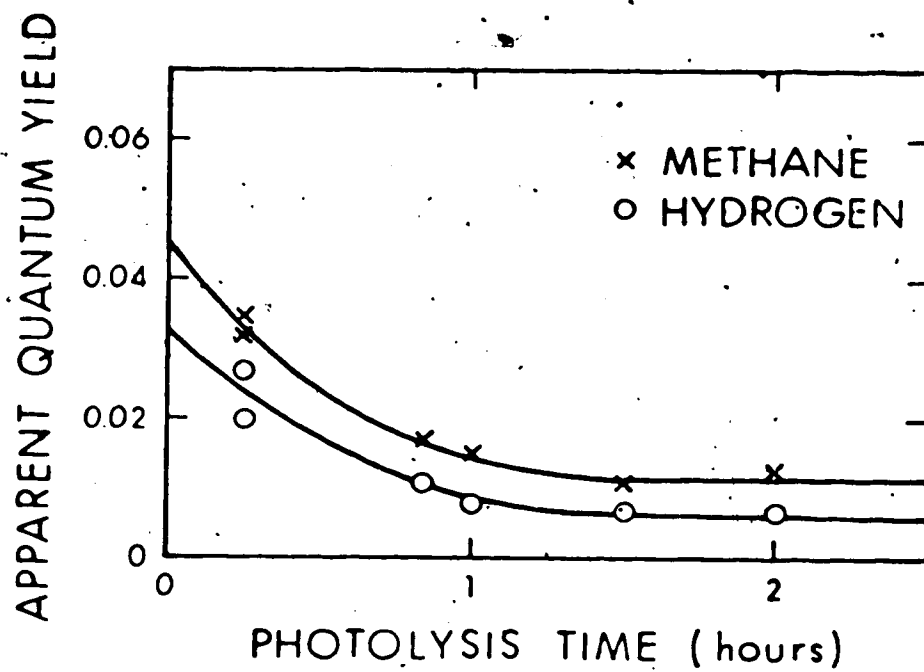
FIGURE III-14. Quantum Yields of Observable Products in the Condensed Phase Xenon Lamp Photolysis of Dimethylsilane.

The mechanism proposed should account for all the observed products as well as all the fragments from the primary photolysis steps.

The nitric oxide scavenging experiments showed that ethane, ethyldimethylsilane, hexamethyldisilane and the three other disilanes were formed by radical combination or abstraction and the radical yield required to bring about the observed products can be calculated from the product quantum yields (Table III-4). An extra significant figure is carried throughout the calculations to prevent round-up error and final results are reported with two significant figures.

Ethane can be obtained by the combination of methyl radicals,

$$CH_3 + CH_3 \longrightarrow C_2H_6 \tag{1}$$

or by abstraction by an ethyl radical from the substrate,

$$C_2H_5 + (CH_3)_4Si \longrightarrow C_2H_6 + CH_2Si(CH_3)_3 \tag{2}$$
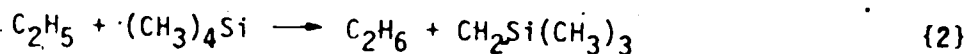
The presence of ethyl radicals in the system would lead to the following reactions

$$2C_2H_5 \longrightarrow n\text{-}C_4H_{10} \tag{3}$$
$$2C_2H_5 \longrightarrow C_2H_4 + C_2H_6 \tag{4}$$
$$C_2H_5 + CH_3 \longrightarrow C_3H_8 \tag{5}$$
$$C_2H_5 + CH_3 \longrightarrow CH_4 + C_2H_4 \tag{6}$$

The observed traces of propane and ethylene and the absence of n-butane indicate that ethyl radicals are probably present in the system but in very small amounts thus reaction {1} is the major source of ethane.

Since $\phi(1) = 0.350$ then from this step $\phi(CH_3) = 0.700$.

Hexamethyldisilane is formed by combination of two trimethylsilyl radicals.

$$2(CH_3)_3Si \longrightarrow (CH_3)_3SiSi(CH_3)_3 \qquad (7)$$
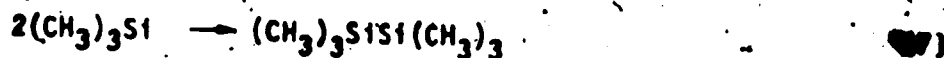
The possibility of dimethylsilylene insertion into substrate to form HMDS

$$(CH_3)_2Si + (CH_3)_4Si \longrightarrow (CH_3)_3SiSi(CH_3)_3 \qquad (8)$$
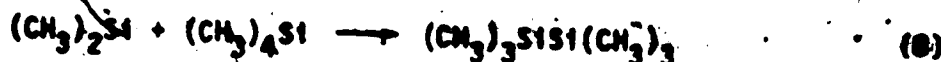
is ruled out because the yield of hexamethyldisilane is completely suppressed in the presence of nitric oxide. $\phi(7) = 0.095$ so the yield of trimethylsilyl radicals required is 0.190.

Ethyldimethylsilane is also wholly scavengeable and here we have more than one possible route of formation.

Simple radical cross-combination reactions such as

$$\cdot CH_3 + CH_2SiH(CH_3)_2 \longrightarrow C_2H_5SiH(CH_3)_2 \qquad (9)$$
$$C_2H_5 + SiH(CH_3)_2 \longrightarrow C_2H_5SiH(CH_3)_2 \qquad (10)$$
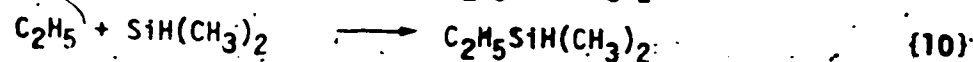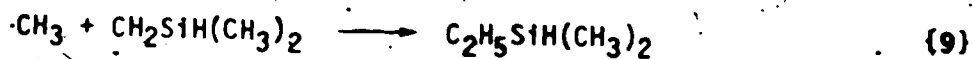
can be ruled out since there are no dimethylsilylmethyl or dimethylsilyl radicals in the system.

One possible route is via combination between a monoradical and a diradical, followed by abstraction from the substrate or another radical:

$$CH_3 + CH_2Si(CH_3)_2 \longrightarrow CH_3CH_2Si(CH_3)_2 \qquad (11)$$
$$C_2H_5Si(CH_3)_2 + (CH_3)_4Si \longrightarrow C_2H_5SiH(CH_3)_2 + CH_2Si(CH_3)_3 \qquad (12)$$
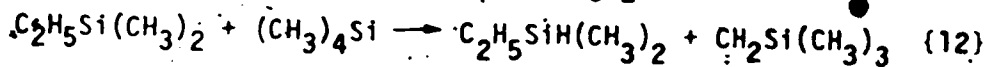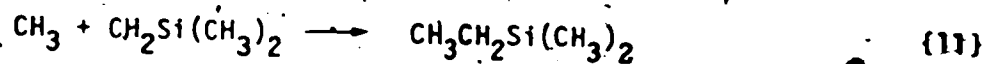
This reaction would be quite favourable if the diradical had a certain degree of π-stabilization (Chapter I, section E) since radical addition to a double bond is a very efficient reaction.

Another possibility is via rearrangement of a monoradical

$$\dot{C}H_2Si(CH_3)_3 \longrightarrow CH_3CH_2\dot{S}i(CH_3)_2 \qquad (13)$$

followed by abstraction (12), or disproportionation with another radical:

$$CH_3CH_2\dot{S}i(CH_3)_2 + \dot{S}i(CH_3)_3 \longrightarrow CH_3CH_2SiH(CH_3)_2 + \dot{C}H_2Si(CH_3)_3 \qquad (14)$$
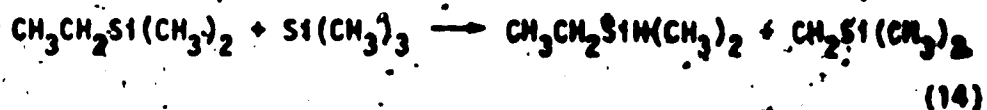
This possibility is more unlikely since radical rearrangements seem to require large activation energies. There is no good evidence for alkyl group migration in free radical isomerizations and even hydrogen transfer is difficult except from the carbon atom on the 4th, 5th or 6th position from the radical centre.[140] We cannot differentiate between these choices experimentally. If ethyldimethylsilane is formed exclusively via reactions (11) and (12), then since $\phi(12) = 0.050$ the yield of methyl radicals required from this step is also 0.050.

The three other disilanes are formed from reactions of the silyl radicals present in the system. It will be shown later that the major silyl monoradicals in the system are $(CH_3)_3\dot{S}i$ and $\dot{C}H_2Si(CH_3)_3$.

The disilane identified as trimethyldisilapentane could be formed by monoradical and diradical combination followed by abstraction from the substrate:

$$(CH_3)_3\dot{S}i + \dot{C}H_2Si(CH_3)_2 \longrightarrow (CH_3)_3SiCH_2\dot{S}i(CH_3)_2 \qquad (15)$$
$$(CH_3)_3SiCH_2\dot{S}i(CH_3)_2 + (CH_3)_4Si \longrightarrow (CH_3)_3SiCH_2SiH(CH_3)_2 + \dot{C}H_2Si(CH_3)_3 \qquad (16)$$
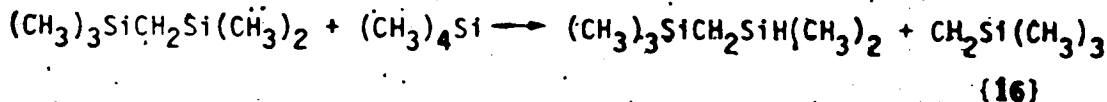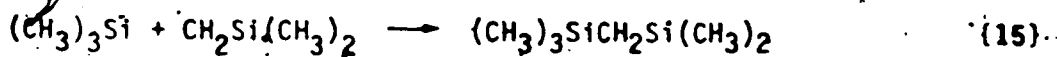
Once again, this could be interpreted as trimethylsilyl radical addition to a quasi double bond.

Tetramethyldisilapentane is formed by cross-combination between the two major silyl radicals:

$$(CH_3)_3Si + CH_2Si(CH_3)_3 \longrightarrow (CH_3)_3SiCH_2Si(CH_3)_3 \qquad \{17\}$$
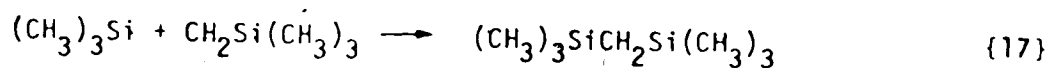
The combination of two trimethylsilylmethyl radicals would form tetramethyldisilahexane,

$$2(CH_3)_3SiCH_2 \longrightarrow (CH_3)_3SiCH_2CH_2Si(CH_3)_3 \qquad \{18\}$$
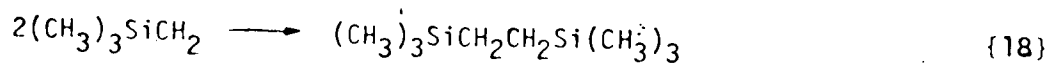
which was tentatively identified as one of the trace products.

Dimethyldisilahexane formation would seem to require combination of two diradicals followed by abstraction

$$2(CH_3)_2SiCH_2 \longrightarrow (CH_3)_2SiCH_2CH_2Si(CH_3)_2 \qquad \{19\}$$

$$(CH_3)_2SiCH_2CH_2Si(CH_3)_2 + 2(CH_3)_4Si \longrightarrow (CH_3)_2SiHCH_2CH_2SiH(CH_3)_2$$
$$+ 2CH_2Si(CH_3)_3 \qquad \{20\}$$
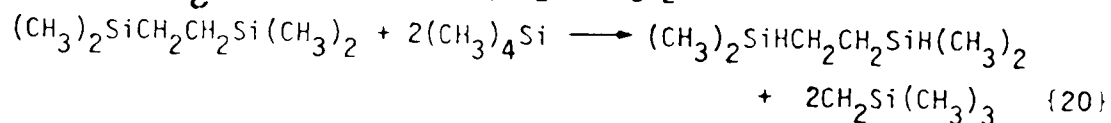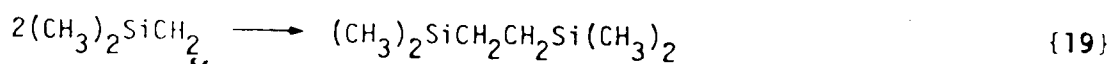
Formation of the disilanes requires a trimethylsilyl radical yield of $\phi\{16\} + \phi\{17\} = 0.055$.

About 30% of the yield of trimethylsilane is unscavengeable in the presence of nitric oxide and this can be formed in a primary step:

$$(CH_3)_4Si \longrightarrow CH_2 + (CH_3)_3SiH \qquad \{21\}$$
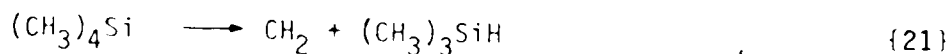
Elimination of carbene has been found to occur in other silyl and alkyl systems. $\phi(\text{Tri-MS}) = 0.135$ so $\phi\{21\} = 0.040$.

It will be shown later that disproportionation of trimethylsilyl radicals is a minor process with $k_d/k_c = 0.04$ (Chapter IV). Thus the yield of trimethylsilane from disproportionation would be 0.04 x 0.095 = 0.004.

$$2(CH_3)_3Si \longrightarrow (CH_3)_3SiH + CH_2Si(CH_3)_2 \qquad \{22\}$$
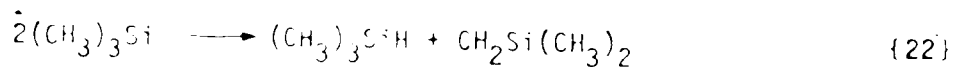
The rest of the trimethylsilane is possibly formed by abstraction by trimethylsilyl radicals from the substrate:

$$(CH_3)_3Si \cdot + (CH_3)_4Si \longrightarrow (CH_3)_3SiH + CH_2Si(CH_3)_3 \qquad \{23\}$$
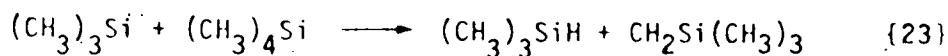
$\phi\{23\} = 0.135 - 0.040 - .004 = 0.091$.

The non-scavengeable yield of ethyltrimethylsilane could be obtained by insertion of carbene into a substrate molecule,

$$CH_2 + (CH_3)_4Si \longrightarrow C_2H_5Si(CH_3)_3 \qquad \{24\}$$
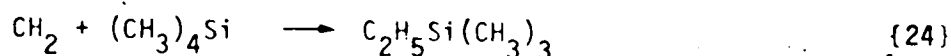
$\phi\{24\} = 0.042 \times 0.5 = 0.021$.

The remainder of the carbene may also insert into the substrate but the product may decompose following the highly exothermic insertion process[141,142]. This decomposition could lead to the traces of ethylene found in the system:

$$CH_2 + (CH_3)_4Si \longrightarrow C_2H_5Si(CH_3)_3^*$$
$$C_2H_5Si(CH_3)_3^* \xrightarrow{+M} C_2H_5Si(CH_3)_3$$
$$\longrightarrow C_2H_4 + (CH_3)_3SiH$$
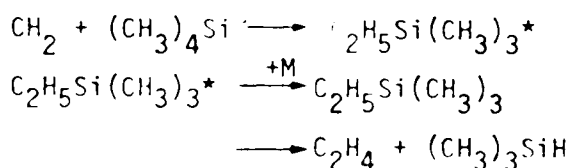
The remainder of the ethyltrimethylsilane must form by monoradical reactions. The major source is most likely methyl radical and trimethyl-silylmethyl radical combination,

$$CH_3 + CH_2Si(CH_3)_3 \longrightarrow C_2H_5Si(CH_3)_3 \qquad \{25\}$$
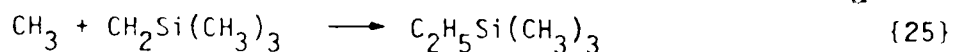
although a small amount may be formed from ethyl radicals

$$C_2H_5 + Si(CH_3)_3 \longrightarrow C_2H_5Si(CH_3)_3 \qquad \{26\}$$
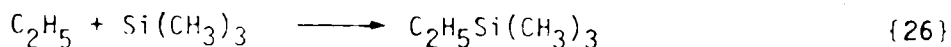
Since the amount of ethyl radicals present in the system has been shown to be small (reactions {3} - {6}) we will discount {26} thus ϕ{25} = 0.042 - 0.021 = 0.021.

The modes of formation of hydrogen and methane were determined from the results of the isotopic labelling study. Ethane has already been shown to be formed entirely by radical combination but it was also measured in the isotopic labelling study since the yield of methyl radicals is related to the yield of methane and of ethane.

Both hydrogen and methane could be produced in primary molecular elimination steps,

$$(CH_3)_4Si \xrightarrow{h\nu} H_2 + (CH)Si(CH_3)_3 \qquad \{27\}$$

$$\xrightarrow{} CH_4 + CH_2Si(CH_3)_2 \qquad \{28\}$$
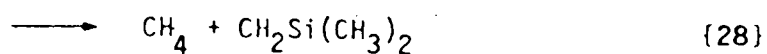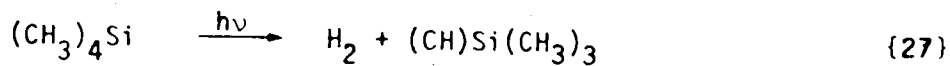
as well as by radical producing steps followed by abstraction from the substrate:

$$(CH_3)_4Si \xrightarrow{h\nu} CH_3 + Si(CH_3)_3 \qquad \{29\}$$

$$\xrightarrow{} 2CH_3 + Si(CH_3)_2 \qquad \{30\}$$

$$\xrightarrow{} H + CH_2Si(CH_3)_3 \qquad \{31\}$$

$$\xrightarrow{} H + CH_3 + CH_2Si(CH_3)_2 \qquad \{32\}$$
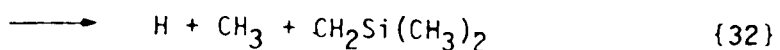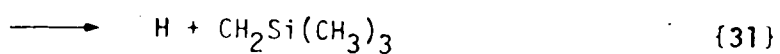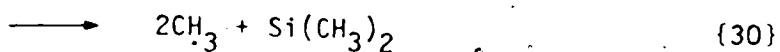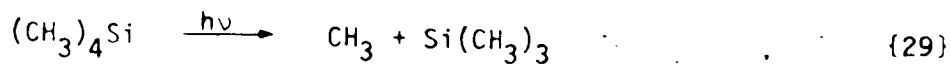
Kinetic schemes for the formation of the different isotopic yields of hydrogen, methane and ethane were drawn up omitting the silicon fragment for clarity.

The primary production of hydrogen is given by

$$TMS-d_{12} + h\nu \xrightarrow{1} [TMS-d_{12}]^* \qquad \{33\}$$

$$[TMS-d_{12}]^* \xrightarrow{2} D_2 \qquad \{34\}$$

$$\xrightarrow{3} D \qquad \{35\}$$

$$\text{TMS} + h\nu \xrightarrow{\ 4\ } [\text{TMS}]^* \qquad \{36\}$$

$$[\text{TMS}]^* \xrightarrow{\ 5\ } H_2 \qquad \{37\}$$

$$\xrightarrow{\ 6\ } H \qquad \{38\}$$
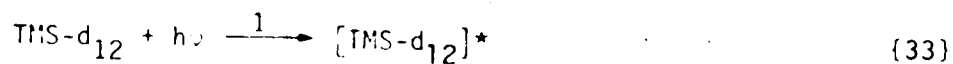
The resulting hydrogen atoms can then abstract from substrate molecules in the following manner:

$$H + \text{TMS} \xrightarrow{\ 7\ } H_2 \qquad \{39\}$$

$$H + \text{TMS-d}_{12} \xrightarrow{\ 8\ } HD \qquad \{40\}$$

$$D + \text{TMS} \xrightarrow{\ 9\ } HD \qquad \{41\}$$

$$D + \text{TMS-d}_{12} \xrightarrow{\ 10\ } D_2 \qquad \{42\}$$
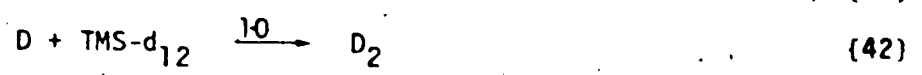
It has been shown in the photolysis of dimethylsilane[139] that exchange reactions of the type

$$H + \text{TMS-d}_{12} \longrightarrow D \qquad \{43\}$$

$$D + \text{TMS} \longrightarrow H \qquad \{44\}$$

$$H + \text{TMS-d}_{12} \longrightarrow CD_3 \qquad \{45\}$$

$$D + \text{TMS} \longrightarrow CH_3 \qquad \{46\}$$

were unimportant so these have been ignored.

A similar kinetic scheme can be drawn up for the production of methane and ethane.

$$\text{TMS} + h\nu \xrightarrow{\ 1\ } [\text{TMS}]^* \qquad \{47\}$$

$$[\text{TMS}]^* \xrightarrow{\ 2\ } CH_4 \qquad \{48\}$$

$$\xrightarrow{\ 3\ } CH_3 \qquad \{49\}$$

$$\text{TMS-d}_{12} + h\nu \xrightarrow{\ 4\ } [\text{TMS-d}_{12}]^* \qquad \{50\}$$

$$[\text{TMS-d}_{12}]^* \xrightarrow{\ 5\ } CD_4 \qquad \{51\}$$

$$\xrightarrow{\ 6\ } CD_3 \qquad \{52\}$$
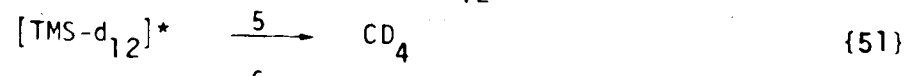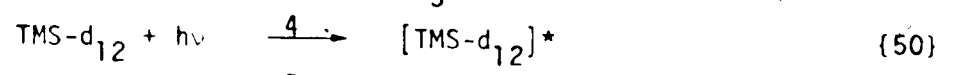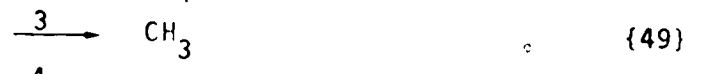
Steps {49} and {52} are meant to summarize the production of methyl radicals as shown in steps {29}, {30} and {32}.

The radicals so produced can react in the following ways:

$$CH_3 + TMS \xrightarrow{7} CH_4 \qquad \{53\}$$

$$CH_3 + TMS\text{-}d_{12} \xrightarrow{8} CH_3D \qquad \{54\}$$

$$CD_3 + TMS \xrightarrow{9} CD_3H \qquad \{55\}$$

$$CD_3 + TMS\text{-}d_{12} \xrightarrow{10} CD_4 \qquad \{56\}$$

$$CH_3 + CH_3 \xrightarrow{11} C_2H_6 \qquad \{57\}$$

$$CH_3 + CD_3 \xrightarrow{12} CH_3CD_3 \qquad \{58\}$$

$$CD_3 + CD_3 \xrightarrow{13} C_2D_6 \qquad \{59\}$$
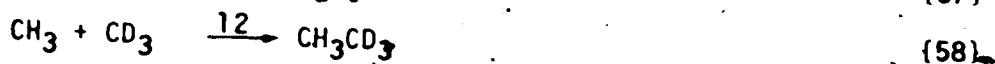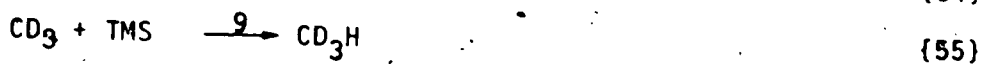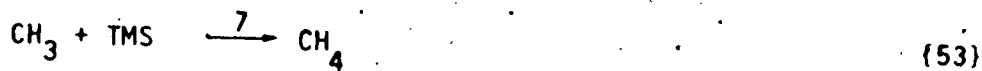
The best method of treatment of this kinetic scheme was found to be computer simulation of the experimental data using iterative numerical integration, varying the relative rate constants for each step until a good fit was obtained. Many of the relative rate constants are not known but fortunately the simulated fit was sensitive to some of the rate constants and relatively insensitive to others. The formation of ethane was used as an internal check in that the total yields of methane and ethane had to give the observed product ratio. Reactions of methyl radicals with other radicals in the system were regarded as minor processes and were omitted to simplify the treatment.

Relative rate constant values used in the calculations are given in Table III-10 and the solid line computer fit to the experimental points is shown on Figures III-11, III-12 and III-13. The values used in the computer analysis were obtained partly from experimental data, partly by comparative assumptions of the most reasonable values and partly dictated by the values required to obtain computer matching to the

TABLE III-10

Relative Rate Constant Values Used In Iterative

Numerical Integration

Rate Constant	A. Hydrogen Analysis	B. Methane/Ethane Analysis
k_1	1.9	2.0
k_2	1.0×10^{-3}	1.5×10^{-1}
k_3	1.0×10^{-1}	8.5×10^{-1}
k_4	1.7	2.1
k_5	3.0×10^{-2}	9.0×10^{-2}
k_6	3.0×10^{-1}	4.5×10^{-1}
k_7	3.0×10^{-2}	1.0×10^{-1}
k_8	3.0×10^{-4}	1.0×10^{-2}
k_9	2.2×10^{-2}	1.0×10^{-1}
k_{10}	2.0×10^{-4}	1.0×10^{-2}
k_{11}	-	9.0×10^{3}
k_{12}	-	9.0×10^{3}
k_{13}	-	9.0×10^{3}

experimental cases.

For the hydrogen scheme k_1/k_4 was taken as 1.13 from the experimental yields of hydrogen produced by photolysis of tetramethylsilane and per-deuterated tetramethylsilane in separate experiments. The values of k_2/k_3 and k_5/k_6 must be extracted from the simulation. We set $k_7/k_8 = k_9/k_{10}$, assuming that the isotope effect for abstraction is independent of the attacking species. It was found that the isotope effect k_7/k_8 could be varied slightly in conjunction with the ratio of molecular to radical elimination, k_5/k_6, thus we have a range of values which are usable, from 10-20% for the yield of molecular H_2 and an isotope effect of 3-10. A reasonable average from these results would give a yield of 15% for molecular H_2 using an isotope effect of 5.

For the methane/ethane scheme k_1/k_4 was set from experimental results at 0.95. Again, k_2/k_3 and k_5/k_6 are the unknown values. To a first approximation we set $k_7/k_8 = k_9/k_{10}$ and $k_{11} = k_{12} = k_{13}$. Again it was found that the isotope effect k_7/k_8 could be varied slightly along with k_2/k_3 to obtain the desired result, thus giving us a range of values of 15-20% for the molecular CH_4 yield with a kinetic isotope effect for abstraction of 3-10. Choosing a value of 5 gives us the molecular CH_4 yield at 15%. One of the results of this simulation is that the rate constants for abstraction by methyl radicals are only four orders of magnitude less than the value for the combination of methyl radicals. This is five orders of magnitude faster than expected since the room temperature rate constant for methyl attack on tetramethyl-silane has been measured and found to be nine orders of magnitude less than that for methyl radical combination. The implication is that hydrogen abstraction is a lot easier than expected either because the methyl

radicals contain a considerable amount of excess energy or possibly that hydrogen is abstracted from other radicals in the system.

Cross-combination and disproportionation of methyl and tri-methylsilyl radicals in the system

$$CH_3 + Si(CH_3)_3 \longrightarrow (CH_3)_4Si \tag{60}$$

$$(CH_3) + Si(CH_3)_3 \longrightarrow CH_4 + CH_2Si(CH_3)_2 \tag{61}$$
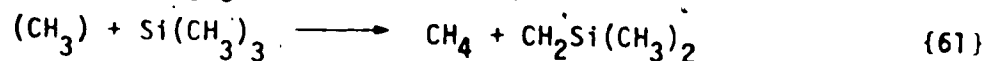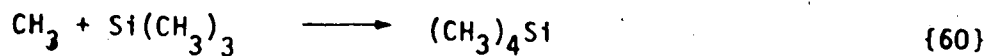
may well account for an appreciable amount of the methane and reaction {61} could be facilitated by the apparent stability of the silicon diradical.

From the results it was found that about 15% of the hydrogen yield arises from molecular elimination,

$$(CH_3)_4Si \xrightarrow{h\upsilon} H_2 + CHSi(CH_3)_3 \tag{62}$$
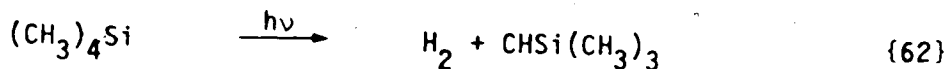
and the rest by hydrogen atom formation followed by abstraction

$$(CH_3)_4Si \xrightarrow{h\upsilon} H + CH_2Si(CH_3)_3 \tag{63}$$

$$\xrightarrow{h\upsilon} H + CH_3 + CH_2Si(CH_3)_2 \tag{64}$$

$$H + (CH_3)_4Si \longrightarrow H_2 + CH_2Si(CH_3)_3 \tag{65}$$
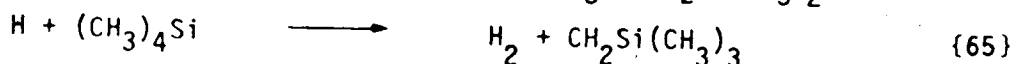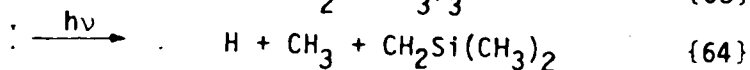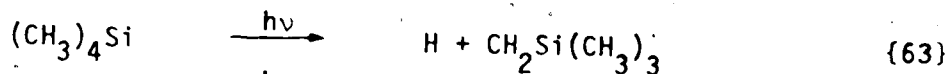
It has been shown in the photolysis of simple alkanes[143] and alkylsilanes[93,139] that single hydrogen atom loss is always a very minor process so reaction {63} has been omitted in favour of reaction {64}. Thus $\phi\{62\} = 0.122 \times 0.15 = .018$ and $\phi\{64\} = 0.122 - .018 = 0.104$. The methane/ethane results show that molecular methane formation accounts for ca. 15% of the total methane and methyl radical production. From the preceeding steps we require a methyl radical yield of $2\phi\{1\} + \phi\{12\} + \phi\{25\} = 0.700 + 0.050 + 0.021 = 0.771$ and we know

that $\phi(CH_4) = 0.330$. Therefore

$$\frac{15}{85} = \frac{\phi[CH_4 \text{ total}] - \phi[CH_4 \text{ abstraction}]}{\phi[CH_3 \text{ total}] + \phi[CH_4 \text{ abstraction}]}$$

$$\frac{15}{85} = \frac{0.330 - \phi[CH_4 \text{ abs}]}{0.771 + \phi[CH_4 \text{ abs}]}$$

Therefore, $\phi[CH_4 \text{ abs}] = 0.165$, and

$$\phi[CH_4 \text{ molecular}] = 0.330 - 0.165$$
$$= 0.165$$

Approximately 50% of the methane is formed in a molecular elimination reaction

$$(CH_3)_4Si \longrightarrow CH_4 + CH_2Si(CH_3)_2 \qquad \{66\}$$
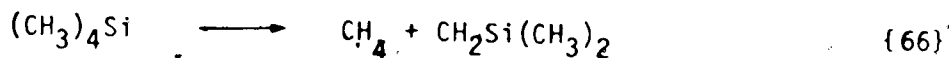
while the rest forms by methyl radical abstraction.

The sum of methyl radicals in the system is now $0.771 + 0.165 = 0.936$ and there are three major processes which can produce primary methyl radicals:

$$(CH_3)_4Si + h\nu \longrightarrow CH_3 + Si(CH_3)_3 \qquad \{67\}$$
$$\longrightarrow 2CH_3 + Si(CH_3)_2 \qquad \{68\}$$
$$\longrightarrow CH_3 + H + CH_2Si(CH_3)_2 \qquad \{69\}$$
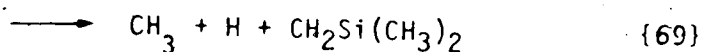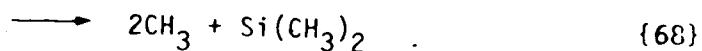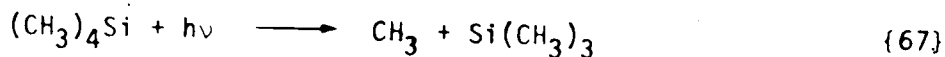
It was not possible to discriminate between the first two steps since the silylene and possibly some of the trimethylsilyl radical will polymerize and be removed from the system. However, a probable scheme can be drawn up to account for all of the secondary products and most of the primary products and fragments. Since the

auxiliary study showed that the quantum yield of fluorescence was less than 0.01, we assumed that the primary quantum yield in our system was 1.00 and apportioned the methyl radical producing steps accordingly. This low fluorescence quantum yield is in line with the values obtained for simple alkanes[144] and for both types of saturated system it seems reasonable that the lower excited states are either unbound or strongly coupled with a dissociative surface.

So far we have a primary quantum yield of $\phi\{21\}$ + $\phi\{62\}$ + $\phi\{64\}$ + $\phi\{66\}$ = 0.040 + 0.018 + 0.104 + 0.165 = 0.327. Thus the remaining primary steps should account for 0.673 of the primary quantum yield, while at the same time they must give a methyl radical yield of 0.936 - 0.104 = 0.832.

i.e. $\phi\{67\}$ + $\phi\{68\}$ = 0.673

$\phi\{67\}$ + $2\phi\{68\}$ = 0.832

Solving these equations gives $\phi\{68\}$ = 0.159 and $\phi\{67\}$ = 0.514.

However it is possible to obtain somewhat different values for $\phi\{67\}$ and $\phi\{68\}$ if we assume that cross-combination and disproportionation does take place between methyl and trimethylsilyl radicals (reactions { 60 }, { 61 }). This postulate might give more likely primary quantum yields for production of methyl radicals while simultaneously accounting for the trimethylsilyl radical yield. We first have to make a reasonable estimate of the k_d/k_c ratio for cross-reaction of methyl and trimethylsilyl radicals and we have chosen a value of 0.1.

Then from the yields of products

$$\phi((CH_3)_3Si) = 2\phi\{7\} + \phi\{15\} + \phi\{17\} + 2\phi\{22\} + \phi\{23\} + \phi\{60\} + \phi\{61\}$$

$$= 2(0.095) + (0.038) + (0.017) + (0.008) + (0.001)$$

$$+ 1.\blacksquare\}$$

$$= 0.344 + 1.1\phi\{60\}.$$

$$\phi(CH_3) \quad = 2\phi\{1\} + \phi\{12\} + \phi\{25\} + 0.165 + \phi\{60\}$$

$$= 0.700 + 0.050 + 0.021 + 0.165 + \phi\{60\}$$

$$= 0.936 + \phi\{60\}.$$

Primary step 4 accounts for some of the methyl radicals so from primary steps 1 and 2 we require a methyl radical yield of $0.936 + \phi\{60\} - 0.104 = 0.832 + \phi\{60\}$.

Since the sum of primary quantum yields $\{67\}$ and $\{68\}$ amounts to 0.673 and the yield of $(CH_3)_3Si$ radicals will come from $\{67\}$ while the yield of methyl radicals is given by $\phi\{67\} + 2\phi\{68\}$ we have

$$\phi((CH_3)_3Si) + \phi(CH_3) = \phi\{67\} + \phi\{67\} + 2\phi\{68\}$$

$$= 2(\phi\{67\} + \phi\{68\})$$

$$= 2(0.673)$$

$$= 1.346.$$

i.e. $0.344 + 1.1\phi\{60\} + 0.832 + \phi\{60\} = 1.346$

$$\phi\{60\} = 0.081$$

Then $\phi\{67\} = 0.344 + 1.1\phi\{60\}$

$$= 0.344 + 0.089$$

$$= 0.433.$$

and $\phi\{68\} = 0.673 - 0.433$

$$= 0.240$$

So we can obtain a slightly different set of primary quantum yields (ϕ_B) if we assume methyl and trimethylsilyl cross-reaction.

The primary quantum yields so obtained are summarized in Table III-11.

D. DISCUSSION

From the data presented it can be seen that the primary decomposition is a multi-step process resulting in a variety of possible final products. Carbon-silicon bond cleavage accounts for ~77% of the decomposition, the rest being carbon-hydrogen cleavage. Decomposition involves both molecular elimination (18%) of methane and hydrogen and radical formation (82%) of methyl radicals and hydrogen atoms, with the silane fragments left behind being monoradicals or diradicals. A minor process is the production of methylene. Combination of radicals and abstraction by radicals from substrate or other radicals result in the observed products. Most of the diradicals and silylene go to form the silicon polymer.

The primary steps chosen are only a few of the many that are allowable on thermochemical grounds. Steps which involved the breaking of three bonds were discounted on statistical grounds since such a simultaneous accumulation of energy in three bonds is not very probable. Also, the loss of a single hydrogen atom has been shown to be very unlikely in the photolysis of hydrocarbons at 1470Å. The excess energy which would be left in the parent molecule and the exothermicity associated with the formation of the hydrogen molecule presumably are enough to eliminate this possibility.

TABLE III-11

Summary of Primary Quantum Yields in the Photolysis of Tetramethylsilane

		ϕ_A	ϕ_B
$(CH_3)_4Si + h\nu \xrightarrow{\ 1\ } CH_3 + Si(CH_3)_3 \cdot$		0.51	0.43
$\xrightarrow{\ 2\ } 2CH_3 + Si(CH_3)_2$		0.16	0.24
$\xrightarrow{\ 3\ } CH_4 + CH_2Si(CH_3)_2$		0.17	0.17
$\xrightarrow{\ 4\ } CH_3 + H + CH_2Si(CH_3)_2$		0.10	0.10
$\xrightarrow{\ 5\ } H_2 + CHSi(CH_3)_3$		0.02	0.02
$\xrightarrow{\ 6\ } CH_2 + (CH_3)_3SiH$		0.04	0.04
		1.00	1.00

ϕ_A: assuming cross-disproportionation does not occur.

ϕ_B: assuming a k_d/k_c ratio of 0.1 for methyl and trimethylsilyl radical cross-reaction.

However, it is impossible to discriminate between parallel primary steps and secondary decompositions of excited fragments.

For example, steps (29) and (30) could be occurring in sequence,

$$(CH_3)_4Si \longrightarrow CH_3 + Si(CH_3)_3^* \qquad (70)$$

$$Si(CH_3)_3^* \longrightarrow CH_3 + Si(CH_3)_2 \qquad (71)$$
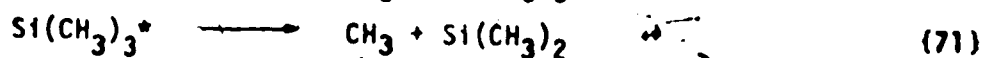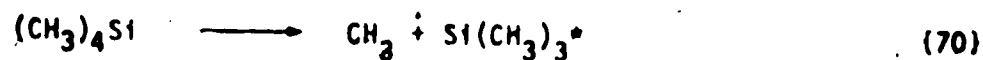
since the silicon fragment in (70) could be carrying as much as 120 kcal mole^{-1} of excess energy. This excited fragment could also be stabilized by losing hydrogen

$$(CH_3)_3Si^* \longrightarrow H + CH_2Si(CH_3)_2 \qquad (72)$$
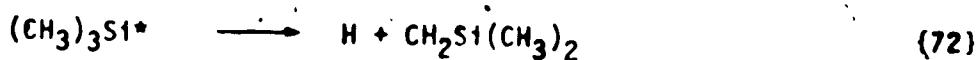
so that the combination of steps (70) and (72) could account for primary step (64).

From the chosen mechanism it can be calculated that approximately 52% of the silicon fragments will form polymer. We can check the validity of the scheme by trying to account for the fate of all the primary products and the modes of formation of final products. The major primary products of photolysis were $\phi(CH_3)$ = 0.936, $\phi(Si(CH_3)_3)$ = 0.514, $\phi(CH_2Si(CH_3)_2)$ = 0.269, $\phi(CH_4)$ = 0.165, $\phi(Si(CH_3)_2)$ = 0.159, $\phi(H)$ = 0.104. The methyl radicals combine to form ethane and also can combine with other radicals in the system. A secondary radical likely to be present in the photolysis is the trimethylsilylmethyl radical, $CH_2Si(CH_3)_3$, obtained by hydrogen atom attack on the substrate, thus $\phi(CH_2Si(CH_3)_3)$ = 0.104 and this can react with other radicals in the system, e.g.

$$CH_3 + CH_2Si(CH_3)_3 \longrightarrow C_2H_5Si(CH_3)_3 \qquad (73)$$
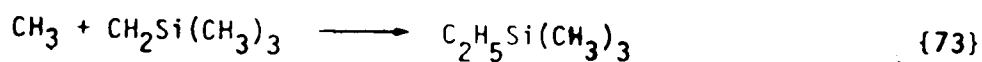
The formation of methane from methyl radicals has been shown to be much faster than expected, indicating that either the activation energy for this process is lowered in some way, or that a disproportionation

reaction of methyl radicals with other larger radicals in the system is occurring.

$$CH_3 + Si(CH_3)_3 \longrightarrow CH_4 + CH_2Si(CH_3)_3 \qquad \{74\}$$
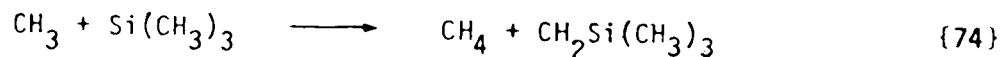
Note also that in this case simple combination would give back substrate

$$CH_3 + Si(CH_3)_3 \longrightarrow (CH_3)_4Si \qquad \{75\}$$
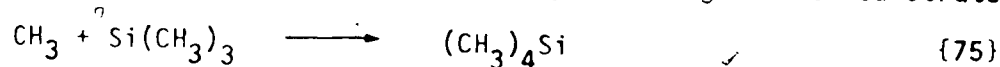
The occurrence of reaction {75} would require changes in primary steps {1} and {2} to produce more methyl radicals as in i_B.

The rate of cross-disproportionation of methyl and t-butyl radicals has been shown to be comparable with that of combination $(k_d/k_c = 0.85)$[59].

$$CH_3 + C(CH_3)_3 \longrightarrow CH_4 + CH_2=C(CH_3)_2 \qquad \{76\}$$
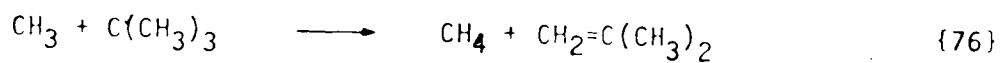
However, the driving force in this reaction to form a stable olefin is not as strong, or at least is only partially present in the silicon radical case. The extent of the double bond in the dimethyl-silylmethyl diradical has been discussed in many reports (Chapter I, section E) and there does appear to be some olefinic behaviour, giving appreciable stability to the diradical.

Very few values are available for k_d/k_c ratios for silyl radicals so no accurate estimation can be made of the extent of participation of this type of reaction in the system. The trimethylsilyl radicals can dimerize or combine with other radicals in the system. This accounts, however, for only 48 of the yield of this radical. Formation of trimethylsilane is 70 scavengeable by nitric oxide and its mode of formation would appear to be via hydrogen abstraction by the trimethylsilyl radical from the substrate, accounting for another 18 of these radicals. This is an unfavourable process with a high activation energy (probably 12 kcals/mole) and would seem to be unlikely unless it is possible that

enough of the excess energy could be located in the appropriate vibrational modes to effectively lower the activation energy for abstraction.

A more probable route is from disproportionation of silyl radicals, a process requiring little, if any, activation energy.

As will be shown later, the room temperature k_d/k_c ratio for trimethylsilyl radicals was found to be 0.04 but perhaps in this system, with more excess energy being available, disproportionation is more favourable. If all of the bimolecularly formed trimethylsilane came from disproportionation this would give a k_d/k_c ratio of 0.5.

In addition, if the bimolecularly formed methane comes from cross-disproportionation of methyl and trimethylsilyl radicals this would account for some 98% of the trimethylsi⁷ ⁻ₗ als in the system and give a diradical $CH_2Si(CH_3)_2$ yield of 0.26 ⁻ ≮5 + 0.095 = 0.529. About 0.114 of this yield ends up as retrievable products and hence the remainder, 0.415, polymerizes.

This together with the amounts of dimethylsilylene and trimethylsilylmethyl radicals produced gives a polymer yield of some 58%, in close agreement with the experimentally obtained value of 53%.

It is also possible as demonstrated on Table III-11 to obtain a slightly different set of primary quantum yield values if we accept cross-reaction of methyl and trimethylsilyl radicals (ϕ_B). In this scheme all of the trimethylsilyl radicals are accounted for and about 10% of the methyl radicals are supposed lost in reformation of substrate.

If the trimethylsilyl radical were to take part in other reactions such as more self-disproportionation or cross-disproportionation with tr⁻ethylsilylmethyl radicals then (1) would be somewhat higher so perhaps a value somewhere between ϕ_A and ϕ_B would be most

appropriate.

The fate of the trimethylsilylmethyl radical, produced by hydrogen atom abstraction, is only accounted for in part (36%) by combination with methyl or trimethylsilyl radicals. This radical, too, could cross-disproportionate with trimethylsilyl radicals.

$$(CH_3)_3SiCH_2 + (CH_3)_3Si \longrightarrow (CH_3)_4Si + CH_2Si(CH_3)_2 \qquad \{77\}$$
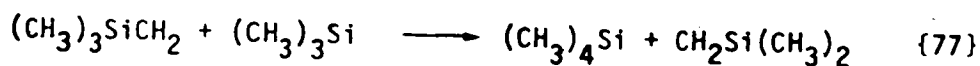
Thus, disproportionation appears to be an important feature of the overall mechanism.

The silylene formed, as was expected[70,145-148], does not insert into either C-H or Si-C bonds and so with no other route of reaction it would polymerize.

The carbene formed in step {62} does not appear to insert into the substrate, however, its yield is very small and possible products may not have been measurable.

Comparing the results from the 147 nm photolysis of the three methylated silanes, monomethyl-[93], dimethyl-[94] and tetramethylsilane, we can see various similarities and differences as a consequence of the varying relative amounts of carbon-hydrogen, silicon-hydrogen and silicon-carbon bonds in these molecules.

The window in the absorption spectrum of tetramethylsilane in the vicinity of 150 nm, which is absent in the other silanes, indicates that the main absorber in this region is the Si-H bond[77]. This is supported by the results from the photolysis of monomethyl-silane where 66% of the bond breakage is from the Si-H bonds although they are some 5 - 10 kcals/mole stronger than the Si-C bond. Similarly in dimethylsilane Si-H cleavage accounts for 43% with the remainder

divided between C-H (29%) and Si-C (28%). In the tetramethylsilane case, Si-C cleavage accounts for 77% of the bonds broken but whether this is due to absorption in the Si-C bond or decomposition of the weakest bond is not clear. It is also not evident at this point how much secondary decompositions contribute to each type of cleavage but in the tetramethylsilane case about half of the C-H cleavage occurs in the molecular formation of methane.

The yield of molecular products decreases from 71% in mono-methylsilane to 22% in tetramethylsilane.

It is very difficult to correlate the primary processes involved with specific optical transitions, even if these were known, because the amount of excess energy available is much larger than the critical energy requirements of some of the primary processes. This complicates the elucidation of two-fragment and three-fragment processes since it is impossible to unambiguously define whether a three-fragment process is a parallel primary reaction or whether it arises from the secondary decomposition of energy rich fragments formed in a two-fragment primary step.

In both monomethylsilane and tetramethylsilane two fragment pro-cesses account for some 70-75% of the decomposition (this drops to 65% for ϕ_B) whereas this decreases to 50% in dimethylsilane, perhaps indicating that in the latter case more of the multifragmentation processes should be redefined as two-fragment steps followed by secondary decomposition.

The mechanism of nitric oxide scavenging is very complex and not completely understood but it appears that the products retain the integrity of the monoradicals present in the system. Insertion reactions and molecular products are not affected by nitric oxide.

As has been shown previously[13] nitric oxide and silyl radicals react by forming a Si-O bond,

$$(CH_3)_3Si + NO \longrightarrow [(CH_3)_3SiON] \qquad \{78\}$$
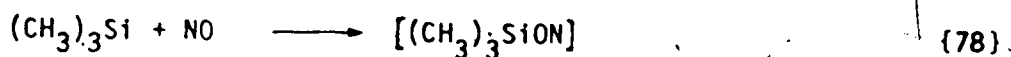
and this intermediate can undergo further reactions

$$(CH_3)_3SiON + NO \longrightarrow (CH_3)_3SiONNO \qquad \{79\}$$

$$(CH_3)_3SiONNO \longrightarrow (CH_3)_3SiO + N_2O \qquad \{80\}$$

$$2(CH_3)_3SiON \longrightarrow (CH_3)_3SiONNOSi(CH_3)_3 \qquad \{81\}$$

$$(CH_3)_3SiONNOSi(CH_3)_3 \longrightarrow 2(CH_3)_3SiO + N_2 \qquad \{82\}$$
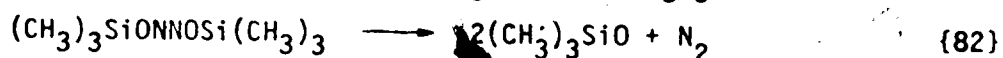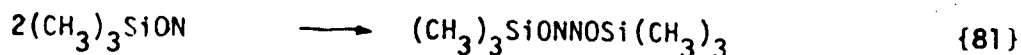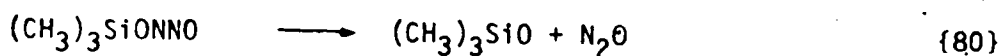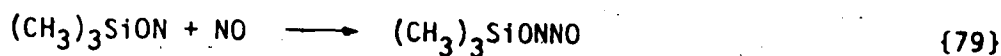
The silyloxy radicals formed can react with the substrate in a displacement reaction facilitated by the strong affinity of silicon for oxygen and made possible by the ability of silicon to expand its valence shell by utilization of its vacant 3d orbitals.

$$(CH_3)_3SiO + (CH_3)_4Si \longrightarrow (CH_3)_3SiOSi(CH_3)_3 + CH_3 \qquad \{83\}$$
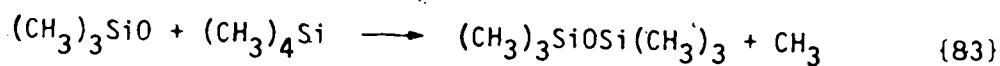
Hexamethyldisiloxane is the main product of the nitric oxide scavenging experiments.

The fates of the H atoms and methyl radicals in the system are less obvious and a large variety of reactions can occur.

Nitric oxide will scavenge H atoms

$$H + NO \longrightarrow HNO \qquad \{84\}$$

and the product can undergo further reactions[149].

HNO can dimerize and then decompose,

$$2HNO \longrightarrow (HNO)_2 \qquad \{85\}$$

$$(HNO)_2 \longrightarrow H_2O + N_2O \qquad \{86\}$$
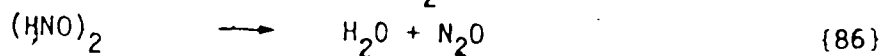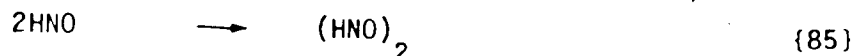
and can react further with more H atoms or NO molecules

$$HNO + H \longrightarrow H_2 + NO \qquad \{87\}$$

$$HNO + 2NO \longrightarrow H + N_2 + NO_3 \qquad \{88\}$$

$$\longrightarrow HNO_3 + N_2 \qquad \{89\}$$
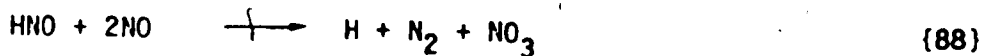
The mechanism of methyl· radical scavenging by nitric oxide is not fully understood[150]. The primary product, nitrosomethane, is not very stable and undergoes numerous further reactions.

$$CH_3 + NO \longrightarrow CH_3NO \qquad \{90\}$$

It was found to dimerize

$$2(CH_3NO) \longrightarrow (CH_3NO)_2 \qquad \{91\}$$
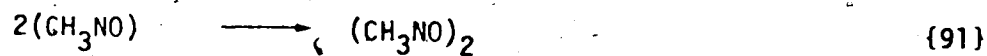
and then to decompose on the cell walls:

$$(CH_3NO)_2 \longrightarrow 2HCN + 2H_2O \qquad \{92\}$$
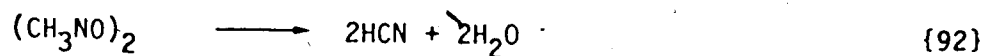
The nitrosomethane could also react further with CH_3 radicals or NO molecules to give trimethylhydroxylamine or methoxy radicals:

$$CH_3NO + 2CH_3 \longrightarrow (CH_3)_2NOCH_3 \qquad \{93\}$$

$$CH_3NO + NO \longrightarrow CH_3O + N_2O \qquad \{94\}$$
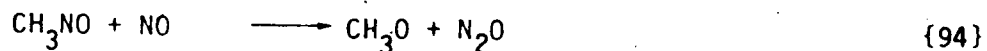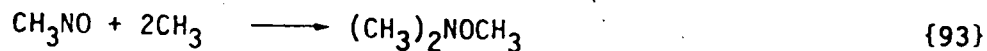
Other reactions possible in the present system are,

$$CH_3 + HNO \longrightarrow CH_4 + NO \qquad \{95\}$$

$$CH_3O + Si(CH_3)_3 \longrightarrow CH_3OSi(CH_3)_3 \qquad \{96\}$$
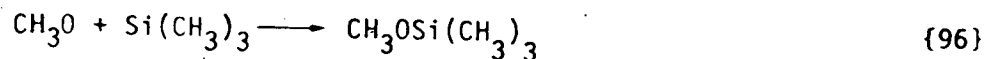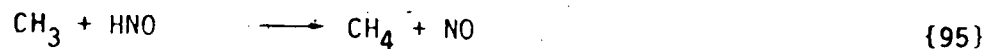
These complications make it impossible to make any worthwhile deductions from alterations in the yields of hydrogen and methane in

the scavenging studies, whereas decreases in the yields of other alkanes and silanes were interpreted as quantitative measures of the extent of monoradical reactions.

The products resulting from the nitric oxide scavenging were not all identified (Table III-6) but estimates could be made of the unknown structures. From the retention times and reactions prevalent in the system, products C and D were thought to be trisiloxanes while A and B were possibly methoxytrimethylsilane and trimethylhydroxyl-amine. The absolute micromole yields are somewhat uncertain since the response factors were not determined for the oxygenated species. The main products appear to be accounted for by the reaction of methyl and trimethylsilyl radicals with nitric oxide (reactions {78} - {83}, {90} - {96}) but the yield of N_2 is high. This could be due to the presence of small chains, e.g. reactions {84}, {87} and {88}.

One point complicating the derivation of a mechanism is the question of the primary quantum yield in the photolysis of carbon dioxide. We have assumed $\phi_{CO} = 1.0$ on the grounds that the majority of papers in the literature agree on this value and since it gave close to the accepted value of $\phi(N_2) = 1.4$ when used for calibration in the photolysis of nitrous oxide carried out with the same xenon resonance lamp.

However, there is some doubt as to whether ϕ_{CO} is exactly unity so two additional sets of primary quantum yields were derived, using $\phi_{CO} = 0.90$ and 0.85 (Table III-12).

It can be seen that this successively increases the amount of two-fragment decompositions at the expense of three-fragment decompositions, from 75% (at $\phi_{CO} = 1.0$) to 90% (at $\phi_{CO} = 0.85$). The biggest

TABLE III-12

Primary Quantum Yields In The Photolysis Of Tetramethylsilane With

Variation In The Actinometric Quantum Yield

Primary Steps	Quantum Yields		
	$\Phi(CO)=1.0$	$\Phi(CO)=0.90$	$\Phi(CO)=0.85^a$
$(CH_3)_4Si + h\nu \xrightarrow{1} CH_3 + Si(CH_3)_3$	0.51	0.65	0.71
$\xrightarrow{2} 2CH_3 + Si(CH_3)_2$	0.16	0.05	-
$\xrightarrow{3} CH_4 + CH_2Si(CH_3)_2$	0.17	0.15	0.14
$\xrightarrow{4} CH_3 + H + CH_2Si(CH_3)_2$	0.10	0.09	0.09
$\xrightarrow{5} H_2 + CHSi(CH_3)_3$	0.02	0.02	0.02
$\xrightarrow{6} CH_2 + (CH_3)_3SiH$	0.04	0.04	0.03
	1.00	1.00	0.99

A primary quantum yield of unity can only be obtained if $\Phi(CO) \geqslant 0.87$.

changes are the large increase in the trimethylsilyl radical yield and the disappearance of dimethylsilylene as a primary product. The increasing yields of trimethylsilyl radicals cannot be correlated with the product distribution even assuming cross-disproportionation; for $\phi(CH_3)_3Si = 0.700$ only about 60% of the radicals can be accounted for.

The same calculation carried out for the ϕ_B results shows the same trends with the added proviso that an actinometric yield of $\phi_{CO} = 0.7$ implies that 33% of the methyl radicals produced end up reforming the substrate.

From these results it is seen that the decomposition of tetramethylsilane is very similar to the decomposition of neo-pentane in that similar types of primary processes occur and free radical steps are more important than molecular modes of elimination.

It is not clear at this point whether hydrogen abstraction by methyl or silyl radicals from the substrate takes place or whether this comes from disproportionation reactions, and how the secondary reactions are affected by the amount of excess energy in the fragments.

It does appear, however, that the results can best be explained by assuming extensive disproportionation and this leads to the conclusion that the diradical $CH_2Si(CH_3)_2$ formed in disproportionation of trimethylsilyl radicals has a large degree of stability.

The main fate of the diradical appears to be polymerization and there is no evidence for the dimer postulated in other studies.

It will be shown later (Chapter V) that the recombination rate constant for trimethylsilyl radicals is about five orders of magnitude less than that for methyl radicals, which explains the relatively low hexamethyldisilane yield which one would expect to be fairly large,

given the large primary yield of trimethylsilyl radicals.

CHAPTER IV

THE PHOTOLYSIS OF BIS(TRIMETHYLSILYL)MERCURY

A. Results

The direct photolysis of bis(trimethylsilyl)mercury in a static system in the gas phase by a medium pressure mercury arc at wavelengths greater than 300 nm was studied as a function of exposure time, total pressure, and concentration of radical scavengers nitric oxide, ethylene and oxygen.

1. Products

The products of photolysis are shown in Table IV-1 and listed here in decreasing order of importance: hexamethyldisilane (HMDS), hexamethyldisiloxane (HMDSO), and trimethylsilane (Tri-MS). In addition to these, traces of tetramethylsilane and another silane were also found and mercury deposited on the walls of the reaction cell. Undecomposed mercurial $(((CH_3)_3Si)_2Hg)$ was found to react with the analytical system to produce mostly hexamethyldisiloxane (80-95%) along with some hexamethyldisilane and trimethylsilane so all photolyses were carried out to 100% reaction to minimize hexamethyldisiloxane formation. Similarly, photolysis of the solid mercurial gave rise to large amounts of siloxane indicating that the trimethylsilyl groups probably react with the cell walls.

2. Exposure Time Study

An exposure time study was carried out to determine the time required to photolyze approximately 0.25 μmoles of mercurial. The relative yields of products reached essentially constant values after

114

TABLE IV-1

Relative Yields of Products from the Photolysis

of Bis(trimethylsilyl)mercury

Product	Relative Yield (%)
Hexamethyldisilane	83.0
Hexamethyldisiloxane	11.5
Trimethylsilane	4.0

-1) so all subsequent photolyses were carried out on this time scale. Although the trimethylsilane yield seems invariant with photolysis time, at the shorter times it is probable that some or all of the trimethylsilane is formed during analysis of the undecomposed mercurial. A blank run of 1 hour gave as products Tri-MS (4%), unknown A (20%), HMDSO (60%) and HMDS (16%), with the total amount of products less than in the photolyses, indicating the probability of loss due to polymerization on the cell wall. To ensure that the change in the relative yields with time was not due to secondary photolyses of the products the following wavelength study was used.

3. Wavelength Study

Trimethylsilane is known to absorb only at wavelengths shorter than 180 nm[77] but the available spectra of hexamethyldisilane show absorption tailing up to 250 nm[78,151]. Use of appropriate glass filters with the medium-pressure mercury lamp showed that at wavelengths above 300 nm there was no measurable yield of products with 0-20 torr of hexamethyldisilane in the reaction cell, while at shorter wavelengths appreciable quantities of trimethylsilane were formed along with minor amounts of unidentified disilanes.

Accordingly all further studies were done at wavelengths greater than 300 nm.

4. Pressure Study

The effect of pressure on the product yields was examined in 90-minute photolyses using from zero to 200 torr of nitrogen as the added gas. Relative yields were found to remain constant (Figure IV-2) indicating that there was no fragmentation of "hot" products at low pressures. Variation in substrate pressure was not studied since the vapour pressure
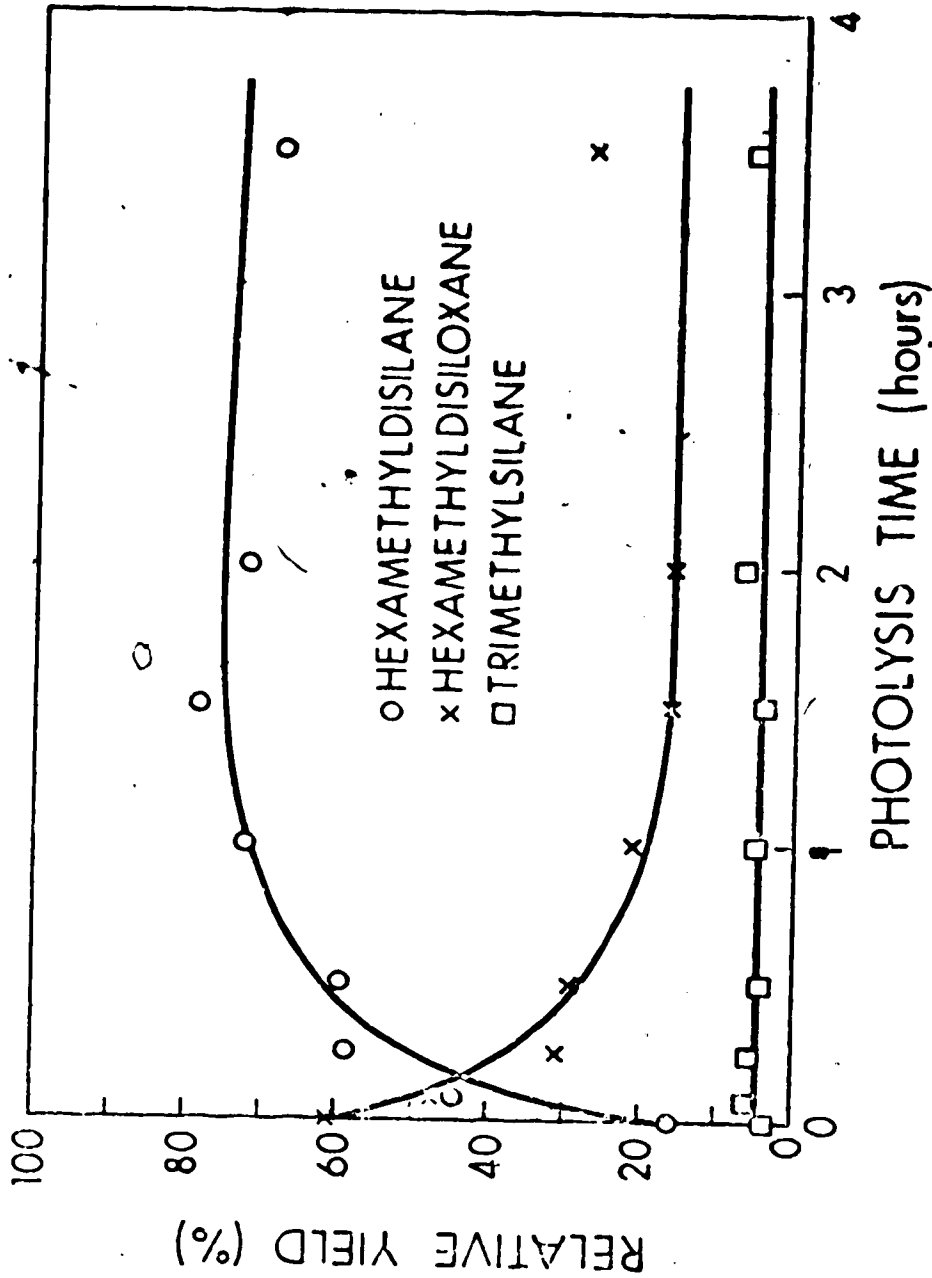
FIGURE IV-1. Relative Yields of HMDS, HMDSO and Tri-MS as a Function of Exposure Time from the Photolysis of Bis(trimethylsilyl)mercury.
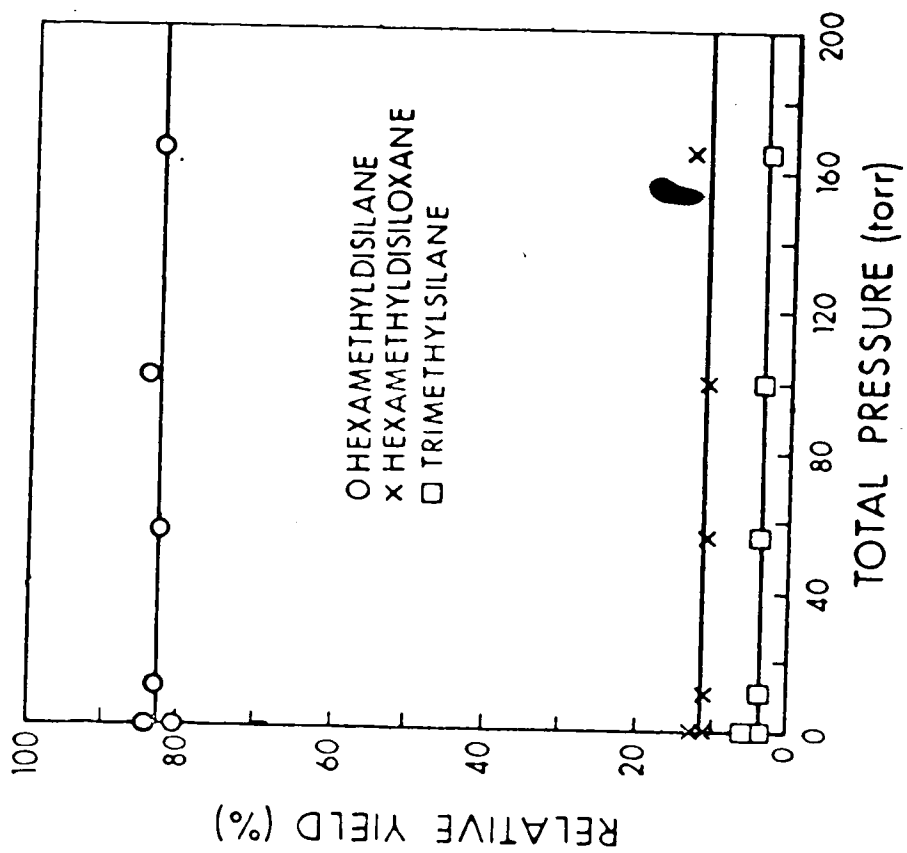
FIGURE IV-2. Relative Yields of HMDS, HMDSO and Tri-MS as a Function of Total Pressure from the Photolysis of Bis(trimethylsilyl)mercury.

of the mercurial at room temperature was so low (ca. 20 microns) and any increase in temperature to increase the vapour pressure resulted in the accelerated decomposition of the mercurial with an increase in the yield of siloxane presumably from reaction of the mercurial with the hot walls of the reaction vessel.

5. Effect of Added Nitric Oxide

The effect of the addition of up to 20 torr of nitric oxide as a radical scavenger is shown in Figure IV-3. Photolysis of the mercurial in the presence of nitric oxide essentially eliminates all of the HMDS and Tri-MS, indicating that both of these products must be formed mainly by monoradical reactions. About 2% of the HMDS remains unscavengeable indicating the presence of a minor molecular route to product formation. Hexamethyldisiloxane is a product of the reaction between nitric oxide and the radicals produced in the photolysis and increases accordingly. It is the major product (~95%) and is accompanied by a minor unidentified product (~4%).

6. Effect of Added Ethylene

Ethylene has been shown to be an efficient scavenger of trimethylsilyl radicals[67] and was used to determine whether, in addition to suppression of the hexamethyldisilane and trimethylsilane yields, the yield of siloxane would be affected. The yield of hexamethyldisilane decreased to 5% and the trimethylsilane was completely scavenged but the siloxane yield remained essentially constant even with photolysis in the presence of 100 torr of ethylene (Figure IV-4).

7. Effect of Added Oxygen

Oxygen was added in a series of photolyses to determine its
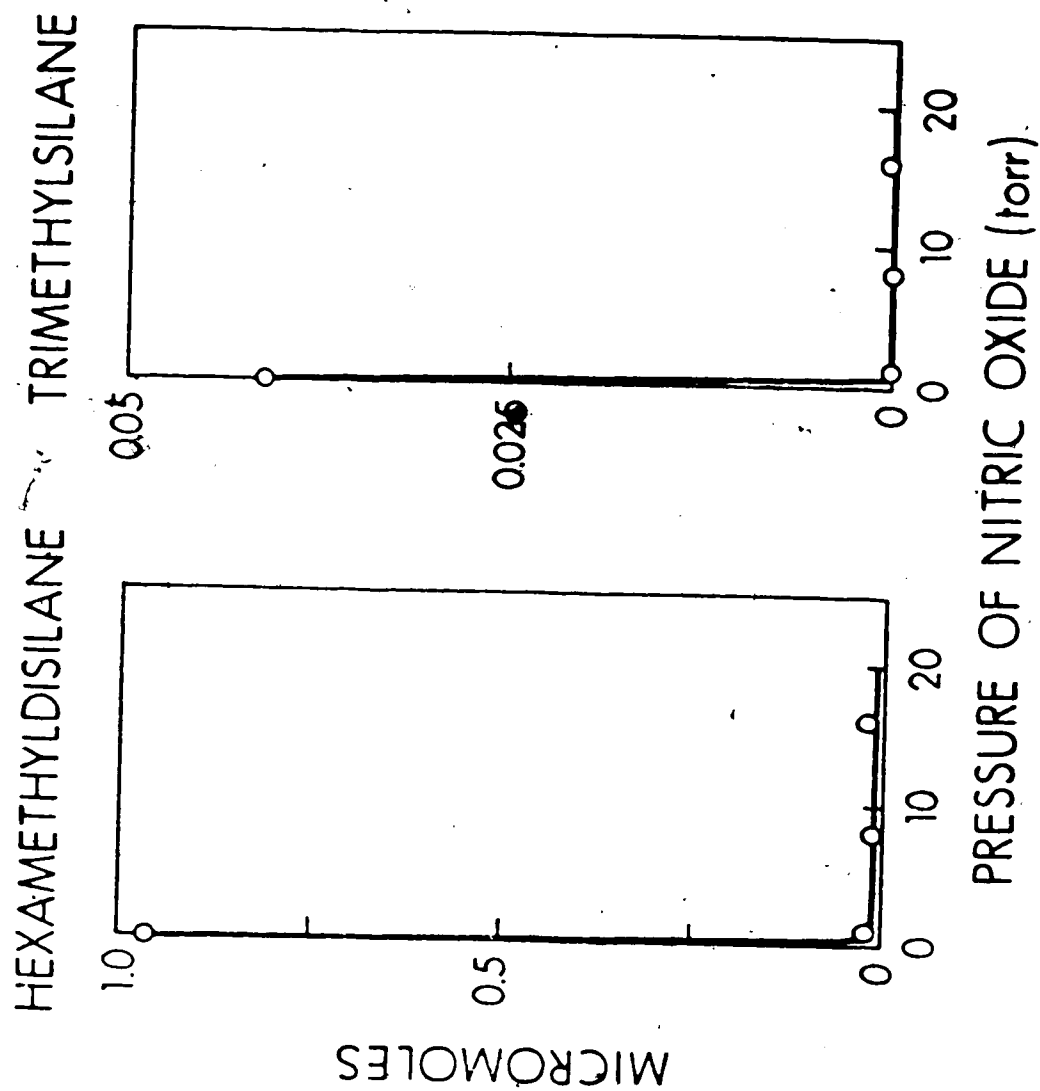
FIGURE–IV-3. Effect of Nitric Oxide on the Yields of HMDS and Tri-MS from the Photolysis of Bis(trimethylsilyl)mercury.
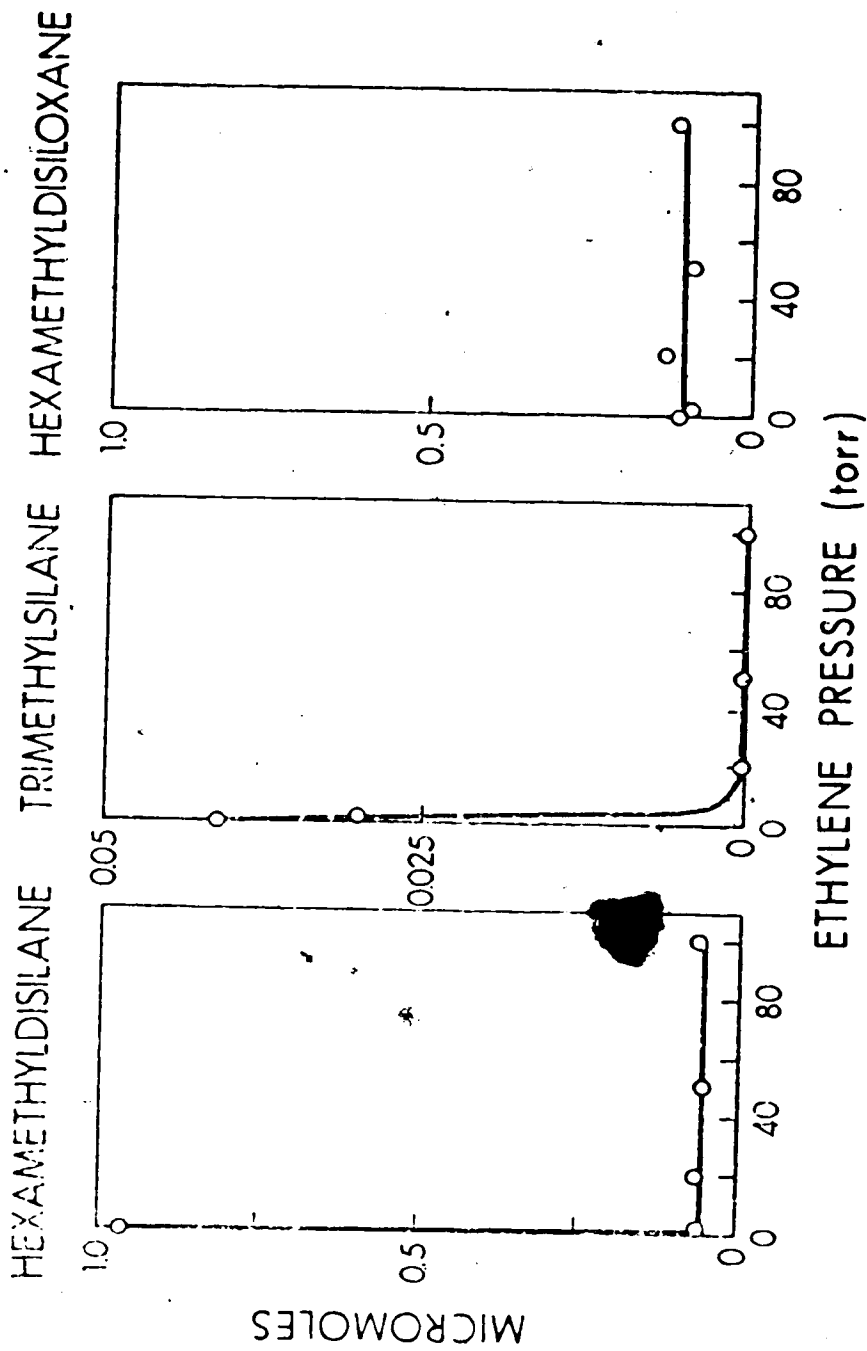
FIGURE IV-4. Effect of Ethylene on the Yields of HMDS, HMDSO and Tri-MS from the Photolysis of Bis(trimethylsilyl)mercury.

scavenging efficiency under the conditions prevalent in the system. As shown in Figure IV-5 less than 40 microns of oxygen suppresses the formation of HMDS and Tri-MS. The products were hexamethyldisiloxane (~80%) and two others, one tentatively identified as the corresponding trisiloxane (~15%) and the other (~4%) unidentified.

The mercurial and oxygen were found to react even in the absence of light indicating the strong affinity of silicon for oxygen.

B. DISCUSSION

1. The Decomposition of Bis(trimethylsilyl)mercury

The mercurial has previously been photolyzed in solution by several workers (Chapter I, Section C-5) and has been found to be a good source of trimethylsilyl radicals. From the results obtained it appears that photolysis in the gas phase is also a fairly clean source of trimethylsilyl radicals. There are only three products, hexamethyldisilane, hexamethyldisiloxane and trimethylsilane, and while the siloxane appears to be formed in a wall reaction the other two seem to be products of trimethylsilyl radical reactions.

The nitric oxide scavenging experiments show that hexamethyldisilane is formed either by combination of two radicals,

$$2(CH_3)_3Si \longrightarrow (CH_3)_3SiSi(CH_3)_3 \tag{1}$$
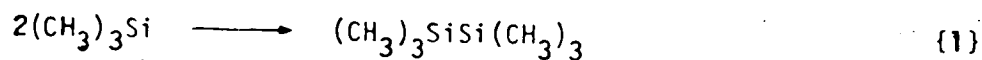
or via a radical reaction with the substrate:

$$(CH_3)_3Si + (CH_3)_3Si-Hg-Si(CH_3)_3 \longrightarrow (CH_3)_3Si-Si(CH_3)_3 + Hg-Si(CH_3)_3 \tag{2}$$

Reaction {1} is favoured since the concentration of substrate is low and the activation energy of reaction {2} is probably quite
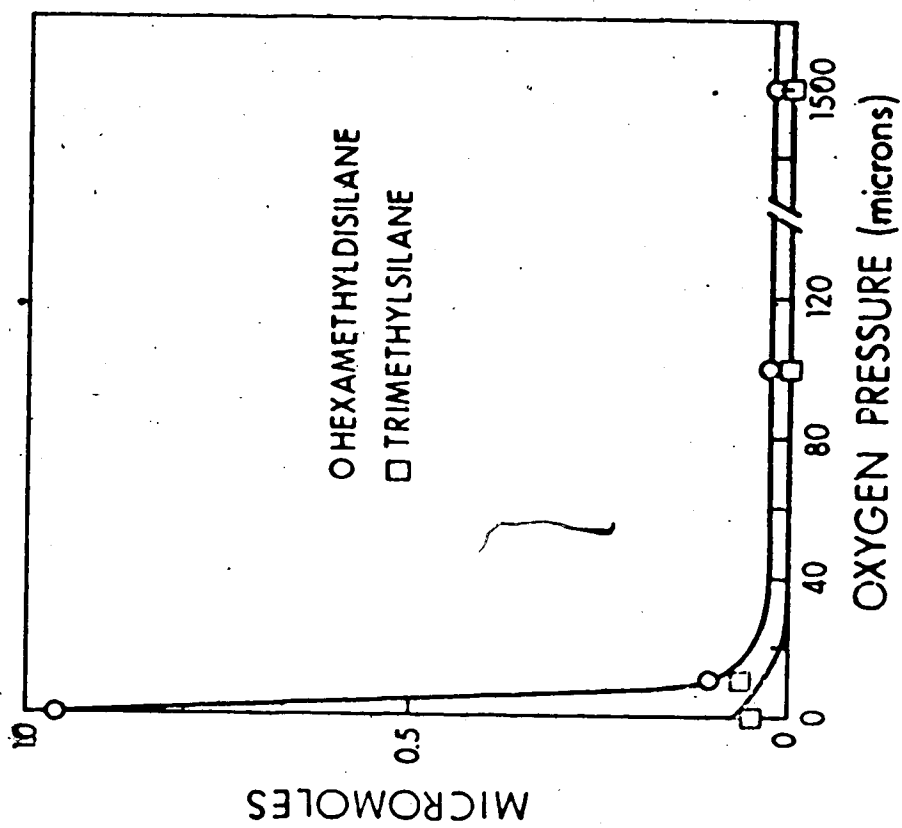
FIGURE IV-5. Effect of Oxygen on the Yield of HMDS and Tri-MS from the Photolysis of Bis(trimethylsilyl)mercury.

substantial. Moreover it will be shown in the following chapter that the kinetic behaviour of the hydrogen abstraction reactions of the tri- methylsilyl radicals can be explained only if formation of HMDS is second order in trimethylsilyl radicals.'

Trimethylsilane is also shown to be formed by radical reaction and the possibilities are the disproportionation of two trimethylsilyl radicals

$$2(CH_3)_3Si \longrightarrow (CH_3)_3SiH + CH_2Si(CH_3)_2 \qquad \{3\}$$

or abstraction from the substrate:

$$(CH_3)_3Si + (CH_3)_3Si-Hg-Si(CH_3)_3 \longrightarrow (CH_3)_3SiH +$$

$$CH_2(CH_3)_2Si-Hg-Si(CH_3)_3 \qquad \{4\}$$
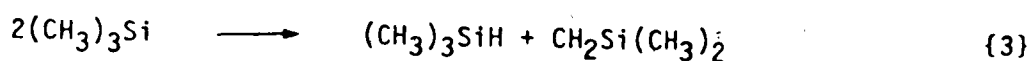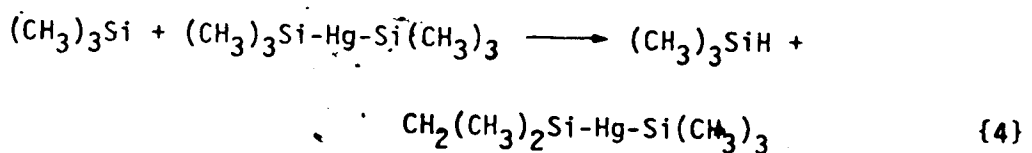
Once again reaction {4} is not considered likely since the activation energy for H-abstraction is likely to be in the order of 10 kcal/mole and the concentration of substrate is low. There are two values available for the Si-Hg bond energy in bis(trimethylsilyl)mercury. One is a very low value of 13.6 kcal/mole[113]. However, this was measured in a system which also gives a very low value for the Si-Si bond energy in hexamethyldisilane, 49-58 kcal/mole, compared to the latest values of ca. 80 kcal/mole, so it may have to be revised upwards.

The other value is a minimum of 48 kcal/mole[111] based on the activation energy for the thermal decomposition of bis(trimethylsilyl)- mercury but the authors admit there is a large error associated with this figure.

Values for alkyl-mercury bond energies[152] indicate that the mean energy is 25-30 kcal/mole and that the first carbon-mercury bond

dissociation energy is much larger than the second. E.g.

$$CH_3-Hg-CH_3 \xrightarrow{h\nu} CH_3-Hg + CH_3 \qquad \{5\}$$

$$CH_3-Hg \longrightarrow CH_3 + Hg \qquad \{6\}$$
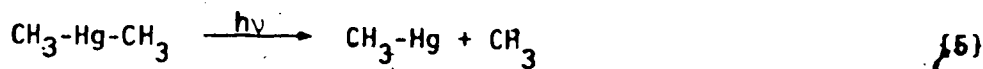
Reaction $\{5\}$ is the rate-determing step and the bond energy is ca. 50 kcals/mole; the subsequent decomposition $\{6\}$ is fast, the dissociation energy being only ca. 7.0 kcals/mole. In higher alkyl substituted mercury compounds, decomposition occurs via simultaneous rupture of both bonds:

$$2(i-Pr)Hg \longrightarrow 2(i-Pr) + Hg \qquad \{7\}$$
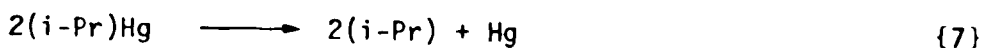
Assignment of bond energies is hazardous since it is very difficult to determine whether the decomposition is a one-step or two-step process and whether simple chain processes such as $\{8\}$, $\{9\}$ and $\{10\}$ take place:

$$((CH_3)_3Si)_2Hg \xrightarrow{h\nu} Hg + 2(CH_3)_3Si \qquad \{8\}$$

$$(CH_3)_3Si + (CH_3)_3Si-Hg-Si(CH_3)_3 \longrightarrow (CH_3)_3SiSi(CH_3)_3 + Hg + Si(CH_3)_3 \qquad \{9\}$$

$$2(CH_3)_3Si \longrightarrow (CH_3)_3SiSi(CH_3)_3 \qquad \{10\}$$
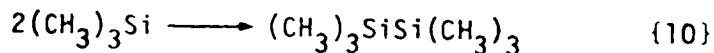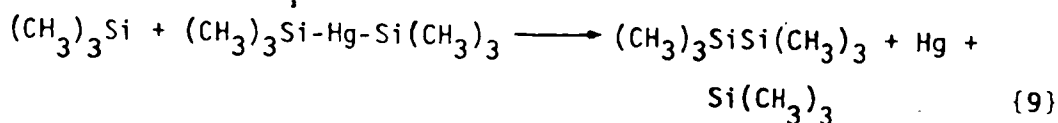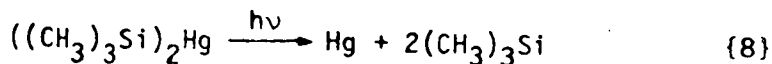
The maximum energy photons entering the cell have ~95 kcals/mole which is probably enough to make a two-step process of decomposition so fast that it is essentially simultaneous. A very minor process ($<1\%$) which is energetically feasible is the concurrent rupture of a Si-C bond to produce a methyl radical. Combination of this with the trimethylsilyl radicals present in the system is the probable cause

of the trace of tetramethylsilane found in the products. Just how much exce§ energy is left in the fragments is difficult to say but it cannot be enough to induce fragmentation of the trimethylsilyl radicals.

The mechanism of decomposition and product formation thus involves the initial formation of two trimethylsilyl radicals and mercury, followed by either combination or disproportionation of the radicals:

$$((CH_3)_3Si)_2Hg \xrightarrow{h\nu} Hg + 2(CH_3)_3Si \qquad \{11\}$$

$$2(CH_3)_3Si \longrightarrow (CH_3)_3SiSi(CH_3)_3 \qquad \{12\}$$

$$2(CH_3)_3Si \longrightarrow (CH_3)_3SiH + CH_2Si(CH_3)_2 \qquad \{13\}$$
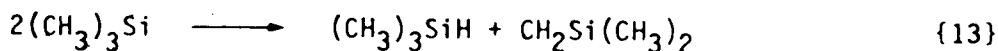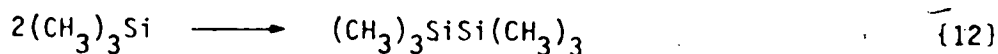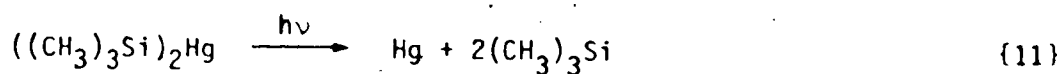
The fate of the diradical, $CH_2Si(CH_3)_2$, in reaction $\{13\}$ is most likely diffusion to the walls. This scheme then gives a $k_{dispro-portionation}$ to $k_{combination}$ ratio of 0.046 which is a much lower value than that for the corresponding carbon radical, t-Bu., where k_d/k_c = 2.3 - 3.1[59], although disproportionation in the carbon case leads to two stable products, an alkane and an alkene. The lack of such a stable olefin-type structure was thought to preclude silyl radical disproportionation but recent results have shown that the Si-C (p-p) π-bonded intermediates have more stability than was originally thought (Chapter I, section E). It has been suggested[116,153], on various grounds, that silicon radicals may disproportionate, but this is the first quantitative measurement reported.

It thus appears likely that disproportionation can occur to a larger extent in those silyl radicals containing Si-H bonds, since these hydrogens should be more readily abstracted than the hydrogen from a

C-H bond.

Photolysis of the mercury compound in the gas phase thus appears to be a good clean source of trimethylsilyl radicals containing little excess energy and is well suited to be used to study the reactions of trimethylsilyl radicals with other species.

2. Stability of Silaethylene

The demonstration that trimethylsilyl radicals disproportionate indicates some degree of stability for the silicon diradical formed in reaction {13}, since the value of 0.046 for k_d/k_c requires an estimated rate increase in the order of 10^5 (cf. Chapter V) for the disproportionation hydrogen transfer reaction over the abstraction reaction

$$(CH_3)_3Si + (CH_3)_4Si \longrightarrow (CH_3)_3SiH + CH_2Si(CH_3)_3 \qquad \{14\}$$
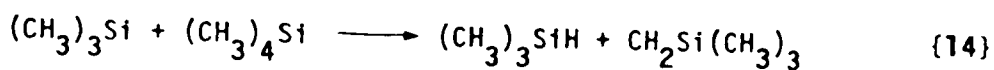
This large difference in rate must be associated with the formation of either a singlet olefinic-type π bond or a strongly interacting triplet 1,2-diradical.

An ab initio molecular orbital calculation was carried out by Drs. I. G. Csizmadia and G. Theodorakopoulos at the University of Toronto on the silaethylene molecule, $H_2Si=CH_2$, aimed at determining the relative stability of the singlet versus the triplet state.

Calculations were carried out with s,p Gaussian type functions contracted to a minimal (STO-4G) basis set[154] using a version of the Gaussian 70 program[155].

Four different structures of silaethylene were optimized starting from the published ab initio results on the i.r. spectrum of silaethylene[156].

The absolute minimum occurs at the skew position in the

pyramidal T_1 state but this is only about 2 kcal/mole below the minimum in the planar S_0 surface. The other two structures, the S_0 and the T_1 planar, appear as transition states on the singlet and triplet hyper-surfaces but all four represent minima in the rotational cross-sections associated with the cis-trans isomerization of silaethylene. The results are shown on Figure IV-6 and the calculated state energies and optimum geometrical parameters are listed in Tables IV-2 and IV-3.

These calculations thus lead to the conclusion that the ground state of silaethylene is a triplet but that the lowest singlet state lies only 2 kcal/mole above it. Even if in reality the order of stability of triplet and singlet states is reversed, it is still likely that the energy splitting between the two is very small. The almost equal stability of the two states is in line with the observations that silaethylene has a fair degree of stability, but is also very reactive, suggesting a diradical character.
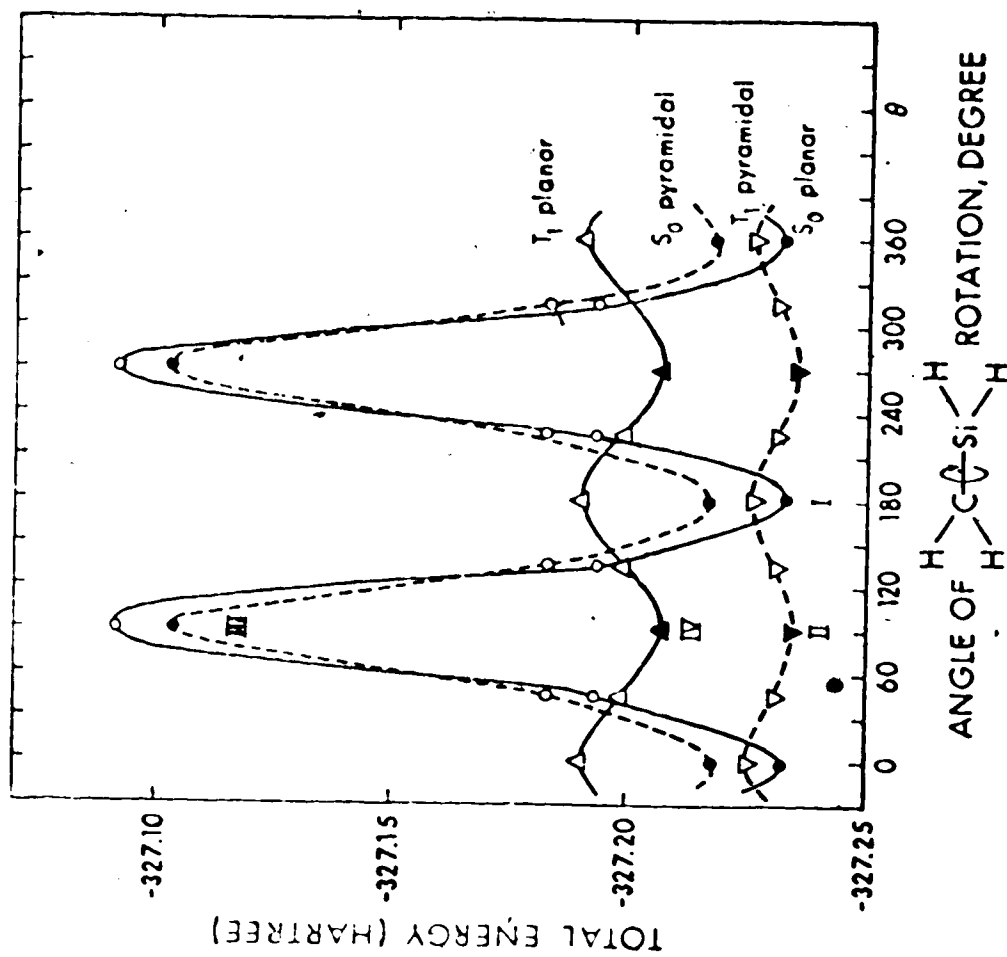
FIGURE IV-6. Cross-sections of the Conformational Hypersurfaces for S_0 and T_1 Silaethylene.

TABLE IV-2

Calculated State Energies in Hartree for S_0 and T_1 Silaethylene

θ (degrees)	Planar Groups		Pyramidal Groups	
	S_0	T_1	S_0	T_1
0 (180)	-327.233137*(I)	-327.189852	-327.217708	-327.226132
45 (135)	-327.192995	-327.198634	-327.182645	-327.230812
90	-327.092329	-327.206975*(IV)	-327.102640*(III)	-327.235380*(II)

* Optimized Values.

TABLE IV-3

Calculated Optimum Geometrical Parameters for S_0 and T_1 Silaethylene

	Planar Groups		Pyramidal Groups	
	S_0	T_1	S_0	T_1
r_{Si-C}	1.637	1.830	1.689	1.846
r_{Si-H}	1.418	1.414	1.444	1.429
r_{C-H}	1.073	1.081	1.065	1.0797
$\angle HSiC$	122.66	120.5	129.34	109.06
$\angle HCSi$	123.13	123.2	117.9	123.0
θ	0°	90°	0°	90°
$\phi HSiH$	0°	0°	0°	30°
ϕHCH	0°	0°	14°	0°

CHAPTER V

REACTIONS OF TRIMETHYLSILYL RADICALS

RESULTS

1. Abstraction from Silanes

It has been demonstrated that the photolysis of bis(trimethyl-silyl)mercury proceeds by the following mechanism:

$$((CH_3)_3Si)_2Hg \quad \xrightarrow{\ h\nu\ } \quad 2(CH_3)_3Si + Hg \qquad \{1\}$$

$$2(CH_3)_3Si\cdot \quad \longrightarrow \quad (CH_3)_3SiSi(CH_3)_3 \qquad \{2\}$$

$$2(CH_3)_3Si \quad \longrightarrow \quad (CH_3)_3SiH + CH_2Si(CH_3)_2 \qquad \{3\}$$
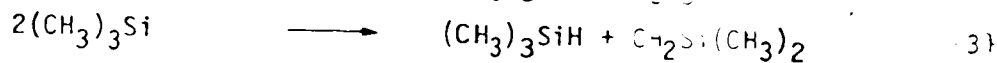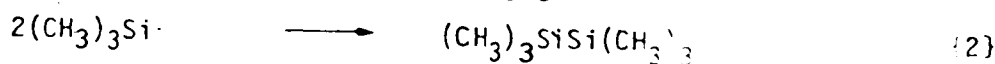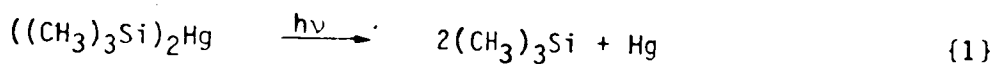
However, when the radicals are produced in the presence of an excess of added silane with a readily abstractable hydrogen the follow-ing abstraction reaction might be expected to occur:

$$(CH_3)_3Si + HSiR_3 \quad \longrightarrow \quad (CH_3)_3SiH + SiR_3 \qquad \{4\}$$
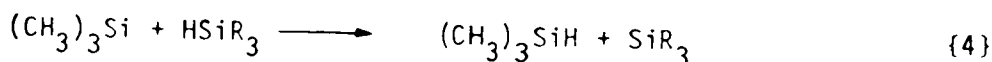
If we make allowance for the formation of trimethylsilane by disproportionation of the trimethylsilyl radicals (reaction {3}) and for the unscavengeable yield of hexamethyldisilane, the rates of formation of trimethylsilane and hexamethyldisilane can be related by the expres-sion

$$\frac{R_{(CH_3)_3SiH} - R_3}{(R_{(CH_3)_6Si_2})^{1/2}} = \frac{k_4 (HSiR_3)}{k_2^{1/2}} \qquad I$$

derived from the steady state treatment of the competing reactions {2}, {3} and {4}.

132

A plot of $R_{(CH_3)_3SiH}/R_{(CH_3)_6Si_2}^{1/2}$ against added silane concentration gives a slope of $k_4/k_2^{1/2}$, the rate constant for abstraction relative to the rate constant for dimerization of trimethylsilyl radicals.

So the mercurial was photolyzed in the presence of a number of silanes over a range of concentrations which would produce from 10% to 90% of the abstraction product, in the expectation that this would provide information on the behaviour of the trimethylsilyl radical.

2. Reaction with Disilane and Disilane-d_6

Rate constants for the abstraction by trimethylsilyl radicals from disilane were determined relative to combination.

$$(CH_3)_3Si + Si_2H_6 \longrightarrow (CH_3)_3SiH + Si_2H_5 \tag{5}$$

$$(CH_3)_3Si + Si_2D_6 \longrightarrow (CH_3)_3SiD + Si_2D_5 \tag{6}$$
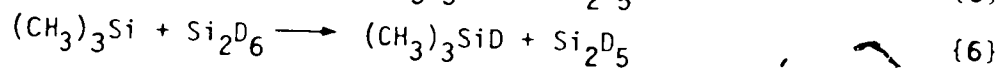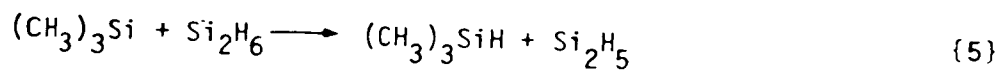
The mercurial was photolyzed in the presence of up to 6 torr of disilane and it was found that ~70 microns were sufficient to give 95% abstraction product. The results are shown in Table V-1 and Figure V-1. The rates of formation were calculated as shown in Table V-2 and the data are plotted on Figure V-2, using least mean squares treatment to obtain the best straight line fit to the points. From the graph,

$$\frac{k_5}{k_2^{1/2}} = 1.01 \pm 0.35 \times 10^3 \text{ moles}^{1/2}\text{cc}^{-1/2}\text{sec}^{-1/2}$$

Photolysis of the mercurial in the presence of up to 500 microns of disilane-d_6 gave the results shown in Table V-3 which were plotted as shown on Figure V-2 to give the result

$$\frac{k_6}{k_2^{1/2}} = 2.70 \pm 0.50 \times 10^2 \text{ moles}^{1/2}\text{cc}^{-1/2}\text{sec}^{-1/2}$$

TABLE V-1

Relative Yields of Products from the Photolysis of $[(CH_3)_3Si]_2Hg$

in the Presence of Si_2H_6

Si_2H_6 Pressure (Torr)	Product Yields	
	% Hexamethyldisilane	% Trimethylsilane
0.030	13.9	86.1
0.060	8.0	92.0
1.56	2.5	97.5
3.12	2.5	97.5
5.50	2.5	97.5
11.50	2.5	97.5
0.038	9.4	90.6
0.018	17.6	82.4
0.010	22.8	77.2
5.50	1.9	98.1
20.50	5.4	94.6
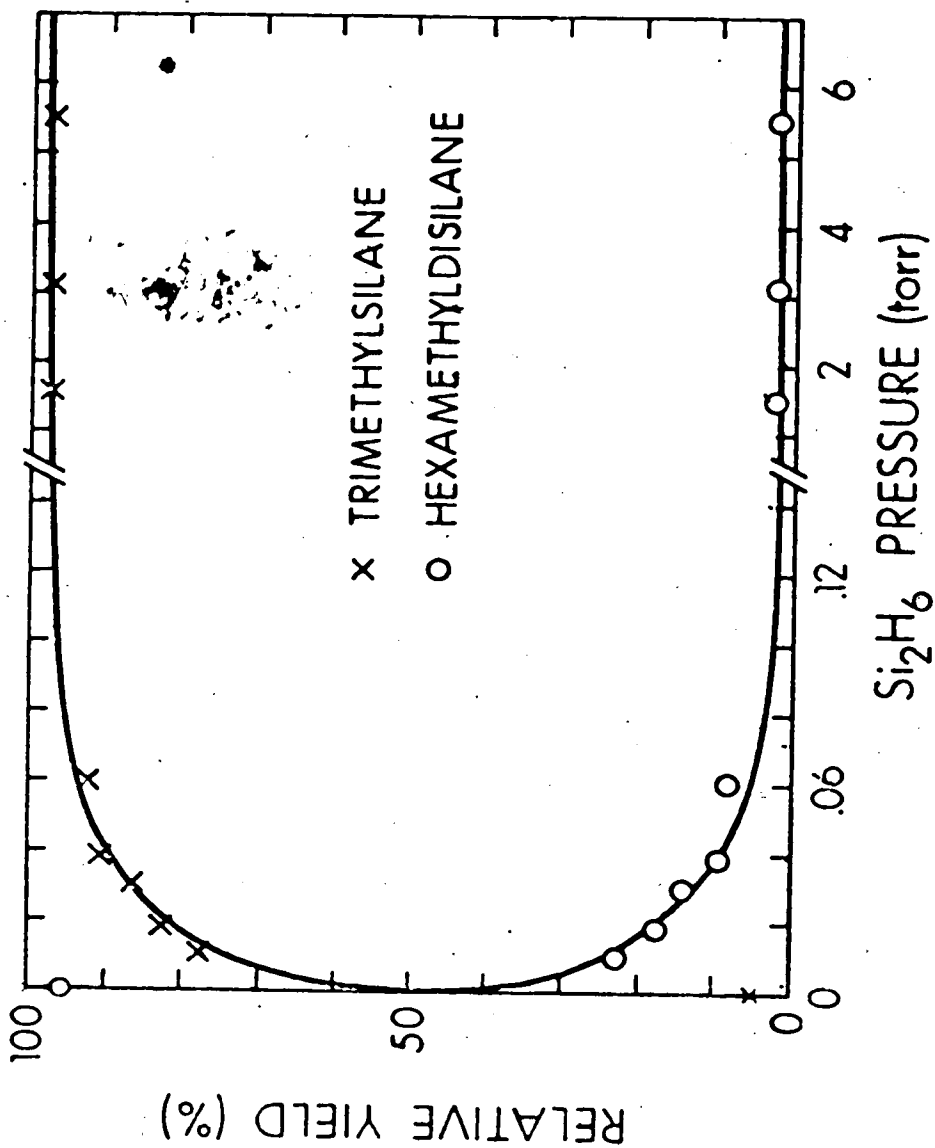
FIGURE V-1. Relative Yields of Products from the Photolysis of Bis(trimethylsilyl)mercury in the Presence of Disilane.

TABLE V-2

Photolysis of $[(CH_3)_3Si]_2Hg$ in the Presence of Si_2H_6 at Constant Pressure**

Si_2H_6 Pressure (microns)	% Yields $(CH_3)_3SiH$	$(CH_3)_6Si_2$	Corrected % Yields* $(CH_3)_3SiH$	$(CH_3)_6Si_2$	$(Rate_1)^{1/2}$ (moles cc^{-1} sec^{-1})$^{1/2}$ x 10^7	$Rate_2$ (moles cc^{-1} sec^{-1}) x 10^{13}	$\dfrac{Rate_2}{(Rate_1)^{1/2}}$ x 10^6	Si_2H_6 concentration moles cc^{-1} x 10^9
30	86.1	13.9	88.2	11.8	2.85	6.18	2.17	1.60
60	92.0	8.0	94.3	5.7	2.06	7.00	3.40	3.20
38	90.6	9.4	92.9	7.1	2.28	6.79	2.90	2.03
18	82.4	17.6	84.4	15.6	3.27	5.71	1.74	0.964
10	77.2	22.8	78.9	21.1	3.70	5.12	1.38	0.535

* Corrected for disproportionation yield of $(CH_3)_3SiH$ and unscavengeable fraction of $(CH_3)_6Si_2$.

** Nitrogen added to keep total pressure at 40 torr.
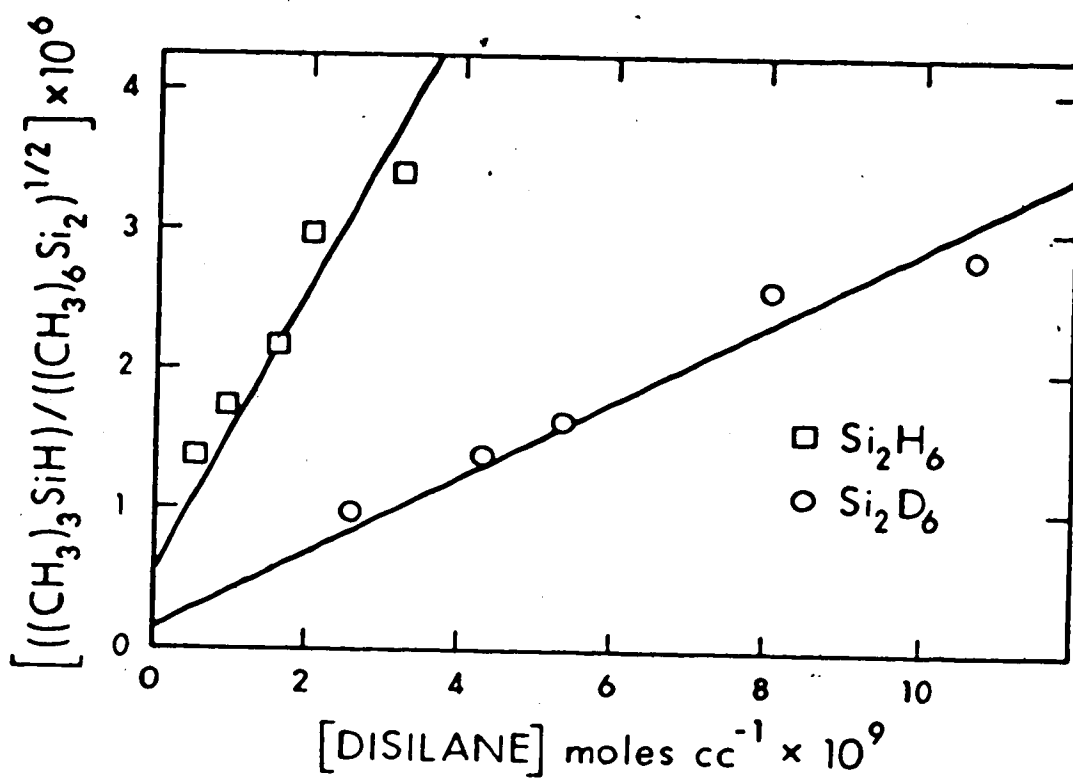
FIGURE V-2. Relative Rate Plots for the Abstraction/Combination Reactions of Trimethylsilyl Radicals with Added Disilane and Disilane-d_6 at Constant Pressure.

TABLE V-3

Photolysis of [(CH$_3$)$_3$Si]$_2$Hg in the Presence of Si$_2$D$_6$ at Constant Pressure**

Si$_2$D$_6$ Pressure (microns)	% Yields		Corrected % Yields*		$(Rate_1)^{1/2}$ (moles·cc^{-1}sec^{-1})$^{1/2}$ x 10^7	$Rate_2$ moles cc^{-1} sec^{-1} x 10^{13}	$\dfrac{Rate_2}{(Rate_1)^{1/2}}$ x 10^6	Si$_2$D$_6$ concentration moles cc^{-1} x 10^9
	(CH$_3$)$_3$SiH	(CH$_3$)$_6$Si$_2$	(CH$_3$)$_3$SiH	(CH$_3$)$_6$Si$_2$				
	93.9	6.3	96.1	3.9	1.73	7.25	4.19	26.0
200	90.0	10.0	92.3	7.7	2.38	6.72	2.82	10.7
100	80.8	19.2	82.9	17.1	3.38	5.56	1.64	5.35
48	68.1	31.9	69.4	30.6	4.28	4.17	0.974	2.57
350	93.8	7.2	95.2	4.8	1.90	7.13	3.75	18.7
150	88.9	11.1	91.1	8.9	2.54	6.56	2.50	8.03
80	75.4	24.6	77.1	22.9	3.84	4.91	1.28	4.28

* Corrected for disproportionation yield of (CH$_3$)$_3$SiH and unscavengeable yield of (CH$_3$)$_6$Si$_2$.

** Nitrogen added to keep total pressure at 40 torr.

Since the rate of abstraction from the disilane was so fast that very low concentrations had to be used to monitor the variation in the amount of abstraction, the possibility that the disilane concentrations were changing appreciably, and consequently affecting the reaction rates, had to be investigated.

Different amounts of mercurial were photolyzed in the presence of 100 microns of disilane-d_6 and the relative yields of products were measured. It can be seen (Table V-4, Figure V-3) that above 1.5 times the usual amount of mercurial the relative yields start to change, so at the concentrations of mercurial used in these rate determinations, some error due to disilane depletion should be expected below 50 microns of disilane. This leads to an uncertainty of about 35% in the value of $k_5/k_2^{\frac{1}{2}}$ for the reaction with disilane.

3. Reaction with Monosilane and Monosilane-d_4

Rate constants for abstraction by trimethylsilyl radicals were determined relative to trimethylsilyl radical recombination

$$(CH_3)_3Si + SiH_4 \longrightarrow (CH_3)_3SiH + SiH_3 \qquad \{7\}$$

$$(CH_3)_3Si + SiD_4 \longrightarrow (CH_3)_3SiD + SiD_3 \qquad \{8\}$$
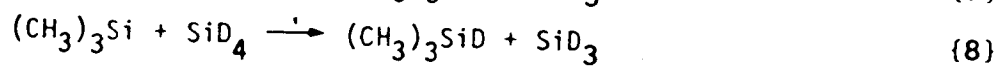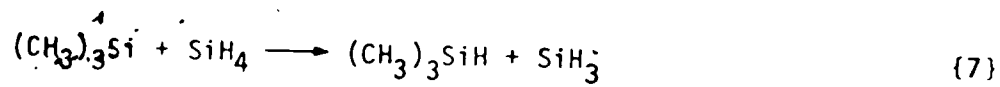
The mercury compound was photolyzed in the presence of up to 3.0 torr of SiH_4 and 25.0 torr of SiD_4 with nitrogen added to keep the total pressure constant at 40 torr.

The results are shown in Tables V-5 and V-6 and Figure V-4 from which

$$\frac{k_7}{k_2^{\frac{1}{2}}} = 1.31 \pm 0.12 \times 10^1 \text{ moles}^{1/2} \text{ cc}^{-1/2} \text{sec}^{-1/2}$$

TABLE V-4

Effect of the Amount of Mercurial on

Relative Product Yields

Si_2D_6 Pressure* (torr)	Relative Amount $((CH_3)_3Si)_2Hg$	% Yields	
		$(CH_3)_6Si_2$	$(CH_3)_3SiH$
0.10	0.25	18.5	81.5
0.10	0.50	17.8	82.2
0.10	1.00	19.2	80.8
0.10	1.50	20.3	79.7
0.10	2.00	10.6	89.4

* Nitrogen added to bring total pressure to 40 torr.
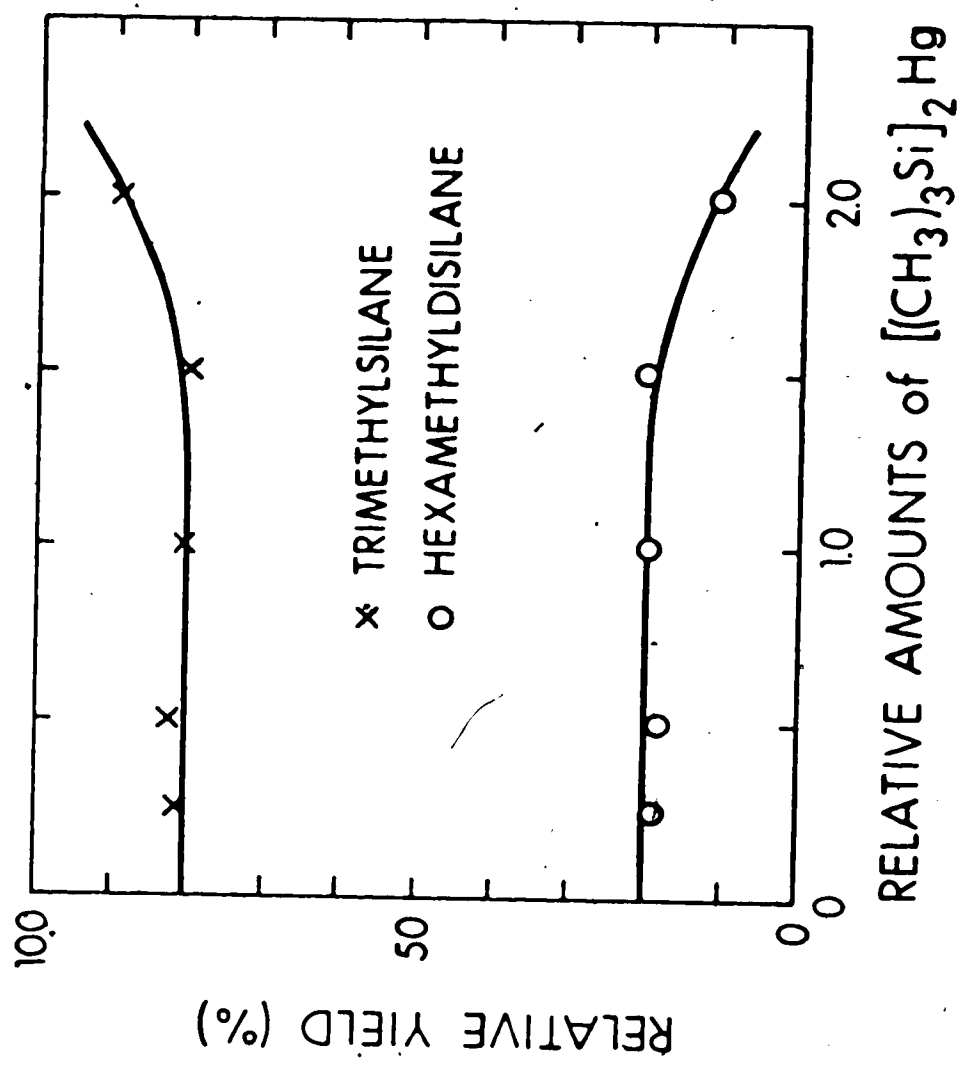
FIGURE V-3. Relative Product Yield Dependence on Amount of Mercurial ($P(Si_2D_6)$ = 0.10 torr).

TABLE V-5

Photolysis of $[(CH_3)_3Si]_2Hg$ in the Presence of SiH_4 at Constant Pressure**

SiH_4 Pressure (torr)	% Yields $(CH_3)_3SiH$	$(CH_3)_6Si_2$	Corrected % Yields* $(CH_3)_3SiH$	$(CH_3)_6Si_2$	$(Rate_1)^{1/2}$ (moles cc^{-1}sec^{-1})$^{1/2}$ $\times 10^6$	$Rate_2$ moles cc^{-1}sec^{-1} $\times 10^{12}$	$\dfrac{Rate_2}{(Rate_1)^{1/2}}$ $\times 10^6$	SiH_4 concentration moles cc^{-1} $\times 10^8$
1.00	57.2	42.8	57.7	42.3	0.480	0.321	0.669	5.35
2.00	78.1	21.9	79.7	20.3	0.358	0.527	1.472	10.70
3.00	78.4	21.6	80.0	20.0	0.358	0.529	1.477	16.05
1.43	65.6	34.4	66.5	33.5	0.441	0.396	0.898	7.65
0.60	44.7	55.3	44.8	55.2	0.528	0.224	0.424	3.21
0.40	34.7	65.3	34.6	65.4	0.560	0.157	0.280	2.14
1.75	73.1	26.9	74.4	25.6	0.396	0.471	1.189	9.36

* Corrected for disproportionation yield of $(CH_3)_3SiH$ and unscavengeable yield of $(CH_3)_6Si_2$.

** Nitrogen added to bring total pressure to 40 torr.

TABLE V-6

Photolysis of $((CH_3)_3Si)_2Hg$ in the Presence of SiD_4 at Constant Pressure**

SiD_4 Pressure (torr)	% Yields $(CH_3)_3SiH$	% Yields $(CH_3)_6Si_2$	Corrected % Yields* $(CH_3)_3SiH$	Corrected % Yields* $(CH_3)_6Si_2$	$(Rate_1)^{1/2}$ (moles $cc^{-1}sec^{-1})^{1/2}$ $\times 10^6$	$Rate_2$ moles $cc^{-1}sec^{-1}$ $\times 10^{12}$	$\frac{Rate_2}{(Rate_1)^{1/2}}$ $\times 10^6$	SiD_4 concentration moles $cc^{-1} \times 10^7$
2.0	27.6	72.4	25.7	74.3	0.574	0.115	0.200	1.07
7.0	45.8	54.2	45.7	54.3	0.525	0.232	0.442	3.74
16.0	69.5	30.4	71.3	28.7	0.417	0.435	1.043	8.56
25.0	82.2	17.8	84.6	15.4	0.324	0.575	1.775	13.37
13.0	58.0	42.0	58.9	41.1	0.478	0.326	0.682	6.95
5.0	46.7	53.3	46.7	53.3	0.522	0.239	0.458	2.67
4.0	34.6	65.4	33.4	66.6	0.560	0.157	0.280	2.14

* Corrected for disproportionation yield of $(CH_3)_3SiH$ and unscavengeable yield of $(CH_3)_6Si_2$.

** Nitrogen added to bring total pressure to 31 torr.
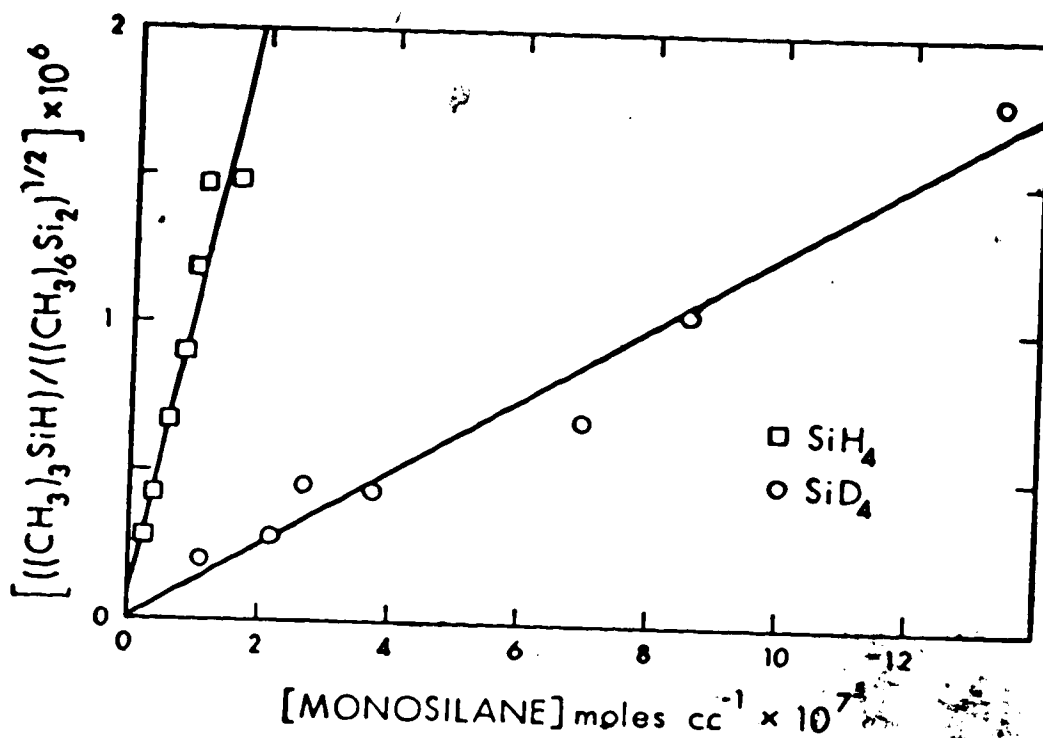
FIGURE V-4. Relative Rate Plots for the Abstraction/Combination Reactions of Trimethylsilyl Radicals with added Monosilane and Monosilane-d_4 at Constant Pressure.

$$\frac{k_8}{k_2^{1/2}} = 1.24 \pm 0.17 \text{ moles}^{1/2} cc^{-1/2} sec^{-1/2}$$

4. Reaction with Methylated Silanes

Rate constants for abstraction by trimethylsilyl radicals from the methylated silanes were determined relative to trimethylsilyl radical recombination

$$(CH_3)_3Si + CH_3SiH_3 \longrightarrow (CH_3)_3SiH + CH_3SiH_2 \qquad (9)$$

$$(CH_3)_3Si + CH_3SiD_3 \longrightarrow (CH_3)_3SiD + CH_3SiD_2 \qquad (10)$$

$$(CH_3)_3Si + (CH_3)_2SiH_2 \longrightarrow (CH_3)_3SiH + (CH_3)_2SiH \qquad (11)$$

$$(CH_3)_3Si + (CH_3)_2SiD_2 \longrightarrow (CH_3)_3SiD + (CH_3)_2SiD \qquad (12)$$

The mercurial was photolyzed in the presence of up to 20 torr CH_3SiH_3, 50 torr CH_3SiD_3, 75 torr $(CH_3)_2SiH_2$ and 50 torr $(CH_3)_2SiD_2$ with nitrogen added to keep the pressure constant. The results are shown in Tables V-7, V-8, V-9, V-10 and Figures V-5, V-6.

Least squares treatment of the plots gave the results

$$\frac{k_9}{k_2^{1/2}} = 2.21 \pm 0.16 \text{ moles}^{1/2} cc^{-1/2} sec^{-1/2}$$

$$\frac{k_{10}}{k_2^{1/2}} = 5.77 \pm 0.74 \times 10^{-1} \text{ moles}^{1/2} cc^{-1/2} sec^{-1/2}$$

$$\frac{k_{11}}{k_2^{1/2}} = 6.99 \pm 0.99 \times 10^{-1} \text{ moles}^{1/2} cc^{-1/2} sec^{-1/2}$$

$$\frac{k_{12}}{k_2^{1/2}} = 3.21 \pm 0.29 \times 10^{-1} \text{ moles}^{1/2} cc^{-1/2} sec^{-1/2}$$

TABLE V-7

Photolysis of $((CH_3)_3Si)_2Hg$ in the Presence of $(CH_3)SiH_3$ at Constant Pressure**

| $(CH_3)SiH_3$ Pressure (torr) | % Yields | | Corrected % Yields* | | $(Rate_1)^{1/2}$ (moles cc^{-1} sec^{-1})$^{1/2}$ x 10^7 | $Rate_2$ moles cc^{-1} sec^{-1} x 10^{13} | $\dfrac{Rate_2}{(Rate_1)^{1/2}}$ x 10^6 | $(CH_3)SiH_3$ concentration moles cc^{-1} x 10^7 |
	$(CH_3)_3SiH$	$(CH_3)_6Si_2$	$(CH_3)_3SiH$	$(CH_3)_6Si_2$				
1.0	28.5	71.5	26.7	73.3	5.76	1.21	0.210	0.535
5.0	49.8	50.2	50.2	49.8	5.11	2.64	0.517	2.67
10.0	75.3	24.7	77.4	22.6	3.79	4.96	1.31	5.35
15.0	85.4	14.6	88.0	12.0	2.88	6.17	2.14	8.02
19.5	85.5	14.5	88.1	11.9	2.88	6.18	2.14	10.4
7.7	71.8	28.2	73.7	26.3	4.04	4.58	1.13	4.12
2.6	47.3	52.7	47.4	52.6	5.19	2.45	.472	1.39

* Corrected for disproportionation yield of $(CH_3)_3SiH$ and unscavengeable yield of $(CH_3)_6Si_2$.

** Nitrogen added to keep total pressure at 40 torr.

TABLE V-8

Photolysis of $((CH_3)_3Si)_2Hg$ in the Presence of CH_3SiD_3 at Constant Pressure**

CH_3SiD_3 Pressure (torr)	% Yields $(CH_3)_3SiH$	% Yields $(CH_3)_6Si_2$	Corrected % Yields* $(CH_3)_3SiH$	Corrected % Yields $(CH_3)_6Si_2$	$(Rate_1)^{1/2}$ (moles cc^{-1} $sec^{-1})^{1/2}$ $\times 10^{12}$	$Rate_2$ moles cc^{-1} sec^{-1} $\times 10^6$	$\frac{Rate_2}{(Rate_1)^{1/2}}$ $\times 10^6$	CH_3SiD_3 concentration moles $cc^{-1} \times 10^6$
20.5	50.2	49.8	50.5	49.5	0.265	0.509	0.521	1.097
52.0	79.4	20.6	81.7	18.3	0.543	0.348	1.560	2.782
10.5	33.7	66.3	32.4	67.6	0.152	0.562	0.270	.562
30.0	63.0	37.0	64.3	35.7	0.372	0.453	0.821	1.605
45.0	78.6	21.4	80.8	19.2	0.532	0.354	1.503	2.407
5.0	20.4	79.6	17.6	82.4	0.076	0.596	0.127	0.267
36.0	66.1	34.9	66.9	33.1	0.397	0.441	0.890	1.926

* Corrected for disproportionation yield of $(CH_3)_3SiH$ and unscavengeable yield of $(CH_3)_6Si_2$.

** Nitrogen added to bring total pressure to 70 torr.

FIGURE V-5. Relative Rate Plots for the Abstraction/Combination
Reactions of Trimethylsilyl Radicals with Added
Monomethylsilane and Monomethylsilane-d$_3$ at Constant
Pressure.

TABLE V-9

Photolysis of $((CH_3)_3Si)_2Hg$ in the Presence of $(CH_3)_2SiH_2$ at Constant Pressure**

$(CH_3)_2SiH_2$ Pressure (torr)	% Yield $(CH_3)_3SiH$	% Yield $(CH_3)_6Si_2$	Corrected % Yields* $(CH_3)_3SiH$	Corrected % Yields* $(CH_3)_6Si_2$	$(Rate_1)^{1/2}$ (moles cc^{-1}sec^{-1})$^{1/2}$ $\times 10^7$	$Rate_2$ moles cc^{-1} sec^{-1} $\times 10^{13}$	$\dfrac{Rate_2}{(Rate_1)^{1/2}} \times 10^7$	$(CH_3)_2SiH_2$ concentration moles cc$^{-1} \times 10^7$
10.0	50.0	50.0	48.7	51.3	5.14	2.53	4.92	5.35
20.0	62.2	37.8	61.4	30.6	4.67	3.48	7.46	10.7
30.0	78.2	21.8	78.0	22.0	3.75	5.02	13.38	16.0
40.0	80.3	19.7	80.1	19.9	3.60	5.24	14.55	21.4
1.0	14.6	85.4	10.9	89.1	6.07	0.455	0.749	0.535
75.0	86.5	13.5	86.4	13.6	3.07	5.96	19.4	40.1
5.0	36.4	63.6	34.3	65.7	5.57	1.63	2.93	2.67

* Corrected for disproportionation yield of $(CH_3)_3SiH$ and unscavengeable fraction of $(CH_3)_6Si_2$.

** Nitrogen added to keep total pressure at 75 torr.

TABLE V-10

Photolysis of ((CH$_3$)$_3$Si)$_2$Hg in the Presence of (CH$_3$)$_2$SiD$_2$ at Constant Pressure**

(CH$_3$)$_2$SiD$_2$ Pressure (torr)	% Yield (CH$_3$)$_3$SiH	% Yield (CH$_3$)$_6$Si$_2$	Corrected % Yields* (CH$_3$)$_3$SiH	Corrected % Yields* (CH$_3$)$_6$Si$_2$	(Rate$_1$)$^{1/2}$ (moles cc^{-1} sec^{-1})$^{1/2}$ x 10^6	Rate$_2$ (moles cc^{-1} sec^{-1}) x 10^{12}	Rate$_2$/(Rate$_1$)$^{1/2}$ x 10^6	(CH$_3$)$_2$SiD$_2$ concentration moles cc^{-1} x 10^6
15.0	37.0	63.0	36.1	63.9	.553	.173	.313	.803
13.0	34.7	65.3	33.5	66.5	.559	.159	.284	.695
8.0	22.3	77.7	19.7	80.3	.590	.0863	.146	.429
25.5	49.3	50.7	49.6	50.4	.512	.259	.506	1.364
35.5	55.3	44.7	54.9	45.1	.492	.298	.604	1.899
52.0	66.1	33.9	67.6	32.4	.438	.402	.918	2.782

* Corrected for disproportionation yield of (CH$_3$)$_3$SiH and unscavengeable yield of (CH$_3$)...

** Nitrogen added to bring total pressure to 75 torr.
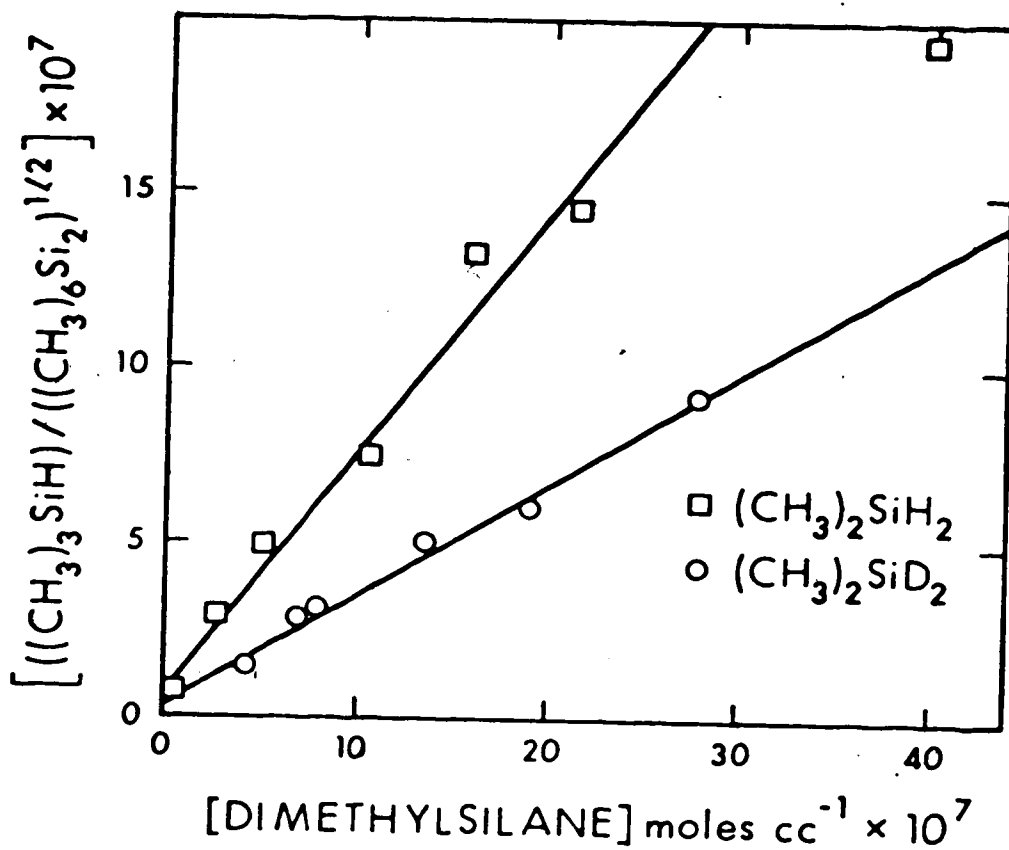
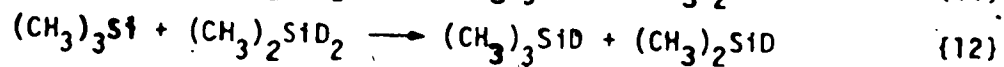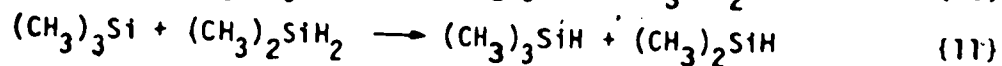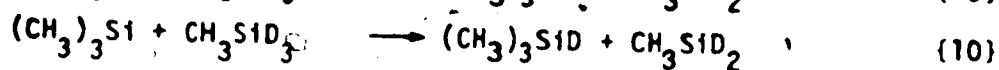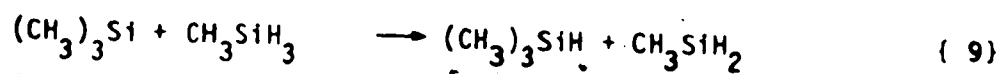FIGURE V-6. Relative Rate Plots for the Abstraction/Combination Reactions of Trimethylsilyl Radicals with Added Dimethylsilane and Dimethylsilane-d$_2$ at Constant Pressure.

The mercurial was also photolyzed in the presence of up to 75 torr of dimethylsilane with no nitrogen added to maintain a constant pressure.

The results are shown in Table V-11 and Figure V-7 from which

$$\frac{k_{11}'}{k_2^{1/2}} = 5.42 \times 10^{-1} \text{ moles}^{1/2} \text{cc}^{-1/2} \text{sec}^{-1/2}$$

5. Reaction with Isobutane

To obtain a comparable rate with a carbon system the mercurial was photolyzed in the presence of up to 200 torr of isobutane.

$$(CH_3)_3Si + (CH_3)_3CH \longrightarrow (CH_3)_3SiH + (CH_3)_3C \qquad \{13\}$$
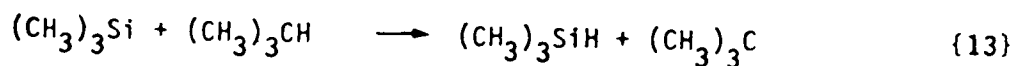
The results are shown in Table V-12 and Figure V-8 and least mean squares treatment of the results gave

$$\frac{k_{13}}{k_2^{1/2}} = 4.78 \pm 1.26 \times 10^{-2} \text{ moles}^{1/2} \text{cc}^{-1/2} \text{sec}^{-1/2}$$

B. KINETICS AND CALCULATIONS

1. Relative Rate Constants and Necessary Corrections

The relative rate constants for abstraction by trimethylsilyl radicals, which are summarized in Table V-13, were obtained on the assumption that abstraction was the sole source of trimethylsilane, but we must take into account the possibility of other sources of tri-methylsilane. The most likely additional source is from cross-disproportionation between a trimethylsilyl radical and the other silyl radical formed in the abstraction step. It is unlikely that

TABLE V-11

Photolysis of $((CH_3)_3Si)_2Hg$ in the Presence of $(CH_3)_2SiH_2$

$(CH_3)_2SiH_2$ Pressure (torr)	% Yields $(CH_3)_3SiH$	% Yields $(CH_3)_6Si_2$	Corrected % Yields* $(CH_3)_3SiH$	Corrected % Yields* $(CH_3)_6Si_2$	$(Rate_1)^{1/2}$ (moles cc^{-1}sec^{-1})$^{1/2}$ $\times 10^7$	$Rate_2$ moles cc^{-1} sec^{-1} $\times 10^{14}$	$\frac{Rate_2}{(Rate_1)^{1/2}}$ $\times 10^7$	$(CH_3)_2SiH_2$ concentration moles cc^{-1} $\times 10^7$
1.0	16.0	84.0	12.9	87.1	6.05	5.33	0.88	0.535
10.5	28.5	71.5	26.8	73.2	5.76	12.1	2.10	5.62
55.0	81.1	18.9	83.5	16.5	3.33	56.2	15.87	29.4
50.0	78.5	21.5	80.8	19.2	3.54	53.3	15.05	26.8
75.0	86.5	13.5	86.4	13.6	3.06	59.6	19.46	40.0
25.5	59.3	40.7	60.3	39.7	4.72	33.9	7.18	13.6
35.5	69.8	30.2	71.6	28.4	4.17	43.6	10.45	19.0

* Corrected for disproportionation yield of $(CH_3)_3SiH$ and unscavengeable fraction of $(CH_3)_6Si_2$.
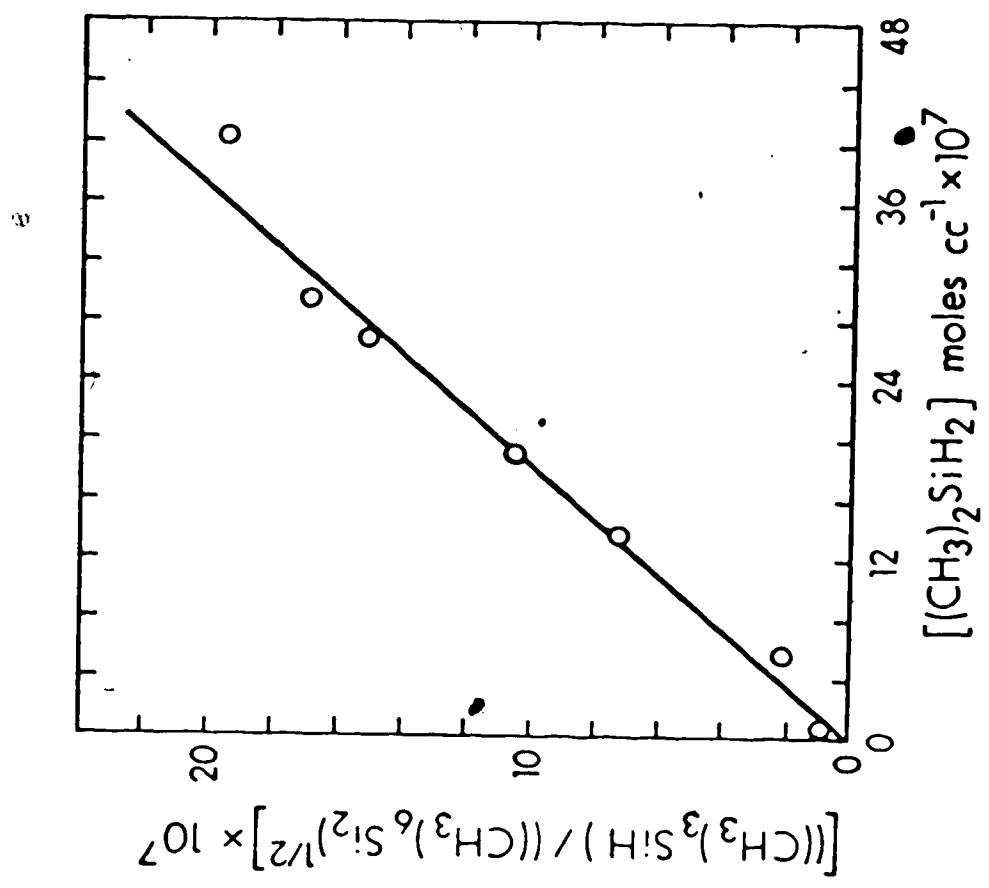
FIGURE 9-7. Relative Rate Plot for the Abstraction/Combination Reactions of Trimethylsilyl Radicals with Added Dimethylsilane.

TABLE V-12

Photolysis of $((CH_3)_3Si)_2Hg$ in the Presence of $(CH_3)_3CH$ at Constant Pressure**

$(CH_3)_3CH$ Pressure (torr)	% Yields $(CH_3)_3SiH$	% Yields $(CH_3)_6Si$	Corrected % Yields* $(CH_3)_3SiH$	Corrected % Yields* $(CH_3)_6Si$	$(Rate_1)^{1/2}$ (moles $cc^{-1} sec^{-1})^{1/2}$ x 10^6	$Rate_2$ moles $cc^{-1} sec^{-1}$ x 10^{13}	$\dfrac{Rate_2}{(Rate_1)^{1/2}}$ x 10^7	$(CH_3)_3CH$ concentration moles cc^{-1} x 10^6
100	26.2	73.8	24.1	75.9	0.582	1.867	1.833	5.35
157	49.5	50.5	49.7	50.3	0.512	2.606	5.090	8.40
206	46.4	53.6	46.3	63.7	0.524	2.355	4.494	11.02
30	14.0	86.0	10.5	89.5	0.609	0.440	0.722	1.60
50	17.3	82.7	14.2	85.8	0.602	0.600	0.997	2.67
75	26.8	73.2	24.8	75.2	0.580	1.115	1.922	4.01
130	40.4	59.6	39.8	60.2	0.543	1.947	3.586	6.95

* Corrected for disproportionation yield of $(CH_3)_3SiH$ and unscavengeable yield of $(CH_3)_6Si_2$.

** Nitrogen added to bring total pressure to 200 torr.

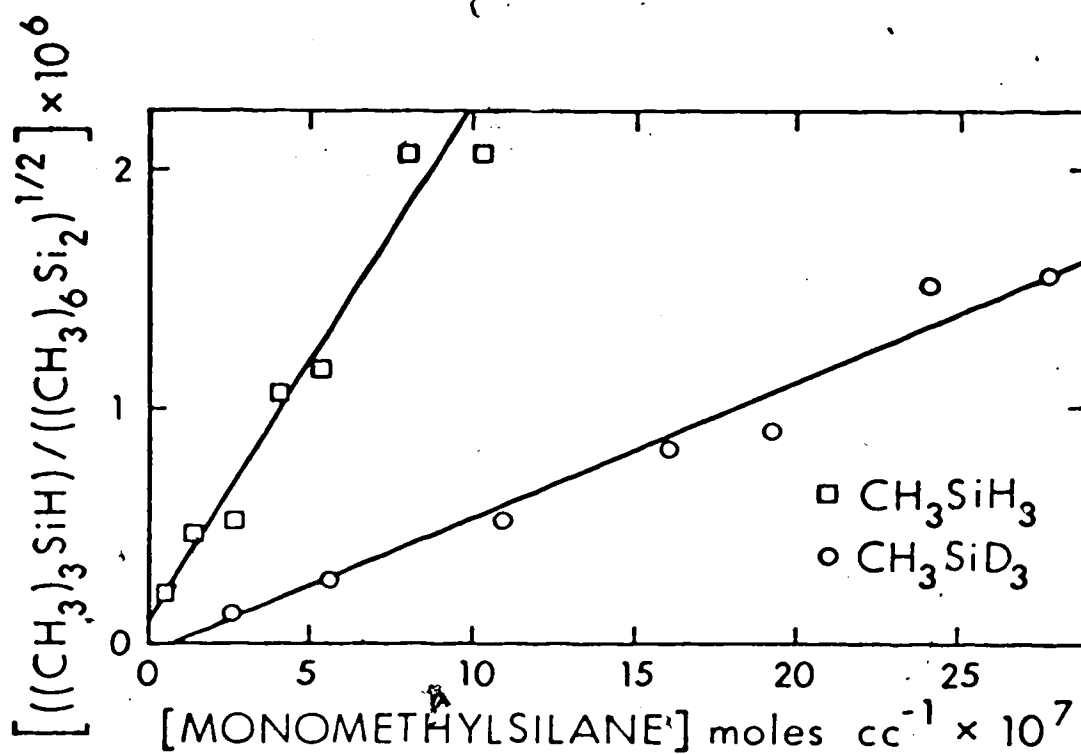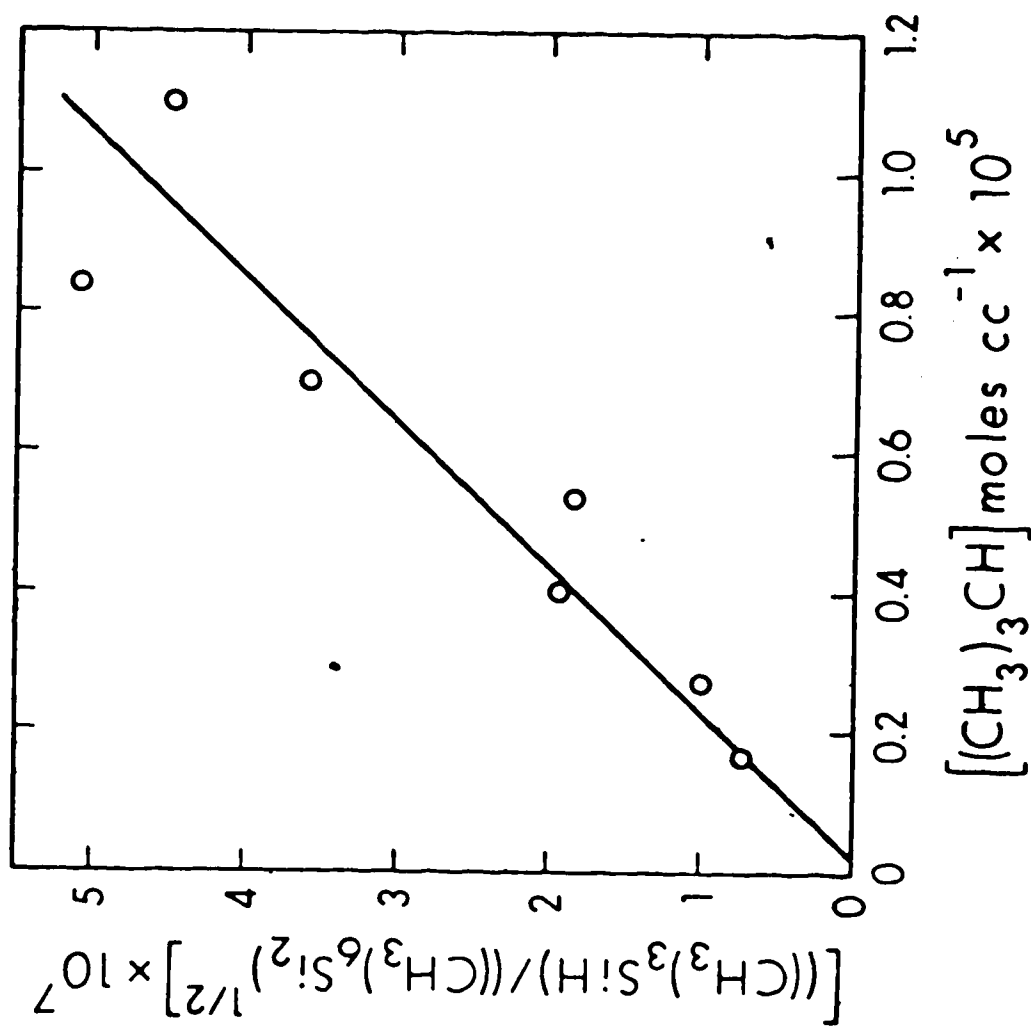FIGURE V-8.   Relative Rate Plot for the Abstraction/Combination Reactions of Trimethylsilyl Radicals with Added 'Isobutane at Constant Pressure.

TABLE V-13

Relative Rate Constants for Reaction of Trimethylsilyl
Radicals with Nondeuterated and Deuterated Silanes

Reaction	$\dfrac{k_{abstraction}}{k^{1/2}_{combination}}$
$(CH_3)_3Si + Si_2H_6$	$1.01 \pm 0.35 \times 10^3$
Si_2D_6	$2.70 \pm 0.50 \times 10^2$
SiH_4	$1.31 \pm 0.12 \times 10^1$
SiD_4	1.24 ± 0.17
CH_3SiH_3	2.21 ± 0.36
CH_3SiD_3	$5.77 \pm 0.74 \times 10^{-1}$
$(CH_3)_2SiH_2$	$6.99 \pm 0.99 \times 10^{-1}$
$(CH_3)_2SiD_2$	$3.21 \pm 0.29 \times 10^{-1}$
$(CH_3)_3CH$	$4.78 \pm 1.26 \times 10^{-2}$

trimethylsilane would result from abstraction by a trimethylsilyl radical from any product of the system since the added silane is present in much greater concentration. In addition, as Table V-13 shows, the rate of abstraction decreases with increasing methylation on the silane, so that abstraction from products would be less favoured since they would be more substituted than the original silane.

2. Corrections for Cross-Disproportionation Yields

The extent of cross-disproportionation can be estimated by using the following scheme for the total reaction mechanism for photolysis of the mercury compound in the presence of added silane, $HSiR_3$, where R = H, CH_3 or SiH_3.

$$[(CH_3)_3Si]_2Hg + h\nu \longrightarrow 2(CH_3)_3Si + Hg \qquad \{14\}$$

$$(CH_3)_3Si + (CH_3)_3Si \longrightarrow (CH_3)_3SiSi(CH_3)_3 \qquad \{15\}$$

$$\longrightarrow (CH_3)_3SiH + CH_2Si(CH_3)_2 \qquad \{16\}$$

$$(CH_3)_3Si + HSiR_3 \longrightarrow (CH_3)_3SiH + SiR_3 \qquad \{17\}$$

$$(CH_3)_3Si + SiR_3 \longrightarrow (CH_3)_3SiSiR_3 \qquad \{18\}$$

$$\longrightarrow (CH_3)_3SiH + \ddot{S}iR_2 \qquad \{19\}$$

$$SiR_3 + SiR_3 \longrightarrow R_3SiSiR_3 \qquad \{20\}$$

$$\longrightarrow HSiR_3 + \ddot{S}iR_2 \qquad \{21\}$$
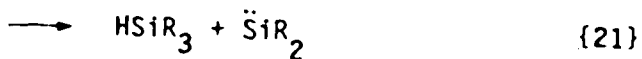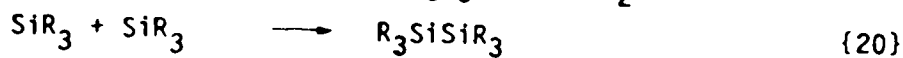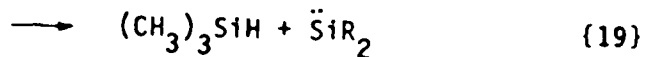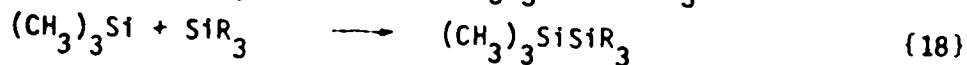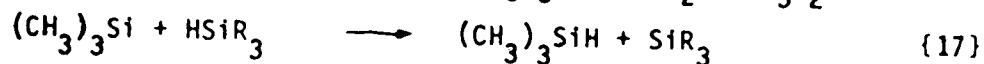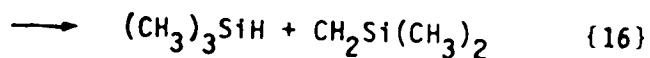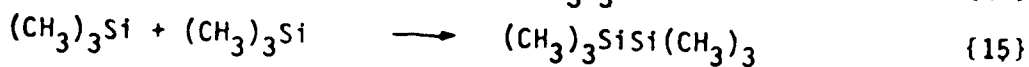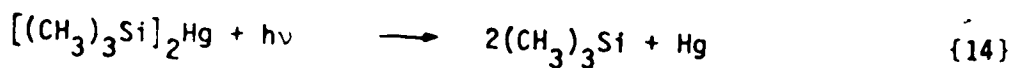
The fate of the diradicals formed in steps {16}, {19} and {21} is probably termination on the walls of the cell but it is possible that if they are formed as the silylene, as is likely in steps {19} and {21}, they could insert into the substrate silane.

For example, the silylene or the diradical can be formed in the monomethylsilane system

$$(CH_3)_3Si + CH_3SiH_2 \longrightarrow (CH_3)_3SiSiH_2CH_3 \qquad (22)$$

$$\longrightarrow (CH_3)_3SiH + CH_3SiH \qquad (23)$$

$$\longrightarrow (CH_3)_3SiH + CH_2SiH_2 \qquad (24)$$
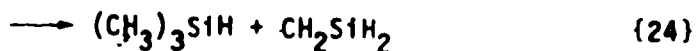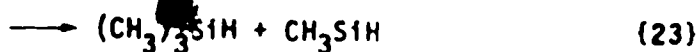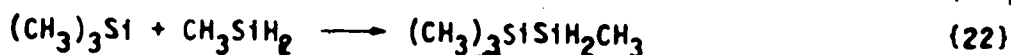
and the silylene can then insert into the substrate silane,

$$CH_3SiH + CH_3SiH_3 \longrightarrow (CH_3)H_2SiSiH_2(CH_3) \qquad (25)$$
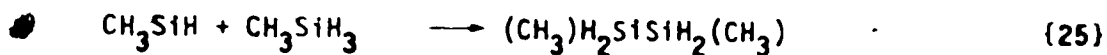
This produces the same product as that formed by combination of two monomethylsilyl radicals and therefore cannot be distinguished as a separate process.

The modes of formation of trimethylsilane can be derived, however, since only steps {16}, {17} and {19} are involved. We accounted for self-disproportionation of the trimethylsilyl radicals (reaction {16}) by using the experimental ratio of trimethylsilane to hexamethyl-disilane obtained in Chapter IV.

The amount of trimethylsilane formed by cross-disproportionation could be calculated by measuring the cross-combination product (reaction {18}) and using the fact that the amount of SiR_3 radicals formed is equal to the trimethylsilane formed by abstraction:

$$(Tri\text{-}MS)_{abstraction} = (CH_3)_3SiSiR_3 + Tri\text{-}MS_{disproportionation} +$$

$$2R_3SiSiR_3 + 2HSiR_3 \, disproportionation \qquad (26)$$
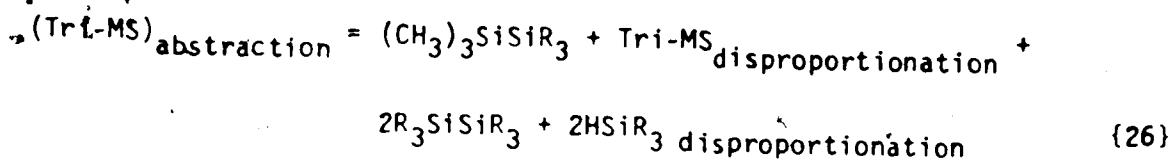
where $(Tri\text{-}MS) = (CH_3)_3SiH$.

Self-combination and disproportionation of SiR_3 radicals to give R_3SiSiR_3 and $HSiR_3$ seems to be relatively unimportant since the yields of the combination product was very small. In any case, since disproportionation yields the original silane substrate, k_{21} could not

be measured. If we ignore reactions {20} and {21} we will obtain a maximum value for the yield of trimethylsilane formed by cross-disproportionation. Thus we can approximate equation {26} to

$$(Tri\text{-}MS)_{abstraction} = (CH_3)_3SiSiR_3 + (Tri\text{-}MS)_{disproportionation} \qquad \{27\}$$

where $(CH_3)_3SiSiR_3$ is the cross-combination product.

Then since $(Tri\text{-}MS)_{total} = (Tri\text{-}MS)_{abs} + (Tri\text{-}MS)_{disp}$

$$(Tri\text{-}MS)_{total} - (Tri\text{-}MS)_{disp.} = (CH_3)_3SiSiR_3 + (Tri\text{-}MS)_{disp.} \qquad \{28\}$$

which reduces to

$$(Tri\text{-}MS)_{disp} = \frac{1}{2}\left[(Tri\text{-}MS)_{total} - (CH_3)_3SiSiR_3\right] \qquad \{29\}$$

Since $(Tri\text{-}MS)_{total}$ and the cross-combination product are measurable quantities, the amount of trimethylsilane formed by cross-disproportionation can be calculated for each silane over the pressure range studied and the cross-disproportionation/combination rate constant ratios for the various silyl radicals can be obtained from equations {18} and {19}.

$$\frac{k_d}{k_c} = \frac{(Tri\text{-}MS)_{disproportionation}}{\text{Cross-combination Product}} \qquad \{30\}$$

The results are shown in Tables V-14, V-15, V-16, V-17 and on Figures V-9 and V-10.

While absolute yields were not measured in all of these experiments, it can be shown that the relative yields of products can be used on an absolute basis since the total yield of the trimethyl-silyl moiety was constant throughout. When the peak areas of each

TABLE V-14

Calculation of the k_d/k_c Ratio for Trimethylsilyl and Disilyl Radicals

Disilane Pressure (microns)	Trimethylsilane total (μmoles)	Cross-Combination Product (μmoles)	Trimethylsilane by Disproportionation (μmoles)	Fraction of Trimethylsilane by Disproportionation	k_d/k_c
10	0.157	0.0002	0.078	0.497	371
18	0.175	0.0003	0.087	0.497	249
30	0.189	0.0053	0.092	0.488	17
38	0.207	0.0025	0.102	0.493	41
60	0.213	0.0026	0.105	0.493	41
			Average	0.494	144
				±0.004	±158

TABLE V-15

Calculation of the k_d/k_c Ratio for Trimethylsilyl and Monosilyl Radicals

Monosilane Pressure (torr)	Trimethylsilane total (μmoles)	Cross-combination Product (μmoles)	Trimethylsilane by Disproportionation (μmoles)	Fraction of Trimethylsilane by Disproportionation	k_d/k_c
0.4	0.100	0.039	0.031	0.310	0.795
0.6	0.133	0.047	0.043	0.323	0.915
1.4	0.211	0.078	0.067	0.317	0.859
1.8	0.236	0.100	0.068	0.288	0.680
2.0	0.260	0.103	0.079	0.304	0.767
3.0	0.255	0.113	0.071	0.278	0.628
			Average	0.303	0.77
				±0.017	±0.11

TABLE V-16.

Calculation of the k_d/k_c Ratio for Trimethylsilyl and Monomethylsilyl Radicals

CH_3SiH_3 Pressure (torr)	Trimethylsilane total (µmoles)	Cross-combination Product (µmoles)	Trimethylsilane by Disproportionation (µmoles)	Fraction of Trimethylsilane by Disproportionation	k_d/k_c
1.0	0.080	0.034	0.023	0.287	0.676
3.0	0.140	0.060	0.040	0.285	0.667
5.0	0.138	0.092	0.023	0.167	0.250
8.0	0.223	0.110	0.057	0.256	0.518
10.0	0.231	0.123	0.054	0.234	0.439
15.0	0.275	0.138	0.069	0.251	0.500
19.0	0.270	0.146	0.062	0.230	0.423
Average				0.244	0.50
				±0.041	±0.15

TABLE V-17

Calculation of the k_d/k_c Ratio for Trimethylsilyl and Dimethylsilyl Radicals

Dimethylsilane Pressure (torr)	Trimethylsilane total (µmoles)	Cross-combination Product (µmoles)	Trimethylsilane by Disproportionation (µmoles)	Fraction of Trimethylsilane by Disproportionation	k_d/k_c
1.0	0.020	0.022	-	-	-
5.0	0.056	0.037	0.009	0.167	0.257
10.0	0.083	0.053	0.015	0.181	0.283
20.0	0.115	0.076	0.019	0.169	0.257
30.0	0.160	0.137	0.011	0.072	0.084
40.0	0.168	0.118	0.025	0.149	0.212
75.0	0.190	0.086	0.052	0.274	0.605
				Average 0.169	0.28
				±0.065	±0.17
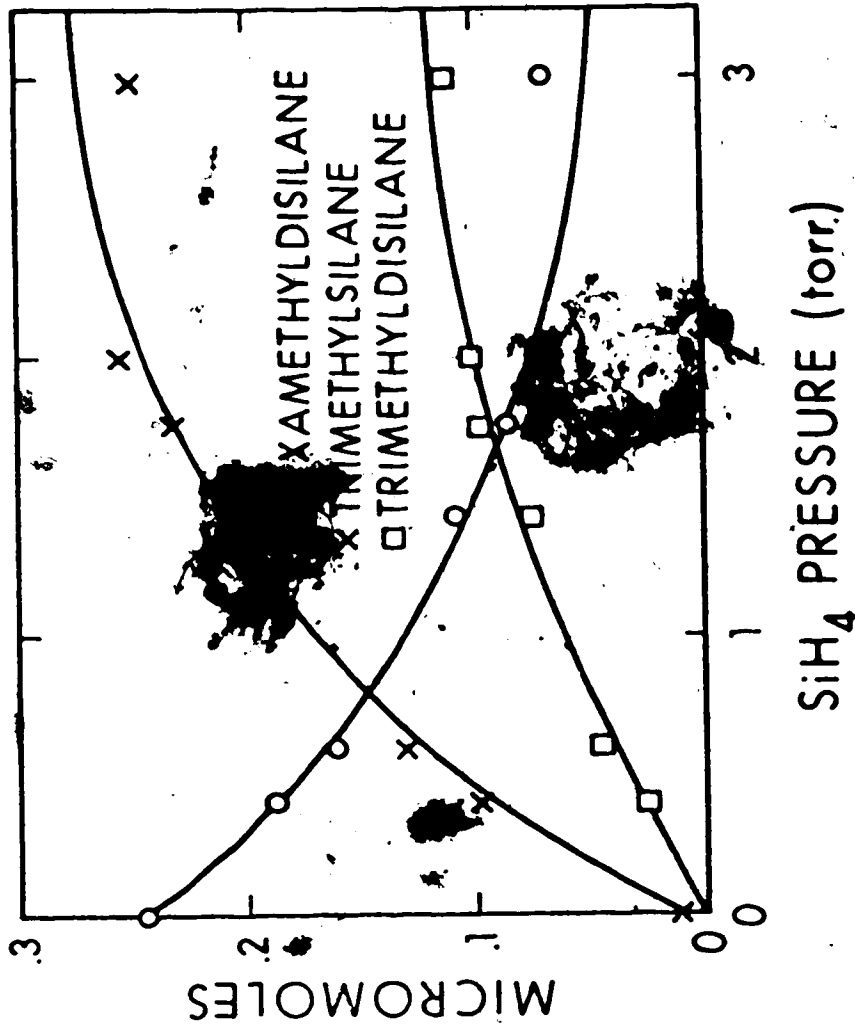
FIGURE V-9. Micromoles of Abstraction, Combination and Cross-combination Products as a function of Monosilane Pressure.
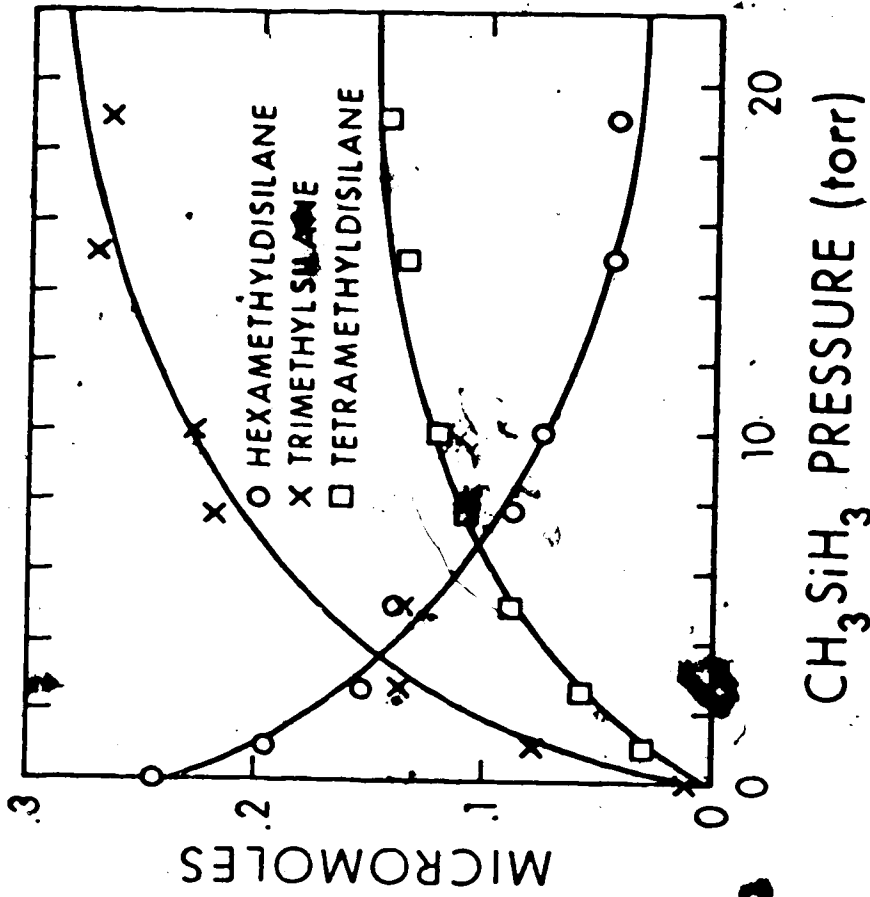
FIGURE V-10. Micromoles of Abstraction, Combination and Cross-combination Products as a Function of Monomethylsilane Pressure.

product were measured, corrected for response factor, and then multiplied by the correct number of trimethylsilyl groups, they were found to be constant, as is shown in Figure V-11, over the full pressure range of the added monomethylsilane.

3. Silyl Radical k_d/k_c Ratios

The calculated k_d/k_c ratios for cross-reactions of trimethyl-silyl radicals with disilyl, monosilyl, monomethylsilyl and dimethyl-silyl radicals are maximum values since no allowance was made for self-reaction of the secondary silyl radicals in the system.

The values obtained for k_d/k_c ratios were:

$(CH_3)_3Si + Si_2H_5$	$<30 \pm 10$	{31}
$(CH_3)_3Si + SiH_3$	$<0.8 \pm 0.4$	{32}
$(CH_3)_3Si + CH_3SiH_2$	$<0.5 \pm 0.2$	{33}
$(CH_3)_3Si + (CH_3)_2SiH$	$<0.3 \pm 0.2$	{34}
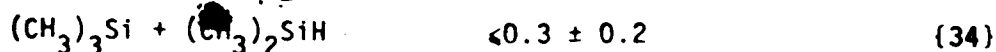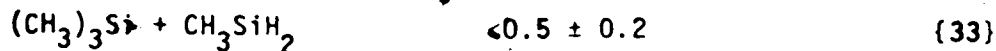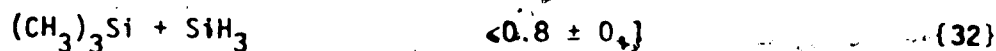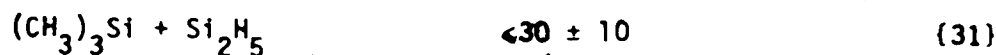
The value for disilyl radicals is obtained if we neglect the first two k_d/k_c values (Table V-14). These are obviously unreliable owing to the very small yields of the combination product at lower pressures.

The k_d/k_c ratios vary somewhat over the pressure ranges employed but it is not certain whether this is real or results from experimental error. The values reported are the average over the range.

These results can be compared with values calculated from earlier work in this laboratory on the Hg photosensitized decomposition of silanes[103,105] and the results are summarized in Table V-18.

It can be seen that the present value of 0.046 for the k_d/k_c
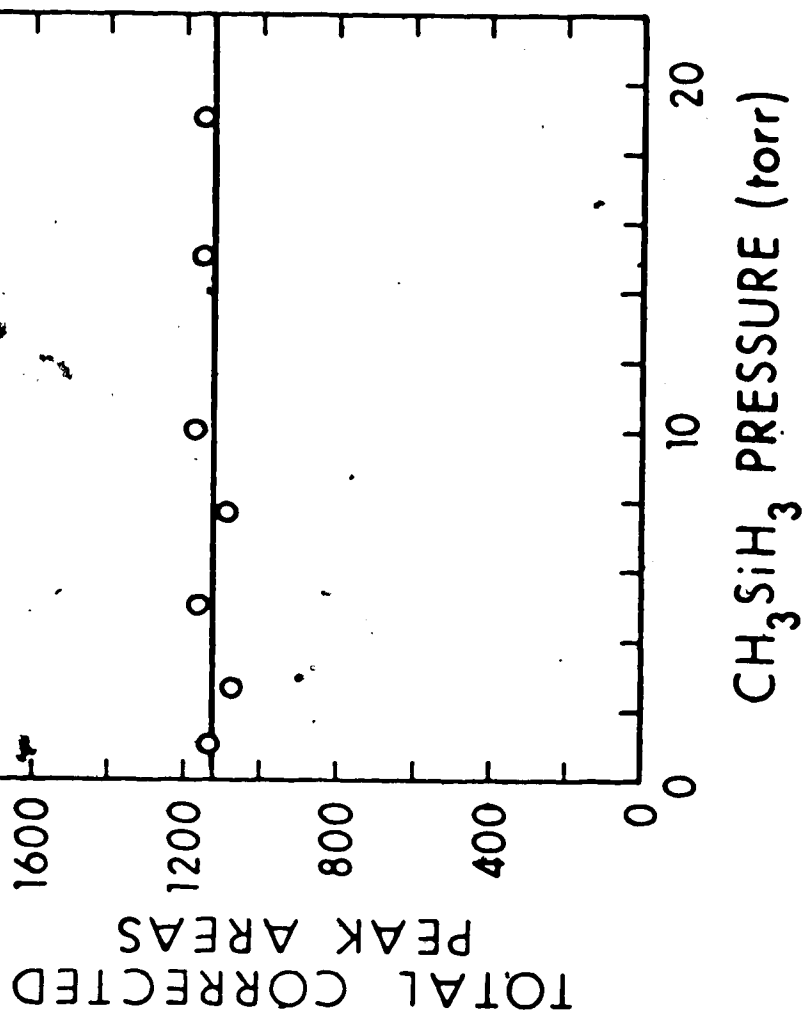
FIGURE V-11. Variation in Total Product Yield as a Function of Monomethylsilane Pressure.

TABLE V-18

Values of k_d/k_c for Various Silyl and Methylated Silyl
Free Radicals

Radicals	$k_d/k_c(25°C)$	Ref.
$(CH_3)_3Si + (CH_3)_3Si$	0.05 ± 0.1	a
$(CH_3)_3Si + (CH_3)_3Si$	0.03	b
$(CH_3)_3Si + (CH_3)_2SiH$	$\leqslant 0.3$	a
$(CH_3)_3Si + (CH_3)SiH_2$	$\leqslant 0.5$	a
$(CH_3)_3Si + SiH_3$	$\leqslant 0.8$	a
$(CH_3)_2SiH + (CH_3)_2SiH$	0.1	b
$CH_3SiH_2 + CH_3SiH_2$	0.1	b
$CH_3SiD_2 + CH_3SiD_2$	0.04	b
$Si_2H_5 + Si_2H_5$	0.1 (400 torr)	c
$SiH_3 + SiH_3$	∞ (up to 1000 torr)	c

[a] Present work.

[b] M. A. Nay, G. N. C. Woodall, O. P. Strausz, H. E. Gunning, J. Amer.
Chem. Soc., **87**, 179 (1965).

[c] T. L. Pollock, H. S. Sandhu, A. Jodhan, O. P. Strausz, J. Amer. Chem.
Soc., **95**, 1017 (1973).

ratio for trimethylsilyl radicals agrees well with the earlier estimate of 0.03, while the values for the self-reactions of other methylated silanes are roughly of the same order of magnitude as those of cross-reactions of trimethylsilyl and secondary radicals. The value for disilyl radicals is quite pressure dependent, reflecting the instability of the excited tetrasilane molecule:

$$Si_2H_5 + Si_2H_5 \longrightarrow Si_4H_{10}^* \qquad (35)$$

$$- \longrightarrow Si_2H_6 + Si_2H_4 \qquad (36)$$

$$Si_4H_{10}^* + M \longrightarrow Si_4H_{10} \qquad (37)$$

$$Si_4H_{10}^* \longrightarrow Si_2H_6 + Si_2H_4 \qquad (38)$$
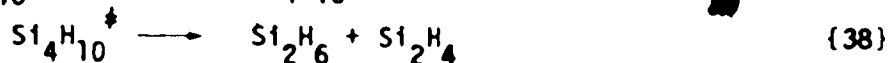
Monosilyl radicals apparently do not recombine up to 1000 torr pressure, in marked contrast to methyl radicals, again due to the instability of the excited Si_2H_6 molecule.

4. Absolute Rate Constant Values

From the series of relative rate constants (Table V-13) we can calculate absolute rate constants for the abstraction reactions with the aid of equation I and a value for k_2, the trimethylsilyl radical recombination rate constant.

The major problem at this point is the uncertainty in the absolute value for k_2. Trotman-Dickenson and co-workers[157] measured a value of $10^{14.25}$ cc mole^{-1}sec^{-1} in a rotating sector experiment using Hg photosensitization of trimethylsilane as a source of trimethylsilyl radicals. This value seems very high, exceeding the value accepted for methyl radical combination by almost an order of magnitude. In addition, when applied to the relative rate constants, it yields absolute

rate constants for abstraction by trimethylsilyl radicals which are orders of magnitude greater than the experimental rate constants for abstraction by methyl radicals from the same silanes. Therefore alternative values for k_2 must be used.

Thynne[158] calculated a value of $10^{5.5}$ cc mole^{-1}sec^{-1} by a thermodynamic method. For the relation

$$2(CH_3)_3Si \xrightleftharpoons[k_{backward}]{k_{forward}} (CH_3)_3SiSi(CH_3)_3 \qquad (39)$$
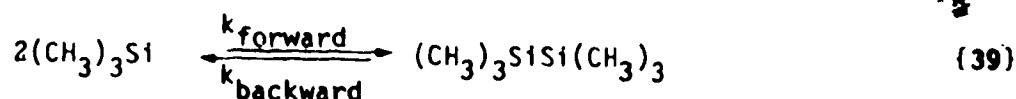
we can write

$$k_{forward} = A_{forward} \, e^{-E_a \, forward/RT} \qquad (40)$$

Using the thermodynamic relationship

$$A_{forward}/A_{backward} = e^{\Delta S/R} \qquad (41)$$

and assuming that there is no activation energy for the forward combination step, equation (40) can be written as

$$\log k_{forward} = \log A_{backward} + \frac{\Delta S}{2.3R} \qquad (42)$$

This is the correct expression in standard atmosphere units and to convert to the more useful concentration units, correction factors must be included. The entropy change at constant pressure can be related to the entropy change in concentration terms by

$$\Delta S_c = \Delta S_p + \Delta nR + \Delta nRlnRT$$

where Δn is the mole change in the reaction. For $\Delta n = 1$ and $T = 298°$,

$$\Delta S_c \ = \ \Delta S_p + 8.3$$

Thus we have a factor of $\frac{8.3}{2.3R}$ for entropy and another factor of 3. to convert from $M^{-1}sec^{-1}$ to $cc.mole^{-1}sec^{-1}$ to give

$$\log k_f \ = \ \log A_b + \frac{\Delta S}{2.3R} + \frac{8.3}{2.3R} + 3 \qquad \{43\}$$

$$= \ \log A_b + \frac{\Delta S}{2.3R} + 4.8 \qquad \{44\}$$

The two variables thus required to calculate $k_{combination}$ the A-factor for decomposition of hexamethyldisilane to two trimethylsilyl radicals and the entropy change for equation {39}.

The A-factor is obtained from pyrolysis experiments on hexamethyldisilane and Thynne used a value of $10^{13.5}$ sec^{-1} in his calculation. This value[159] was later retracted and a more detailed study[28,160] yielded $10^{17.5}$ sec^{-1}, showing that the pyrolysis was more complex than originally believed, with short chains being postulated in the decomposition mechanism. This latter result is in better agreement with the usually accepted range[12,72], $10^{15} - 10^{17}$ sec^{-1}, for decomposition of organic molecules into two polyatomic radicals.

The other variable, the entropy change, is given by

$$\Delta S \ = \ S^\circ(\text{Hexamethyldisilane}) - 2S^\circ(\text{Trimethylsilyl radical}) \qquad \{45\}$$

The entropy of the trimethylsilyl radical is calculated from the well-accepted experimental value[161] for the entropy of trimethylsilane (79.03 e.u.), by applying a correction for the loss of one hydrogen atom and adding $R\ln2$ for the electronic contribution to give

$$S^\circ((CH_3)_3Si) = 80.4 \ cal.deg^{-1}mole^{-1}.$$

There is less agreement on the entropy of hexamethyldisilane. This has not been determined experimentally and the values available are derived from a variety of calculations, comparisons and approximations and give a range from 100 to 120 cal.deg^{-1}mole^{-1}.

Thynne used the Benson and Buss Atomic Additivity Rules[162] and obtained S°(HMDS) = 105 e.u. He then applied an arbitrary correction of 2.5 e.u. for steric strain to this value to obtain 102.5 e.u.

Trotman-Dickenson used the bond additivity values from Ring and O'Neal[163] along with a calculated value of -10.7 e.u. for the Si-Si bond entropy to calculate a value of 120 ± 10 e.u.

Using these two values for S°(HMDS) gives ΔS = -58.3 or -40.8 e.u. and insertion of these data into equation {44} along with the A-factor of 10$^{17.5}$ sec^{-1} produces k_f values of 10$^{9.6}$ or 10$^{13.4}$ cc.mole^{-1} sec^{-1}.

Use of the higher value, 10$^{13.4}$ cc.mole^{-1}sec^{-1}, derived from S°(HMDS) = 120 e.u., gave unacceptably high absolute rate constants for abstraction by trimethylsilyl radicals and since the other value was so much lower, by some four orders of magnitude, better values of k_2 must be used.

The entropy of hexamethyldisilane can be estimated in a number of ways, one of which is to compare the entropies of isobutane[164] (70.4 e.u.) and trimethylsilane (79.0 e.u.), which should reflect any entropy differences between the $C(CH_3)_3$ and $Si(CH_3)_3$ systems, and then compare hexamethylethane[164] (93.1 e.u.) and hexamethyldisilane where the same differences should exist.

$$\frac{S°(Isobutane)}{S°(Trimethylsilane)} = \frac{S°(Hexamethylethane)}{S°(Hexamethyldisilane)} \qquad \{46\}$$

This gives $S°(HMDS) = 104.5$ e.u. and a correction for the Si-Si bond in hexamethyldisilane instead of the C-C bond in hexamethylethane should not add more than ~5 e.u., to give $S°(HMDS) = 110$ e.u. It becomes clear that this type of estimation can provide any value between 100 and 120 e.u.

Another approach is to calculate the cross-combination rate constant for methyl and trimethylsilyl radicals from the equation

$$CH_3 + (CH_3)_3Si \underset{k_b}{\overset{k_f}{\rightleftharpoons}} (CH_3)_4Si \qquad \{47\}$$
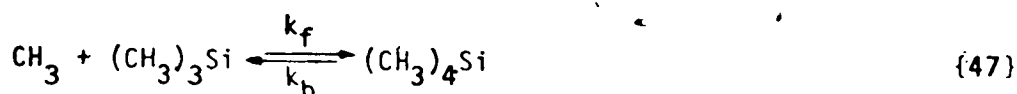
In a similar thermodynamic calculation

$$\log k_f = \log A_b + \frac{\Delta S}{2.3R} + 4.8 \qquad \{44\}$$

The A-factor for tetramethylsilane pyrolysis[116] is given as $10^{14.3}$ sec^{-1} and

$$\Delta S = S°((CH_3)_4Si) - S°(CH_3) - S°((CH_3)_3Si) \qquad \{48\}$$
$$= 85.6 - 46.1 - 80.4$$
$$= -40.9 \text{ e.u.}$$

Insertion of these values into equation {44} gives $\log k_f = 10.2$.

If we take this as the geometric mean of the two self-combinations

$$k_{cross} = 2(k_{methyl} \cdot k_{trimethylsilyl})^{1/2} \qquad \{49\}$$

and since $k_{methyl} = 10^{13.34}$ cc.mole^{-1}sec^{-1}, we obtain

$$k_{trimethylsilyl} = 10^{6.38} \ cc.mole^{-1}sec^{-1}.$$

The fact that this value is very low and is not consistent with the value obtained from hexamethyldisilane pyrolysis is evidence of discrepancies in the calculations. In this case it is probably the experimental A-factor which is too low.

The method we have chosen is based on the assumption that abstraction by trimethylsilyl radicals from silanes will be no faster than abstraction by a correspondingly large alkyl radical. We used the experimental rate constant for abstraction by iso-propyl radicals from monosilane reported by Berkley and co-workers[75] and equated this with the rate constant for abstraction by trimethylsilyl radicals from the same silane to obtain $k_{combination} = 10^{8.0} \ cc.mole^{-1}sec^{-1}$.

If we assume that the $10^{9.6}$ value obtained by modifying Thynne's calculation is the A-factor for the recombination, since he assumed zero activation energy, then from the calculated rate constant of $10^{8.0} \ cc.mole^{-1}sec^{-1}$ we obtain an activation energy of -2.2 kcal. $mole^{-1}$ for the recombination:

$$k_2 = 10^{9.6} \ exp(-2200/RT) = 10^{8.0} \ cc.mole^{-1}sec^{-1} \qquad \{50\}$$

Determination of rate constants for radical dimerization have been made in solution and were found to be very similar to the high values reported for gas phase measurements. Ingold[165] has used electron paramagnetic resonance to measure the rate constants of recombination for a variety of alkyl and other Group IV radicals such as CH_3 (1.1×10^{13} $cc.mole^{-1}sec^{-1}$), $(CH_3)_3C$ ($8.1 \times 10^{12} \ cc.mole^{-1}sec^{-1}$) and $(CH_3)_3Si$ ($5.5 \times 10^{12} \ cc.mole^{-1}sec^{-1}$). Gaspar and co-workers[166], using a flash photolysis-

epr technique measured values for SiH_3 $(4 \times 10^{12}$ cc.mole^{-1}sec$^{-1})$ and $(CH_3)_3Si$ $(3 \times 10^{12}$ cc.mole^{-1}sec$^{-1})$.

These rates are near the diffusion controlled limits for solution and it is somewhat surprising that the gross structural changes between gas and liquid phases should have such minor effects. In any case meaningful comparisons of gas and solution rates are complicated by solution effects such as the frequency of encounters and primary/-secondary recombination[167].

In addition the interpretation of the results is perhaps too simple in that no account is taken of possible reactions of the silicon radicals such as cross-combination or reaction with the initiator, t-butylperoxide. The high affinity of silicon for oxygen, forming a strong bond of about 106 kcal mole^{-1} [41] indicates that such reactions are quite likely. The oversimplification is borne out by the fact that recalculation of the supposed second-order results of Gaspar can give a more reasonable straight line when plotted as a first order reaction. There are also unexplained anomalies concerning product formation which leave these results open to question.

Application of the values $10^{14.25}$ and $10^{8.0}$ cc.mole^{-1}sec^{-1} for the recombination rate constant to the experimental relative rates gives the absolute values shown in Table V-19. The first and second columns show the ranges using $10^{14.25}$ and $10^{8.0}$ respectively. The third column shows the change in values from column 2 when the maximum correction for cross-disproportionation is applied. It can be seen that columns 2 and 3 differ at most by a factor of 2 and while the best value will lie between the two, the error is minimal compared to that between columns 1 and 2.

TABLE V-19

Absolute Rate Constants for Abstraction from Silanes
by Trimethylsilyl Radicals

Reaction	a	Rate Constant $(cc. mole^{-1} sec^{-1})$	
		b	
		uncorrected	corrected
$(CH_3)_3Si + Si_2H_6$	1.35×10^{10}	1.02×10^7	5.15×10^6
Si_2D_6	3.60×10^9	2.72×10^6	1.39×10^6
SiH_4	1.75×10^8	1.32×10^5	9.22×10^4
SiD_4	1.65×10^7	1.25×10^4	9.63×10^3
CH_3SiH_3	2.95×10^7	1.73×10^4	1.68×10^4
CH_3SiD_3	7.70×10^6	4.83×10^3	4.77×10^3
$(CH_3)_2SiH_2$	9.32×10^6	6.56×10^3	5.86×10^3
$(CH_3)_2SiD_2$	4.28×10^6	3.25×10^3	2.62×10^3
$(CH_3)_3CH$	6.38×10^5	4.83×10^2	2.42×10^2

a: using $k_{combination} = 10^{14.25} cc\ mole^{-1}sec^{-1}$.

b: using $k_{combination} = 10^{8.0}\ cc\ mole^{-1}sec^{-1}$.

Shown for comparison in Table V-20 are the experimental absolute rate constants reported by a number of workers[11,39,75,76,168-171] for the hydrogen abstraction reactions by methyl radicals from the same silanes and corresponding alkanes.

It can be seen that the rate constants obtained using the $10^{14.25}$ cc.mole^{-1}sec^{-1} value for the recombination rate constant are between 10 and 200 times larger than the values for methyl radical abstraction, which suggests that they are too high. On the other hand the smaller values derived from $k_2 = 10^{8.0}$ cc.mole^{-1}sec^{-1} are between 10 and 150 times smaller than the rates for methyl radicals.

. Another point of difference is that the methyl abstraction values range over a factor of 70-fold from disilane to dimethylsilane while in the trimethylsilyl case this factor is approximately 1500.

Abstraction by trimethylsilyl radicals from isobutane was found to be slower, by a factor of 15, than abstraction from dimethyl-silane compared to a factor of 2 when the abstraction was by methyl radicals. The absolute value for abstraction by methyl radicals from isobutane lies between the absolute values on columns 1 and 2 of Table V-19 and closer to the high value.

5. BEBO Calculations

Having obtained a set of absolute rate constants for hydrogen abstraction by trimethylsilyl radicals it was decided to employ the BEBO method to calculate activation energies for these reactions and subsequently to derive A-factors.

This empirical method developed by Johnston and co-workers[172] has been shown[31,173] to be able to predict activation energies for

TABLE V-20

Absolute Rate Constants for Abstraction from Silanes and Alkanes by Methyl Radicals

Reaction	Rate Constant (25°C) $cc. mole^{-1} sec^{-1}$
$CH_3 + Si_2H_6$	6.9×10^7
Si_2D_6	1.2×10^7
SiH_4	5.0×10^6
SiD_4	9.5×10^5
CH_3SiH_3	2.1×10^6
CH_3SiD_3	3.1×10^5
$(CH_3)_2SiH_2$	1.0×10^6
$(CH_3)_2SiD_2$	2.8×10^5
$(CH_3)_3SiH$	4.0×10^5
$(CH_3)_3SiD$	1.1×10^5
$(CH_3)_4Si$	1.9×10^4
$CH_3 + CH_4$	1.2×10^1
CH_3CH_3	3.8×10^3
$CH_3CH_2CH_3$	2.5×10^4
$(CH_3)_3CH$	5.1×10^5
$(CH_3)_4C$	3.2×10^3

some hydrogen transfer reactions to within a few $kcal.mole^{-1}$. Details of the method and types of parameters used are given in Appendix II.

The calculations were carried out using the input parameters shown in Table V-21 and the potential energies of activation along with bond lengths and orders in the activated complex are given in Table V-22.

The corrected activation energies derived from the above potential energies of activation are shown in Table V-23 along with A-factors calculated from the lower set of absolute rate constants obtained previously (Column 3, Table V-19). It became clear that if the higher set of rate constants were used abnormally high A-factors for a hydrogen abstraction reaction (10^{15} $cc.mole^{-1}sec^{-1}$) would be obtained, reinforcing the rejection of the rate constant of $10^{14.25}$ $cc.mole^{-1}sec^{-1}$.

Comparison of these values with experimental Arrhenius parameters for abstraction by methyl radicals from silanes (Table V-23) shows that similar trends exist in activation energies, with $E_a(Si_2H_6)$ being the lowest and the values for the methylated silanes being a few kilocalories higher and essentially the same, within the error of the calculation. The A-factors obtained in the calculation seem to indicate a decreasing trend with increased methylation but whether this is real or just an artifact of the method is not clear. The value for dimethylsilane does seem very low, however the average of the four values is $10^{11.5}$, just slightly lower than the average value of $10^{12.1}$ obtained by one group of workers[76] for abstraction by methyl radicals from the same silanes. However, the results from a number of different workers[76] show A-factors for abstraction methyl radicals ranging from $10^{11.0}$ to $10^{12.6}$ $cc.mole^{-1}sec^{-1}$.

It must be kept in mind that the BEBO method is an empirical

TABLE V-21

Input Parameters for BEBO Calculations

Bond Dissociation Energies[a] (kcal mole^{-1})		Reference
$D(SiH_3 - H)$	98	31
$D(Si_2H_5 - H)$	95	Est
$D(CH_3SiH_2 - H)$	96	Est
$D((CH_3)_2SiH - H)$	94	
$D((CH_3)_3Si - H)$	92	
$D(SiH_3 - SiH_3)$	81	19
Bond Distances	Å	
Si-H	1.48	174-177
Si-Si	2.32	178,179
Stretching Frequencies	cm^{-1}	
$SiH_3 - H$	2182	180
$Si_2H_5 - H$	2159	180,182
$CH_3SiH_2 - H$	2167	180,183
$(CH_3)_2SiH - H$	2143	180,184
$(CH_3)_3Si-H$	2125	180,184
$SiH_3 - SiH_3$	434	181
Morse Parameter β	cm^{-1}	
$(CH_3)_3Si + SiH_4$	1.601	b
Si_2H_6	1.979	b
CH_3SiH_3	1.659	b
$(CH_3)_2SiH_2$	1.796	b

TABLE V-21 (cont'd)

Input Parameters for BEBO Calculations

Bond Energy Index[c]	p
Si-H	1.004

[a] Includes zero point energy.

[b] Calculated from $\beta = 1.2177 \times 10^7 \; \omega_e \sqrt{\dfrac{\mu}{E_{ss}}}$

[c] Calculated from $p = \dfrac{0.26[\ln(E_{1s}/E_s)]}{R_x - R_{1s}}$

TABLE V-22

Potential Energies of Activation Calculated by the

BEBO Method

Reaction	Bond Order (Bond Breaking)	Energy (kcal mole^{-1})	Bond Lengths (Å)	
			Bond Breaking	Bond Forming
$(CH_3)_3Si + SiH_4$	0.31	11.2	1.79	1.57
Si_2H_6	0.38	7.6	1.74	1.60
CH_3SiH_3	0.38	10.9	1.73	1.60
$(CH_3)_2SiH_2$	0.44	9.6	1.70	1.63

TABLE V-23

Calculated and Experimental Arrhenius Parameters
for Abstraction from Silanes

Reaction	Log A ($cc\ mole^{-1}sec^{-1}$)	E_a ($kcal\ mole^{-1}$)
	Calculated Arrhenius Parameters	
$(CH_3)_3Si + SiH_4$	12.3	10.0
Si_2H_6	11.3	6.2
CH_3SiH_3	11.4	9.8
$(CH_3)_2SiH_2$	10.9	9.6
	Experimental Arrhenius Parameters	
$CH_3 + SiH_4$	12.2	7.5
Si_2H_6	12.0	5.6
CH_3SiH_3	12.3	8.1
$(CH_3)_2SiH_2$	12.1	8.3

calculation and that the output can be no more accurate than the values used for input parameters.

The bond lengths and vibrational frequencies are reasonably well known but there is a wide range in silicon bond energies (Table I-1). Earlier results favoured 81 kcal mole^{-1} for $D((CH_3)_3Si-H)$ while more recent measurements give 88-90 kcals mole^{-1}. There is good agreement on $D(SiH_3-H)$ as 94 kcal mole^{-1} but the values for the other partially substituted silanes are usually interpolated. We have chosen the set of higher values since the relative ease of abstraction by trimethylsilyl radicals would indicate that a reasonably strong Si-H bond is being formed. In addition, abstraction becomes more difficult with increasing methylation, pointing to the possibility that Si-H bond energies do not decrease as much with methylation as was formerly suggested.

This point of view is reinforced by calculation of the Si-H bond energies by the method of Benson and Luria[185-187]. This model proposes that the difference in C-H bond enthalpies in hydrocarbons is due to the electrostatic energy arising from the interaction of formal negative (carbon) and positive (hydrogen) charges on each atom. The model satisfactorily explains the deviations from the law of bond additivity which are observed for alkanes and predicts the decrease in carbon-hydrogen bond strength from methane to isobutane.

The same calculation can be applied to silanes (see Appendix III) and although absolute bond energies cannot be derived because of the lack of data on additional parameters, the differences between the silicon-hydrogen bond energies can be calculated. These are found to be relatively insensitive to small changes in the absolute

value of the formal electrostatic charge and, when combined with the literature value for $D(H-SiH_3)$, they give the silicon-hydrogen bond energies shown along with the corresponding alkanes on Table V-24.

It can be seen that the method reproduces the carbon-hydrogen bond energies to within one kcal.mole^{-1} and that the values for the silanes vary over a much smaller range with the disilane bond energy being the lowest. This result may help to explain why abstraction from disilane was the fastest of the silanes studied.

C. DISCUSSION

The results obtained allow us to propose a description of the abstraction, combination and disproportionation reactions of various silyl radicals and in particular those of the trimethylsilyl radical.

On the basis of the experimental data and known A-factors for abstraction reactions it appears that the recombination rate constant for trimethylsilyl radicals is some orders of magnitude slower than the collision frequency. Assuming an effective collision diameter of 7.22Å for trimethylsilane[141] the room temperature collision frequency is found to be 2×10^{13} cc.mole^{-1}sec^{-1}.

The results seem to indicate a value for k_2 of $10^{8.0}$ cc.mole^{-1} sec^{-1} and it is somewhat difficult to explain such a low rate constant.

The same situation exists for large alkyl radicals (Table I-3) where work of the last few years points to a value of $10^{8.4}$ cc.mole^{-1} sec^{-1} for the t-butyl recombination rate constant[57]. These lower values agree more readily with the thermochemistry in the alkyl radical systems but it is not clear if the same holds true for silyl systems since in this case the thermochemical parameters are less well defined.

· TABLE V-24

Carbon-Hydrogen and Silicon-Hydrogen Bond Energies
Calculated by the Electrostatic Interaction Method

| Molecule | Bond Energies (kcal mole^{-1}) | |
	Obsd.[a]	Calcd.
H-CH$_3$	104	104
H-C$_2$H$_5$	98	98.3
H-i-C$_3$H$_7$	94.5	93.7
H-t-C$_4$H$_9$	91	90.3
H-SiH$_3$	94[b]	94
H-SiH$_2$CH$_3$	-	93.8
H-SiH(CH$_3$)$_2$	-	93.3
H-Si(CH$_3$)$_3$	80-90[b]	92.0
H-Si$_2$H$_5$	-	90.8

a: Reference 12.

b: Table I-1.

The existence of rotational barriers which could contribute to activation energies in the combination of larger radicals might be expected to decrease the recombination rate but there is no real evidence for any activation energy for recombination since no temperature dependence has yet been established.

One might expect this activation energy to be present since the combination of two t-butyl radicals involves the re-orientation of the methyl groups of the planar radicals into the tetrahedral arrangement of the molecule which should increase the methyl group rotational barriers.

Since silyl radicals are pyramidal[47,66,188,189] rather than planar this explanation is not valid but the recombination rate should be lowered due to repulsions in improperly oriented collisions (i.e. back-to-back) since only head-on silicon-silicon collisions would be expected to be effective. The larger covalent radius of the silicon atom[13] and the availability of empty d-orbitals could partially negate this effect.

Most of the recombination rate constants for alkyl radicals are similar, with values around 10^{13} cc.mole^{-1}sec^{-1}, but these do not agree with known thermodynamic data on alkanes and alkyl radicals[58,190]. Some values of the last few years, in contrast, are orders of magnitude lower[53,55,57]. The latest determination of the t-butyl recombination rate constant[191] does, however, point to a high value, 1.2×10^{12} cc.mole^{-1}sec^{-1}.

It appears that current thermochemical data are reliable and errors in the heats of formation and entropies are much smaller than the discrepancies in the values for the recombination rate constants.

It is not surprising that the rate constants for silyl radical recombinations are open to question since even the values for alkyl radicals, which have been studied for far longer, are still not settled.

However, our experimental results would seem to indicate that the rate of trimethylsilyl radical recombination must be some four or five orders of magnitude less than that of methyl radical combination, if it is assumed that the rate of abstraction by trimethylsilyl radicals is less than or equal to the rate of abstraction by methyl radicals from the same silane.

The situation on abstraction from alkanes or silanes is also open to different interpretations. A lot of data are available on the rates of hydrogen abstraction by hydrogen atoms or methyl radicals from alkanes or silanes, but the spread in the reported values makes detailed analysis very speculative.

For abstraction by hydrogen atoms[192] from alkanes the reported A-factors range from 10^{10} to $10^{14.8}$ cc.mole^{-1}sec^{-1} and the activation energies from 4 to 15 kcal.mole^{-1} and it is generally accepted that the A-factors should be 10^{13} - 10^{14} and be essentially constant for all the simple alkanes. The activation energies seem to show a decrease from ~12 kcal.mole^{-1} for methane to ~8 kcal.mole^{-1} for isobutane.

For abstraction by hydrogen atoms from silanes the results are more sparse[193-195] but the A-factors seem to be within the same range as for the alkanes while the activation energies appear to be in the order of 2-3 kcal.mole^{-1}. The BEBO computations on these systems persistently gave values which were too high, from 4 - 9 kcal.mole^{-1}, indicating that the BEBO method may not be applicable to abstraction by hydrogen from silanes.

For methyl radical abstraction from alkanes[11] the A-factors range from 10^{11} - $10^{12.5}$ cc.mole^{-1}sec^{-1} and the activation energies decrease from 14.6 kcal.mole^{-1} for methane to 8.0 kcal.mole^{-1} for isobutane. Thus the activation energies seem to follow the trend in the C-H bond strengths which decrease from 104 kcal.mole^{-1} (CH_3-H) to 91 kcal.mole^{-1} (($CH_3)_3$C-H).

For abstraction by methyl radicals from silanes[75,76] this same trend is not apparent since the activation energies are quite similar: $E_a(SiH_4)$ = 7.1; $E_a(CH_3SiH_3)$ = 8.1, $E_a((CH_3)_2SiH_2)$ = 8.3; $E_a((CH_3)_3SiH)$ = 7.7; $E_a(Si_2H_6)$ = 5.6.

This does not bear any simple relationship to the accepted trend in Si-H bond energies.

Our results also indicate that the activation energies for abstraction by trimethylsilyl radicals from SiH_4, CH_3SiH_3 and $(CH_3)_2SiH_2$ are almost the same with the value for Si_2H_6 being a few kcals.mole^{-1} less.

The values of the activation energies for trimethylsilyl radical abstraction calculated by the BEBO method are 0.6 - 2.5 kcal. mole^{-1} higher than the activation energies for abstraction by methyl radicals. This difference, small as it is, may be related to the large difference in the energy of the bond formed in the abstraction: $D(CH_3$-H) = 104 kcal.mole^{-1} and $D((CH_3)_3Si$-H) = 90 kcal.mole^{-1}.

However, as the BEBO calculations show, the largest contributor to the activation energy is the triplet repulsion between the two atoms which are exchanging the hydrogen. Thus the effect of the bond dissociation energies might be small compared to the differences in the triplet repulsion energy.

Zavitsas and co-workers[196,197], in predicting activation energies, also postulate high triplet repulsion. Thus in the reaction

$$X + H\text{-}Y \longrightarrow X\cdots\cdot H\cdots\cdot Y \longrightarrow X\text{-}H + Y$$
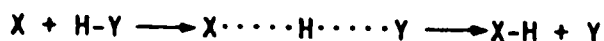
the properties of the X-Y molecule are of great importance even though it is never formed in the reaction. A strong X-Y bond increases the activation energy and vice-versa. In addition, such factors as lower stretching frequencies and greater bond lengths, which broaden the X-Y Morse curve, will result in greater repulsion at a given distance and so give a higher activation energy.

Thus it might be expected that abstraction by trimethylsilyl radicals would require slightly higher activation energies but the observation that the activation energies for abstraction by methyl or trimethylsilyl radicals from silanes seem to be relatively independent of the silane (except for Si_2H_6) would indicate that either the Si-H bond energies are a lot closer than presently accepted values or that the silicon somehow affects the abstraction in such a way that the overall exothermicity becomes less important than triplet repulsion. However, if this were the case, one might expect to see a bigger difference between the triplet interaction of C and Si in abstraction by methyl radicals and the triplet interaction of two Si atoms in abstraction by trimethylsilyl radicals.

Arrhenius parameters have been determined by Trotman-Dickenson and co-workers[198] for the gas phase abstraction of chlorine atoms by trimethylsilyl radicals in a series of experiments with alkyl chlorides. Using their aforementioned value for the recombination rate constant of trimethylsilyl radicals ($10^{14.25}$ cc.mole^{-1}sec^{-1}) they obtained from their

relative rates a range of A-factors from $10^{11.0}$ - $10^{11.3}$ and activation energies from 4.06 kcal.mole^{-1} for methyl chloride to 2.96 kcal.mole^{-1} for t-butyl chloride. These compare with activation energies of 12.9 kcals.mole^{-1} and 10.1 kcals.mole^{-1} for abstraction by methyl radicals from carbon tetrachloride and hexachloroethane respectively[199].

There is at present a controversy over the strength of the Si-Cl bond dissociation energy in chlorotrimethylsilane. Values obtained range from 88[37] to 123[45] kcal.mole^{-1}. This compares to a value of 78.5 kcals.mole^{-1} for $D((CH_3)_3C-Cl)$[12]. The Si-Cl bond is obviously the stronger but by how much is open to question. The activation energies for abstraction by trimethylsilyl radicals are seen to be much lower than the values for abstraction by methyl radicals, and it is not known whether this is in fact due to the higher Si-Cl bond energy or to experimental error.

The experimental isotope effects for the systems studied are shown in Table V-25. It can be seen that the values decrease with methylation and are all smaller than the k_H/k_D ratio for abstraction by methyl radicals except for the monosilane value which is exceptionally high. They do not bear any simple relation to the values for methyl radical abstraction but are closer to the values for iso-propyl and n-propyl radical abstraction from monosilane and disilane[75]. The extremely high value for monosilane would imply that hydrogen quantum tunnelling may be important in this reaction. Quantitative interpretation of the measured isotope effects is not possible.

Primary kinetic hydrogen isotope effects[200-202] are caused primarily by the difference in zero-point energies of the isotopic molecules being compared, but other factors which influence the ratio

TABLE. V-25

Isotope Effects for Abstraction by Trimethylsilyl Radicals

Reaction	k_H/k_D (25°C)
$(CH_3)_3Si$ + monosilane	10.6
disilane	3.7
monomethylsilane	3.8
dimethylsilane	2.2

Isotope Effects for Abstraction by Methyl Radicals

Reaction	k_H/k_D (25°C)
CH_3 + monosilane	5.0
disilane	5.4
monomethylsilane	6.8
dimethylsilane	3.4

include the effect of isotopic substitution on translational motion and on vibrational and rotational levels.

Comparison of experimental[203] and theoretical values for kinetic isotope effects show that present theories are inadequate. Other factors which have to be taken into account include the transmission coefficient and quantum-mechanical tunnelling. The transmission coefficient is the relative probability of decomposition of the activated complex in the forward direction. The value cannot be computed on theoretical grounds and is usually assumed to be unity. The concept of tunnelling admits that there is a finite probability of a particle crossing an energy barrier even if it has less energy than the highest point in the barrier. It depends on mass and so is most noticeably different between H and D isotopes. Because of the lack of data it is impossible to make a quantitiative estimate of the contribution of tunnelling in this case.

Experimental isotope effects can be reproduced in some cases by assuming a model of the activated complex and inserting likely values for geometrical parameters, force constants and frequencies but agreement is often not good[204], reflecting the inadequacies of present theories.

Disproportionation seems to require little or no activation energy and if a small barrier does exist it appears to have the same magnitude as that for combination[205]. Under these circumstances the k_d/k_c ratios do not vary with temperature, thus one determination produces the specific ratio for any pair of radicals.

Values of auto. and cross-disproportionation/combination ratios[59] for a variety of alkyl radicals are given in Table V-26 to

TABLE V-26

Disproportionation-Combination Ratios for Alkyl Radicals

Radical	k_d/k_c
Auto-Disproportionation	
CH_3	-
CH_3CH_2	0.13
$CH_3CH_2CH_2$	0.15
CH_3CHCH_3	0.66
$(CH_3)_3C$	2.3,3.1,2.7
Cross-Disproportionation	
$CH_3CHCH_3 + CH_3CH_2$	0.16
$CH_3CHCH_3 + CH_3CH_2CH_2$	0.41
$(CH_3)_3C + CH_3CH_2$	0.32
$(CH_3)_3C + CH_3CHCH_3$	0.67

contrast with the silyl radical values. It can be seen that combination is usually the favoured process (except for t-butyl radicals) but that the disproportionation rate constant is usually within an order of magnitude of the combination value except for methyl radicals where no disproportionation is observed. In cross reactions, either radical can abstract a hydrogen from the other, in most cases, and the k_d/k_c ratios are usually similar.

As shown in Table V-18 the trend for silicon radicals is in the opposite direction to the trend for alkyl radicals in that monosilyl radicals wholly disproportionate and the k_d/k_c ratio decreases to 0.046 for trimethylsilyl radicals.

It is only possible to compare the relative k_d/k_c ratios with those of alkanes for a few cases since the thermodynamic data are not available for most silicon mono- and di-radicals and the range of values is large even for stable molecules.

A calculation can be made for the monosilyl radical reaction:

$$2SiH_3 \xrightarrow{\quad 1 \quad} Si_2H_6 \qquad \{51\}$$

$$\xrightarrow{\quad 2 \quad} SiH_4 + SiH_2 \qquad \{52\}$$

If we utilize the thermodynamic values in Table V-27

$$\Delta S_{51} = 65.6 - 2(51.4)$$
$$= -37.2 \text{ cal.deg}^{-1}\text{mole}^{-1}$$

$$\Delta S_{52} = 48.9 + 49.6 - 2(51.4)$$
$$= -4.3 \text{ cal.deg}^{-1}\text{mole}^{-1}$$

$$\Delta H_{51} = 17.0 - 2(51.0)$$
$$= -85 \text{ kcal.mole}^{-1}$$

TABLE V-27

Thermodynamic Properties of Some Silicon Compounds

Species	S^b cal mole^{-1}deg^{-1}	ΔH_f° kcal mole^{-1}	Reference
SiH_3	51.4	51.0	206,207
SiH_2	49.6	59.3	206,206
SiH_4	48.9	8.2	12,12
Si_2H_6	65.6	17.0	12,12
$(CH_3)_3Si$	80.4	9.0, -25.6	158,45,37
$(CH_3)_3SiSi(CH_3)_3$	105 - 120	-50, -118	158,157,45,37
$(CH_3)_3SiH$	79.0	-18.1, -55	161,45,37
$(CH_3)_2Si=CH_2$	[79.0]^a	-19.9	43

a: estimated

$$\Delta H_{52} = 8.2 + 59.3 - 2(51.0)$$

$$= -34.5 \text{ kcal.mole}^{-1}$$

Then from $\Delta G = T\Delta S$ {53}

$$\Delta G_{51} = -85 - 298 (-0.372)$$

$$= -73.9 \text{ kcal.mole}^{-1}$$

$$\Delta G_{52} = -34.5 - 298 (-.0043)$$

$$= -33.2 \text{ kcal.mole}^{-1}$$

Thus it would appear from the thermodynamic calculation that combination is much preferred over disproportionation. However, the formation of disilane is so exothermic that it may readily decompose again through a low energy path. It has been shown[208] that disilane pyrolysis gives SiH_4 and SiH_2 as products

$$Si_2H_6 \xrightarrow{\ 600°K\ } SiH_4 + SiH_2$$ {54}

with $k_{54} = 10^{14.31} \exp(-48600/RT) \text{ sec}^{-1}$. Combination of monosilyl radicals thus seems to be an efficient path for disproportionation to monosilane and silene. This low energy decomposition path is also available to methyldisilane and trisilane[209].

The same calculation for methyl radicals

$$2CH_3 \longrightarrow C_2H_6^{\#}$$ {55}

$$\longrightarrow CH_4 + CH_2$$ {56}

gives $\Delta G_{55} = -77.1 \text{ kcal.mole}^{-1}$ and

$$\Delta G_{56} = +3.4 \text{ kcal.mole}^{-1}$$

using values from Benson[12]. Again, combination is much preferred over

disproportionation which is even endothermic, and in this case there is no low energy path for decomposition. The energy rich ethane can either be pressure stabilized or it will fall apart again to give two methyl radicals.

For trimethylsilyl radicals the calculation is complicated by the appearance of the silicon-carbon diradical, or "double-bonded" species, and the unreliability of the available thermodynamic data for silicon molecules.

$$2(CH_3)_3Si \longrightarrow (CH_3)_3SiSi(CH_3)_3 \tag{57}$$
$$\longrightarrow (CH_3)_3SiH + CH_2=Si(CH_3)_2 \tag{58}$$
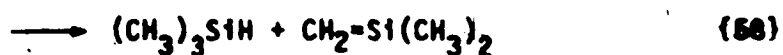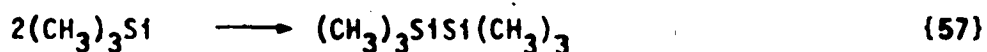
It has been shown earlier that the entropy of hexamethyl-disilane lies between 100 and 120 $cal.deg^{-1}mole^{-1}$ and that the entropies of trimethylsilane and the radical are reliable. The entropy of the dimethylsilaethylene can be estimated from the observation that the corresponding alkene, isobutene, has an entropy value (70.2 e.u.) which is almost the same as its saturated parent, isobutane (70.4 e.u.). The loss of the freely rotating methyl group, of the mass of two hydrogens, of the two C-H stretching frequencies and the change in the C-C frequency from 1000 cm^{-1} to 1650 cm^{-1} in the double bond appear to be compensated for by the formation of the double bond. So if we assume that the same changes take place in the silicon radical case we can approximately equate the dimethylsilaethylene entropy with that of trimethylsilane (79.0 e.u.). So from the data in Table V-27

$$\Delta S_{57} = 105 - 2(80.4) \text{ to } 120 - 2(80.4)$$
$$= -55.8 \text{ to } -40.8 \text{ cal.deg}^{-1}\text{mole}^{-1}.$$

$$\Delta S_{58} = 79.0 + 79.0 - 2(80.4)$$

$$= -2.8 \text{ cal.deg}^{-1}\text{mole}^{-1}.$$

The heats of formation vary to quite a large extent but if we chose a self-consistent set of values, we obtain

$$\Delta H_{57} = -50 - 2(9)$$

$$= -68 \text{ kcal.mole}^{-1}$$

$$\Delta H_{58} = -18.1 - 19.9 - 2(9)$$

$$= -56 \text{ kcal.mole}^{-1}.$$

Then

$$\Delta G_{57} = -68 - 298(-.0558) \text{ or } -68 - 298(-.0408)$$

$$= \underline{-51.4} \text{ or } \underline{-55.8} \text{ kcal.mole}^{-1}$$

$$\Delta G_{58} = -56 - 298(-.0028)$$

$$= \underline{-55} \text{ kcal.mole}^{-1}.$$

Using a different self-consistent set of heats of formation gives

$$\Delta H_{57} = -118 - 2(-25.6) = -66.8 \text{ kcal.mole}^{-1}$$

$$\Delta H_{58} = -55 - 19.9 - 2(-25.6) = -23.7 \text{ kcal.mole}^{-1}$$

Thus

$$\Delta G_{57} = \underline{-50.2} \text{ kcal.mole}^{-1}$$

$$\Delta G_{58} = \underline{-22.9} \text{ kcal.mole}^{-1}$$

The first results suggest that combination and dispropor-
tionation have almost equal probability while the second favours
combination over disproportionation.

Data for the partially methylated radicals is more sparse so
reliable correlations cannot really be made.

Data for t-butyl radical[164,210]

$$2(CH_3)_3C^{\bullet} \longrightarrow (CH_3)_3CC(CH_3)_3 \qquad \{59\}$$

$$\longrightarrow (CH_3)_3CH + CH_2=C(CH_3)_2 \qquad \{60\}$$
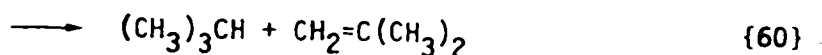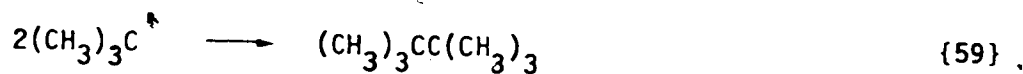
gave the following results:

$$\Delta G_{59} = -51.6 \text{ kcal.mole}^{-1}$$

$$\Delta G_{60} = -47.1 \text{ kcal.mole}^{-1}$$

showing that combination and disproportionation are almost equivalent
although the slightly more favoured combination reaction is not
reflected by the k_d/k_c ratio of 2 to 3.

The calculation of heats of formation may be aided by exten-
sion of the new electrostatic model of Benson and Luria[185-187] which
can account for the observed values for saturated and unsaturated
hydrocarbons and alkyl free radicals.

Correlation of the experimental results with thermodynamic
data will remain difficult until the mechanism of disproportionation
is fully understood.

The present consensus[59] is that combination is a head-to-head
process

$$CH_3CD_2 + D_2CCH_3 \longrightarrow CH_3CD_2CD_2CH_3 \qquad \{61\}$$
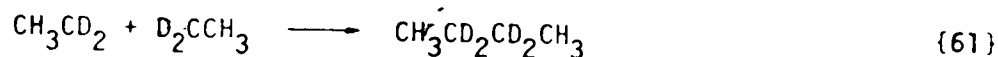
while disproportionation is a head-to-tail process.

$$CH_3CD_2 + CH_3CD_2 \longrightarrow CH_3CD_2H + CH_2=CD_2 \qquad (62)$$
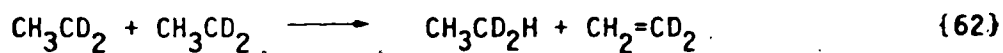
The activated complexes are thought to be different for the two pathways, but both require a very loose transition state and the abnormally high A-factors are difficult to explain on the basis of simple covalent bonding[211].

The values obtained in Table V-18 for cross-disproportionation are upper limits and may have to be revised downward in the light of more information.

Disproportionation does seem to increase with decreasing methylation on the silyl radicals in both auto- and cross-disproportionation reactions, and this suggests increasing stability of the silicon diradical.

Dewar et al.[43] have calculated heats of formation and π-bond energies for a variety of silicon compounds and from their calculated bond lengths the $Si=C$ bond in silaethylene appears to be stronger than that in dimethylsilaethylene.

CHAPTER VI

SUMMARY AND CONCLUSIONS

The present investigation gives a reasonably self-consistent picture of the photochemical decomposition of tetramethylsilane and the reactions of the free radicals produced. The direct photolysis of tetramethylsilane was accomplished with a xenon resonance lamp and the photolysis of bis(trimethylsilyl)mercury with a medium pressure mercury lamp. The hydrogen transfer reactions of trimethylsilyl radicals with a number of silanes were examined separately. The resulting product distributions were accounted for in both photolyses and detailed mechanisms were proposed.

The photo-decomposition of tetramethylsilane gave ten measurable products and a polymer deposit. The mechanism was deduced from the interpretation of pressure studies, time studies, radical scavenging and deuterium labelling and was found to be initiated by at least six primary steps. A few of these could be further subdivided since they involve the loss of two fragments, but these could not be differentiated quantitatively because many of the silicon residues were lost to the polymer. Although the 147 nm line falls in the silicon-hydrogen absorption region, and carbon-hydrogen bonds outnumber silicon-carbon bonds by twelve to four, the predominant mode of decomposition is silicon-carbon cleavage. Radical formation (78%) is favoured over molecular elimination and the product distribution suggests the occurrence of radical cross-disproportionations. The accuracy of the primary quantum yield of the actinometer, carbon

203

dioxide, and the subsequent tetramethylsilane decomposition quantum yield were verified by auxiliary experiments using nitrous oxide as the actinometer. In addition, fluorescence was found to be negligible and a tetramethylsilane decomposition primary quantum yield of unity could only be obtained when the primary quantum yield of carbon monoxide was assumed to be greater than 0.87.

.The trimethylsilyl radical was one of the major primary products in this system and this led to the photolysis of bis(trimethyl-silyl)mercury as a low energy source of the radical. The mechanism was determined from the effect of pressure, exposure time, and radical scavenging with nitric oxide, ethylene and oxygen. The photolysis was a clean source of trimethylsilyl radicals which reacted to give dimerization and disproportionation products.

The k_d/k_c ratio of 0.046 obtained for the trimethylsilyl radicals is much lower than that for the corresponding t-butyl radical but even this low value implies formation of a quasi double-bonded silaethylene in the disproportionation step. Ab initio molecular orbital calculations show that the planar singlet and skew triplet silaethylene are of equivalent stability.

The relative rates of hydrogen abstraction by trimethylsilyl radicals were found to be fastest with disilane and to decrease with methylation by more than three orders of magnitude in dimethylsilane.

Combination of these results with literature data led to the estimation of a trimethylsilyl radical recombination rate constant of $10^{8.0}$ cc mole^{-1}sec^{-1}. Arrhenius parameters for the hydrogen transfer reactions were calculated by the BEBO method and compared with the experimental results for abstraction by methyl radicals. The

calculated activation energíes were similar to, but 1 - 2 kcals mole^{-1} higher than, the methyl values, indicative of the lower reactivity of the trimethylsilyl radical.

While the calculated A-factors showed a decrease with methylation they could also be considered to be constant within the error limits and the average value was within the error range for the methyl abstraction A-factors.

Estimates could also be made of the k_d/k_c ratios for cross-reactions of trimethylsilyl and other silyl radicals and it could be shown that the k_d/k_c ratios exhibit a trend opposite to that for alkyl radicals since k_d/k_c decreased with substitution. This is due partly to the existence of low energy decomposition paths for the excited combination product of two silyl radicals.

The results of this study highlight some of the difficulties inherent in present attempts to explain the photochemistry of silicon compounds and the subsequent abstraction, combination and disproportionation reactions.

The electronic spectra of alkanes are complex and not fully resolved as yet and for silanes only crude approximations, simple correlations between spectra and experiment, are available.

Lack of an agreed self-consistent set of thermodynamic data makes predictions difficult and even where this exists, as for the alkanes, values derived from equilibrium calculations do not always agree well with kinetic results.

It is still not evident if combination reactions have an activation energy or whether there is any activation energy difference between combination and disproportionation. More systematic and

extensive temperature studies should eliminate these doubts.

Notwithstanding the number of detailed and useful interpretations in the literature, explanations of abstraction rates and combination-disproportionation ratios have to be semi-empirical since the full mechanisms of these events are not well understood.

Further work needs to be carried out in the determination of absolute rate constants for radical dimerization by different methods and in the collection and systemization of thermodynamic properties.

In addition more total product measurements and elucidation of detailed mechanisms should be attempted in radical systems to ensure that the reaction studied is not complicated by unknown concurrent processes. In particular the occurrence of disproportionation reactions in silane systems could account for appreciable quantities of abstraction products or reformation of substrate.

Although present results indicate that silaethylene is very reactive, being very polar and with a π-bond energy only half that of a carbon system, it is possible that proper correlation of calculated predictions with experimental results may yet result in the production of a stabler silicon-carbon or silicon-silicon double bond with a measurable lifetime.

BIBLIOGRAPHY

1. R. W. Bott, Organometallic Chem. Rev., **B4**, 427 (1968).

2. R. F. Cunico, J. Organometal. Chem., **83**, 65 (1974).

3. H. Sakurai, Free Radicals, Volume II (ed. by J. K. Kochi), John Wiley and Sons, New York, 1973, Chapter 25.

4. S. S. Washburne, J. Organometal. Chem., **83**, 155 (1974).

5. P. R. Jones, J. Organometal. Chem., **83**, 213 (1974).

6. O. W. Steward, J. Organometal. Chem., **83**, 265 (1974).

7. I. M. T. Davidson, Quarterly Rev., 111 (1971).

8. R. A. Jackson, Adv. Free Radical Chem., **3**, 231 (1969).

9. W. H. Atwell and D. R. Weyenberg, Angew. Chem., **8**, 469 (1969).

10. V. Bažant, V. Chvalousky and J. Rathousky, Organosilicon Compounds, Academic Press, New York (1965).

11. A. F. Trotman-Dickenson, Adv. Free Radical Chem., **1**, 1 (1965).

12. S. W. Benson, Thermochemical Kinetics, John Wiley & Sons, Inc., New York (1968).

13. L. Pauling, The Nature of the Chemical Bond, Cornell University Press, Ithaca, 1960.

14. K. M. Mackay and R. Watt, Organometallic Chem. Rev. A, **4**, 137 (1969).

15. L. C. Glasgow, G. Olbrich and P. Potzinger, Chem. Phys. Lett., **14**, 466 (1972).

16. H. Burger, Angew. Chem., **12**, 474 (1973).

17. C. E. Moore, Atomic Energy Levels, Nat. Bur. Stds., U.S. Circ., 467, Vol. 1 (1948), Vol. 11 (1952), Vol. 111 (1958).

18. J. Higuchi, S. Kubota, T. Kumamoto and I. Tokue, Bull. Chem. Soc. Jap., **47**, 2775 (1974).

19. C. F. Shaw and A. L. Allred, Organometallic Chem. Rev. A, 5, 95 (1970).

20. J. Attridge, Organometallic Chem. Rev. A, 5, 323 (1970).

21. J. Nagy, J. Reffy, J. Organomatallic Chem., 22, 565 (1970).

22. A. N. Egorochkin, N. S. Vyazankin, N. S. Ostasheva, O. V. Kuz'min, N. S. Nametkin, I. F. Kovalev, M. G. Voronkov, J. Organometallic Chem., 59, 117 (1973).

23. E. A. V. Ebsworth, Organometallic Compounds of Group IV Elements, Vol. I, edited by A. G. MacDiarmid (New York: M. Dekker, Inc.), Chapter 1.

24. J. H. Mackey and D. E. Wood, Molecular Physics, 18, 783 (1970).

25. S. W. Benson, J. Chem. Educ., 42, 502 (1965).

26. K. W. Egger and A. T. Cocks, Helvet. Chim. Acta., 56, 1516 (1973).

27. J. A. Kerr, Chem. Rev., 66, 465 (1966).

28. I. M. T. Davidson and A. V. Howard, J. Chem. Soc. Faraday I, 69 (1975).

29. G. G. Hess, F. W. Lampe and L. H. Sommer, J. Amer. Chem. Soc., 87, 5327 (1965).

30. M. A. Ring, M. J. Puentes and H. E. O'Neal, J. Amer. Chem. Soc., 92, 4845 (1970).

31. O. P. Strausz, E. Jakubowski, H. S. Sandhu and H. E. Gunning, J. Chem. Phys., 51, 552 (1969).

32. P. Potzinger and F. W. Lampe, J. Phys. Chem., 74, 587 (1970).

33. A. Hosaka and F. S. Rowland, J. Phys. Chem., 77, 705 (1973).

34. I. M. T. Davidson and A. V. Howard, Chem. Commun., 323 (1973)

35. R. Walsh and J. M. Wells, Chem. Commun., 513 (1973).

36. W. C. Steele, L. D. Nichols and F. G. A. Stone, J. Amer. Chem. Soc., 85, 4441 (1962).

37. S. J. Band, I. M. T. Davidson and C. A. Lambert, J. Chem. Soc. A, 2068 (1968).

38. M. F. Lappert, J. Simpson and T. R. Spalding, J. Organometal. Chem., 17, P1 (1969).

39. J. A. Kerr, A. Stephens and J. C. Young, Int. J. Chem. Kinetics, 1, 339 (1969).

40. S. R. Gunn and L. G. Green, J. Phys. Chem., 65, 779 (1961).

41. A. E. Beezer and C. T. Mortimer, J. Chem. Soc. (A), 514 (1966).

42. Nat. Bur. Std., U.S., Tech. Note 270-3 (1968).

43. M. J. S. Dewar, D. H. Lo, and C. A. Ramsden, J. Amer. Chem. Soc., 97, 311 (1975).

44. D. Quane, J. Phys. Chem., 75, 2480 (1972).

45. P. Potzinger and F. W. Lampe, J. Phys. Chem., 74, 719 (1970).

46. J. M. Gaidis, P. R. Briggs and T. W. Shannon, J. Phys. Chem., 75, 974 (1971).

47. L. Pauling, J. Chem. Phys., 51, 2767 (1969).

48. N. Basco, D. G. L. James and R. D. Suart, Int. J. Chem. Kinetics, 2, 215 (1970).

49. H. E. Van Den Bergh, A. B. Callear and R. J. Norstrom, Chem. Phys. Lett., 4, 102 (1969).

50. G. B. Kistiakowsky and E. K. Roberts, J. Chem. Phys., 21, 1637 (1953).

51. A. Shepp and K. O. Kutschke, J. Chem. Phys., 26, 1020 (1957).

52. R. Hiatt and S. W. Benson, J. Amer. Chem. Soc., 94, 6886 (1972).

53. D. G. Hughes and R. M. Marshall, J. Chem. Soc. Faraday I, 413 (1975).

54. E. L. Metcalfe and A. F. Trotman-Dickenson, J. Chem. Soc., 4620 (1962).

55. R. Hiatt and S. W. Benson, Int. J. Chem. Kinetics, 4, 151 (1972).

56. E. L. Metcalfe, J. Chem. Soc., 3560 (1963).

57. R. Hiatt and S. W. Benson, Int. J. Chem. Kinetics, 5, 385 (1973).

58. D. F. McMillen, D. M. Golden and S. W. Benson, J. Amer. Chem. Soc., 94, 4403 (1972).

59. M. J. Gibian and R. C. Corley, Chem. Rev., 73, 441 (1973).

60. W. B. De More and S. W. Benson, Adv. Photochem., 2, 219 (1964).

61. J. R. McNesby and R. V. Kelly, Int. J. Chem. Kinetics, 3, 293 (1971).

62. W. L. Hase, W. G. Brieland, P. W. McGrath and J. W. Simons, J. Phys. Chem., 76, 459 (1972).

63. W. L. Hase, W. G. Brieland and J. W. Simons, J. Phys. Chem., 73, 4401 (1969).

64. P. M. Kelley, W. L. Hase and J. W. Simons, J. Phys. Chem., 79, 1043 (1975).

65. J. H. Sharp and M. C. R. Symons, J. Chem. Soc. (A), 3068 (1970).

66. R. L. Morehouse, J. J. Christiansen and W. Gordy, J. Chem. Phys., 45, 1751 (1966).

67. K. Y. Choo and P. P. Gaspar, J. Amer. Chem. Soc., 96, 1284 (1974).

68. A. F. Trotman-Dickenson, Chem. & Industry, 379 (1965).

69. O. M. Nefedov, M. N. Manakov, Angew. Chem. Int. Edit., 5, 1021 (1966).

70. B. Cox and H. Purnell, J. Chem. Soc. Faraday I, 71, 859 (1975).

71. R. L. Jenkins, R. A. Kedrowski, L. E. Elliott, D. C. Tappen, D. J. Schlyer and M. A. Ring, J. Organometal. Chem., 86, 347 (1975).

72. H. M. Frey and R. Walsh, Chem. Rev., 69, 103 (1969).

73. F. O. Rice and K. F. Herzfeld, J. Phys. Colloid. Chem., 55, 975 (1951).

74. J. G. Calvert and J. N. Pitts, Photochemistry, John Wiley & Sons, Inc., New York (1966).

75. R. E. Berkley, I. Safarik, H. E. Gunning and O. P. Strausz, J. Phys. Chem., 77, 1741 (1973).

76. R. E. Berkley, I. Safarik, H. E. Gunning and O. P. Strausz, J. Phys. Chem., 77, 1734 (1973).

77. A. G. Alexander, O. P. Strausz, R. Pottier and G. P. Semeluk, Chem. Phys. Lett., 13, 608 (1972).

78. Y. Harada, J. N. Murrell and H. H. Sheena, Chem. Phys. Lett., 1, 595 (1968).

79. B. A. Lombos, P. Sauvageau and C. Sandorfy, J. Molec. Spectros., 24, 253 (1967).   c

80. J. W. Raymonda and W. T. Simpson, J. Chem. Phys., 47, 430 (1967).

81 R. J. Buenker and S. D. Peyerimhoff, Chem. Phys., 8, 56 (1975).

82. S. G. Lias and P. Ausloos, J. Chem. Phys., 43, 2748 (1965).

83. I. D. Clark, J. Atmospheric Sci., 28, 847 (1971).

84. B. H. Mahan, J. Chem. Phys., 33, 959 (1960).

85. L. F. Loucks and R. J. Cvetanovic, J. Chem. Phys., 56, 321 (1972).

86. I. D. Clark and J. F. Noxon, J. Geophys. Rev., 75, 7307 (1970).

87. W. Felder, W. Morrow and R. A. Young, J. Geophys. Res., 75, 7311 (1970).

88. T. G. Slanger, R. L. Sharpless and G. Black, J. Chem. Phys., 61, 5022 (1974).

89. E. C. Y. Inn, J. Geophys. Res., 77, 1991 (1972).

90. M. C. Dodge and J. Heicklen, Int. J. Chem. Kinetics, 3, 269 (1971).

91. J. Y. Yang and F. M. Servedio, J. Chem. Phys., 47, 4817 (1967).

92. M. Zelikoff and L. M. Aschenbrand, J. Chem. Phys., 22, 1680 (1954).

93. K. Obi, A. Clement, H. E. Gunning and O. P. Strausz, J. Amer. Chem. Soc., 91, 1622 (1969).

94. A. G. Alexander and O. P. Strausz, to be published.

95. T. L. Pollock and O. P. Strausz, to be published.

96. M. A. Ring, G. D. Beverly, F. H. Koester and R. P. Hollandsworth, Inorg. Chem., 8, 2033 (1969).

97. H. Okabe and J. R. McNesby, J. Chem. Phys., 34, 668 (1961).

98. R. F. Hampson, Jr., J. R. McNesby, H. Akimoto and I. Tanaka, J. Chem. Phys., 40, 1099 (1964).

99. H. Akimoto and I. Tanaka, Ber. des Bunsenges., 72, 134 (1968).

100. K. Obi, H. Akimoto, Y. Ogata and I. Tanaka, J. Chem. Phys., 55, 3822 (1971).

101. J. R. McNesby, Action Chimique. Biolog. Rad., 37 (1966).

102. P. J. Ausloos and S. G. Lias, Ann. Rev. Phys. Chem., 22, 85 (1971).

103. T. L. Pollock, H. S. Sandhu, A. Jodhan and O. P. Strausz, J. Amer. Chem. Soc., 95, 1017 (1973).

104. S. Siegel and T. Stewart, J. Phys. Chem., 73, 823 (1969).

105. M. A. Nay, G. N. C. Woodall, O. P. Strausz and H. E. Gunning, J. Amer. Chem. Soc., 87, 179 (1965).

106. H. Niki and G. J. Mains, J. Phys. Chem., 68, 304 (1964).

107. E. Siberg, O. Stecher, H. J. Andrascheck, L. Kreuzbichler and E. Staude, Angew. Chem. Int. Edit., 2, 507 (1963).

108. S. W. Bennett, C. Eaborn, R. A. Jackson and R. Pierce, J. Organometal. Chem., 28, 59 (1971).

209. S. ...orn and R. A. Jackson, J. Organometal. Chem., 21, 79 (1970).

110. C. Eaborn, R. A. Jackson and R. W. Walsingham, J. Chem. Soc. (C), 2188 (1967).

111. C. Eaborn, R. A. Jackson and R. W. Walsingham, J. Chem. Soc. Perkin II, 366 (1973).

112. R. Fields, R. N. Haszeldine and R. E. Hutton, J. Chem. Soc. (C), 2559 (1967).

113. J. A. Connor, G. Finney, G. J. Leigh, R. N. Haszeldine, P. J. Robinson, R. D. Sedgwick and R. F. Simmons, Chem. Commun., 178 (1966).

114. G. J. Mains and J. Dedinas, J. Phys. Chem., 74, 3476 (1970).

115. R. A. Shaw, Pure and Applied Chem., 13, 297 (1966).

116. R. P. Clifford, B. G. Gowenlock, C. A. F. Johnson and J. Stevenson, J. Organometal. Chem., 34, 53 (1972).

117. P. Jutzi, Angew. Chem., 14, 232 (1975).

118. L. E. Gusel'nikov, N. S. Nametkin and V. V. Vdovin, Acc. Chem. Research, 8, 18 (1975).

119. B. E. Douglas and D. H. McDaniel, Concepts and Models of Inorganic Chemistry, Ginn, Boston (1965), p. 58.

120. L. E. Gusel'nikov, N. S. Nametkin and V. V. Vdovin, Russian Chemical Rev., 43, 620 (1972).

121. T. J. Barton, G. Marquardt and J. A. Kilgour, J. Organometal. Chem., 85, 317 (1975).

122. C. M. Golino, R. D. Bush, D. N. Roark and L. H. Sommer, J. Organometal. Chem., 66, 29 (1974).

123. R. D. Bush, D. M. Golino, G. D. Homer and L. H. Sommer, J. Organometal. Chem., 80, 37 (1974).

124. C. M. Golino, R. D. Bush, P. On and L. H. Sommer, J. Amer. Chem. Soc., 97, 1957 (1975).

125. P. Boudjouk and L. H. Sommer, Chem. Commun., 54 (1973).

126. D. N. Roark and L. H. Sommer, Chem. Commun., 167 (1973).

127. D. N. Roark and G. J. D. Peddle, J. Amer. Chem. Soc., 94, 5837 (1972).

128. M. D. Curtis, J. Organometal. Chem., 60, 63 (1973).

129. R. Damrauer and D. R. Williams, J. Organometal. Chem., 66, 241 (1974).

130. R. Walsh, J. Organometal. Chem., 38, 245 (1972).

131. B. G. Gowenlock and C. A. F. Johnston, Roy. Inst. Chem. Rev., 107 (1968).

132. J. R. McNesby and H. Okabe, Advances in Photochemistry, 3, 157 (1964), ed. W. A. Noyes, Jr., G. S. Hammond and J. N. Pitts, Jr. Interscience Publishers (1964).

133. H. Okabe, J. Optical Soc. Amer., 54, 478 (1964).

134. A. H. Laufer, J. A. Pirog and J. R. McNesby, J. Optical Soc. Amer., 55, 64 (1965).

135. E. Karamatos and F. W. Lampe, J. Phys. Chem., 74, 2267 (1970).

136. R. E. Rebbert and P. Ausloos, J. Chem. Phys., 46, 4333 (1967).

137. R. A. Holroyd, J. Amer. Chem. Soc., 91, 2208 (1969).

138. W. M. Jackson, J. Faris and N. J. Buccos, J. Chem. Phys., 45, 4145 (1966).

139. A. G. Alexander and O. P. Strausz, submitted for publication.

140. S. W. Benson, Adv. in Chem. Series, 97, 1 (1970).

141. W. L. Hase, R. L. Johnson and J. W. Simons, Int. J. Chem. Kinetics, IV, 1 (1972).

142. W. L. Hase and J. W. Simons, J. Organometal. Chem., 32, 47 (1971).

143. K. Obi, H. Akimoto, Y. Ogata and I. Tanaka, J. Chem. Phys., 55, 1300 (1971).

144. W. Rothman, B. Hirayama and S. Lipsky, J. Chem. Phys. 58, 1300 (1973).

145. M. D. Sefcik and M. A. Ring, J. Amer. Chem. Soc., 95, 5168 (1973).

146. P. John and J. H. Purnell, J. Chem. Soc. Faraday I, 69, 1455 (1973).

147. O. F. Zeck, Y. Y. Su, G. P. Gennaro and Y. N. Tang, J. Amer. Chem. Soc., 96, 5967 (1974).

148. P. S. Skell and P. W. Owen, J. Amer. Chem. Soc., 94, 5434 (1972).

149. F. C. Kohout and F. W. Lampe, J. Chem. Phys., 46, 4075 (1967).

150. D. E. Hoare, Can. J. Chem., 40, 2012 (1962).

151. H. Gilman, W. H. Atwell and G. L. Schwebke, J. Organometal. Chem., 2, 369 (1964).

152. H. A. Skinner, Adv. Organometal. Chem., 2, 49 (1964).

153. I. M. T. Davidson and C. A. Lambert, J. Chem. Soc. A, 882 (1971).

154. W. J. Hehre, R. F. Stewart and J. A. Pople, J. Chem. Phys., 51, 2656 (1969).

155. W. J. Hehre, W. A. Latham, R. Ditchfield, M. D. Newton and J. A. Pople, Gaussian 70 Program No. 236, QCPE Indiana University, Bloomington, Indiana, U.S.A.

156. H. B. Schlegel, S. Wolfe and K. Mislow, Chem. Commun., 246 (1975).

157. P. Cadman, G. M. Tilsley and A. F. Trotman-Dickenson, J. Chem. Soc. Faraday I, 68, 1849 (1972).

158. J. C. J. Thynne, J. Organometal. Chem., 17, 155 (1969).

159. I. M. T. Davidson and I. L. Stephenson, J. Chem. Soc. (A), 282 (1968).

160. I. M. T. Davidson, C. Eaborn and J. M. Simmie, J. Chem. Soc. Faraday I, 70, 249 (1974).

161. H. J. Spangenberg and M. Pfeiffer, Z. Physik. Chem., 232, 343 (1966).

162. S. W. Benson and J. H. Buss, J. Chem. Phys., 29, 546 (1958).

163. H. E. O'Neal and M. A. Ring, Inorg. Chem., 5, 435 (1966).

164. S. W. Benson, F. R. Cruickshank, D. M. Golden, G. R. Haugen, H. E. O'Neal, A. S. Rodgers, R. Shaw and R. Walsh, Chem. Rev., 69, 2 (1969).

165. G. B. Watts and K. U. Ingold, J. Amer. Chem. Soc., 94, 491 (1972).

166. P. P. Gaspar, A. D. Haizlip and K. Y. Choo, J. Amer. Chem. Soc., 94, 9032 (1972).

167. K. J. Laidler, "Chemical Kinetics", McGraw-Hill Book Co., Toronto, 1965.

168. E. R. Morris and J. C. J. Thynne, J. Phys. Chem., 73, 3294 (1969).

169. A. U. Chaudhry and B. G. Gowenlock, J. Organometal. Chem., 16, 221 (1968).

170. T. N. Bell, P. Slade and A. G. Sherwood, Can. J. Chem., 52, 1662 (1974).

171. J. A. Kerr and D. Timlin, J. Chem. Soc. A, 1241 (1969).

172. H. S. Johnston and C.   J. Amer. Chem. Soc., 85, 2544 (1963).

173. E. Jakubowski, H. S. Sandhu, H. E. Gunning and O. P. Strausz, J. Chem. Phys., 52, 4242 (1970).

174. A. C. Bond and L. O. Brockway, J. Amer. Chem. Soc., 76, 3312 (1954).

175. L. Pierce, J. Chem. Phys., 34, 498 (1961).

176. R. W. Kilb and L. Pierce, J. Chem. Phys., 27, 108 (1957).

177. L. Pierce and D. H. Petersen, J. Chem. Phys., 33, 907 (1960).

178. B. Beagley, J. J, Monaghan and T. G. Hewitt, J. Molec. Struct., 8, 401 (1971).

179. M. S. Gordon and L. Neubauer, J. Amer. Chem. Soc., 96, 5690 (1974).

180. R. P. Hollandsworth and M. A. Ring, Inorg. Chem., 7, 1635 (1968).

181. G. W. Bethke and M. Kent Wilson, J. Chem. Phys., 26, 1107 (1957).

182. R. E. Wilde, J. Molec. Spectros., 8, 455 (1962).

183. M. Randic, Spectrochimica Acta, 18, 115 (1962).

184. D. F. Ball, P. L. Goggin, D. C. McKean and L. A. Woodward, Spectrochemica Acta, 16, 1358 (1960).

185. S. W. Benson and M. Luria, J. Amer. Chem. Soc., 97, 704 (1975).

186. S. W. Benson and M. Luria, J. Amer. Chem. Soc., 97, 3337 (1975).

187. M. Luria and S. W. Benson, J. Amer. Chem. Soc., 97, 3342 (1975).

188. D. E. Milligan and M. E. Jacox, J. Chem. Phys., 52, 2594 (1970).

189. L. H. Sommer and L. A. Ulland, J. Org. Chem., 37, 3878 (1972).

190. D. G. Hughes, R. M. Marshall and J. H. Purnell, J. Chem. Soc. Faraday I, 70, 594 (1974).

191. D. A. Parkes and C. P. Quinn, Chem. Phys. Lett., 33, 483 (1975).

192. W. E. Jones, S. D. Macknight and L. Teng, Chem. Rev., 73, 407 (1973).

193. K. Obi, H. S. Sandhu, H. E. Gunning and O. P. Strausz, J. Phys. Chem., 76, 3911 (1972).

194. J. A. Cowfer, K. P. Lynch and J. V. Michael, J. Phys. Chem., 79, 1139 (1975).

195. M. A. Contineanu, D. Mihelcic, R. N. Schindler and P. Potzinger, Ber. Bunsen. Ges., 75, 426 (1971).

196. A. A. Zavitsas, J. Amer. Chem. Soc., $\underline{94}$, 2779 (1972).

197. A. A. Zavitsas and A. A. Melikian, J. Amer. Chem. Soc., $\underline{97}$, 2757 (1975).

198. P. Cadman, G. M. Tilsley and A. F. Trotman-Dickenson, J. Chem. Soc. Faraday I, $\underline{69}$, 914 (1973).

199. D. M. Tomkinson and H. O. Pritchard, J. Phys. Chem., $\underline{70}$, 1579 (1966).

200. R. P. Bell, J. Chem. Soc. Chem. Rev., 513 (1975).

201. F. H. Westheimer, Chem. Rev., $\underline{61}$, 265 (1961).

202. M. Wolfsberg, Ann. Rev. Phys. Chem., $\underline{20}$, 449 (1969).

203. P. Gray, A. A. Herod and A. Jones, Chem. Rev., $\underline{71}$, 247 (1971).

204. I. Safarik, R. Berkley and O. P. Strausz, J. Chem. Phys., $\underline{54}$, 1919 (1971).

205. D. G. Hooper, M. Simon and M. H. Back, Can. J. Chem., $\underline{53}$, 1237 (1975).

206. P. John and J. H. Purnell, J. Organometal. Chem., $\underline{29}$, 233 (1971).

207. P. Potzinger and F. W. Lampe, J. Phys. Chem., $\underline{73}$, 3912 (1969).

208. M. Bowrey and J. H. Purnell, Proc. Roy. Soc. A, $\underline{321}$, 341 (1971).

209. A. J. Vanderwielen, M. A. Ring and H. E. O'Neal, J. Amer. Chem. Soc., $\underline{97}$, 993 (1975).

210. H. E. O'Neal and S. W. Benson, Int. J. Chem. Kinetics, I, 221 (1969).

211. S. W. Benson and W. DeMore, Ann. Rev. Phys. Chem., $\underline{16}$, 397 (1965).

212. R. F. Stewart, J. Chem. Phys., $\underline{50}$, 2485 (1969).

213. C. C. J. Roothaan, Rev. Mod. Phys., $\underline{23}$, 69 (1951).

214. R. M. Pitzer, J. Chem. Phys., $\underline{46}$, 4871 (1967).

215. R. Ditchfield, W. J. Hehre and J. A. Pople, J. Chem. Phys., 54, 724 (1971).

216. J. A. Pople and R. K. Nesbet, J. Chem. Phys., 22, 571 (1954).

217. H. S. Johnston, "Gas Phase Reaction Rate Theory", Ronald Press, New York, 1966.

218. L. Pauling, J. Amer. Chem. Soc., 69, 542 (1947).

219. H. S. Johnston, Advan. Chem. Phys., 3, 131 (1960).

220. S. Sato, J. Chem. Phys., 23, 592, 2465 (1955).

APPENDIX I

AB INITIO MOLECULAR ORBITAL CALCULATION ON SINGLET AND
TRIPLET SILAETHYLENE

This calculation was done by Drs. I. G. Csizmadia and G. Theodorakopoulos at the University of Toronto on four different structures of the silaethylene molecule using s and p Gaussian type functions contracted to a minimal STO-4G basis set.

This method developed by Pople and co-workers[154] replaces the full Slater type atomic orbitals of the form

$$\phi_{1s}(\zeta_1, r) = (\zeta_1^3/\pi)^{1/2} \exp(-\zeta_1 r)$$

$$\phi_{2s}(\zeta_2, r) = (\zeta_2^5/3\pi)^{1/2} r \exp(-\zeta_2 r)$$

$$\phi_{2p}(\zeta_2, r) = (\zeta_2^5/\pi)^{1/2} r \exp(-\zeta_2 r) \cos\theta$$

by a linear combination of a small number of Gaussian type orbitals, since integrals involving Gaussian functions can be evaluated analytically[212,213].

This method is much less time consuming than the full linear combination of atomic orbitals self-consistent field (LCAO SCF) method, which utilizes the full Slater type orbitals as a minimal basis set and for which calculations have been published for a few small molecules[214].

Pople's method approximates the Slater orbitals as atomic orbitals, ϕ_u', which are sums of K Gaussian type orbitals (K = 2 - 6),

$$\phi_{1s}'(1, r) = \sum_{k}^{K} d_{1s,k} \, g_{1s}(\alpha_{1k}, r)$$

$$\phi'_{2s}(1,r) = \sum_{k}^{K} d_{2s,k} \, g_{1s}(\alpha_{2k}, r)$$

$$\phi'_{2p}(1,r) = \sum_{k}^{K} d_{2p,k} \, g_{2p}(\alpha_{2K}, r)$$

where g_{1s} and g_{2p} are the Gaussian type orbitals

$$g_{1s}(\alpha, r) = (2\alpha/\pi)^{3/4} \exp(-\alpha r^2)$$

$$g_{2p}(\alpha, r) = (128\alpha^5/\pi^3)^{1/4} r \exp(-\alpha r^2) \cos\theta$$

The results approach the full Slater type calculation as the Gaussian Set increases and the STO-4G level was chosen for our calculation since the rate of convergence tapers off markedly at this point.

Calculations were carried out using a version of the Gaussian 70 program[155] and the starting point for the variation in energy with the angle of rotation round the Si-C bond was the optimized geometry obtained in the recent ab initio molecular orbital calculation which produced the theoretical infrared spectrum of silaethylene[156].

In this study the scale factors for H and C were taken as those optimized for ethylene[215] and standard scale factors were used for the silicon core shells while the values for the valence shells were optimized.

In our relative stability comparison, the singlet closed shell SCF problem was solved with Roothaan's restricted Hartree-Fock method[213], while for the lowest triplet state problem we used Pople's unrestricted Hartree-Fock method[216].

Absolute minima on the conformational hypersurfaces for the S_0 closed shell singlet and the T_1 orbitally excited lowest triplet were

obtained as well as for two other structures appearing on the S_o and T_1 hypersurfaces. All four structures represent minima in the rotational cross-sections associated with cis-trans isomerization of silaethylene.

APPENDIX II

THE BOND ENERGY-BOND ORDER (BEBO) METHOD OF CALCULATING

POTENTIAL ENERGIES OF ACTIVATION

This empirical method for determining the activation energy of bimolecular hydrogen transfer reactions developed by Johnson and co-workers[172,217] has been shown to be able to predict values to within 2 kcal.mole^{-1}. The method is based on the concept that the energy necessary to break a bond is supplied to a large extent by the formation of the new bond. This strong correlation is approximated for hydrogen atom transfer by the assumption that the path of lowest energy on the potential energy surface exists where the sum of bond orders is unity

$$n_1 + n_2 = 1$$

The bond order n is related to the bond length by the Pauling equation[218]

$$R = R_s - 0.26 \ln n$$

where the subscript s stands for "single" and R_s is the equilibrium bond length.

An empirical log-log plot of dissociation energies against bond order also gives a linear relationship

$$E = E_s n^p$$

where E is bond energy and p is a coefficient which can be calculated from the assumed linear relationship of bond energy against bond length

for single-order bonds and the corresponding Lennard-Jones zero-order bond in the "molecule" of two noble gas atoms[219]:

$$P = \frac{0.26 \ln (E_s/E_x)}{R_x - R_s}$$

where E_x and R_x are the Lennard-Jones parameters for the noble gases.

For the hydrogen transfer reaction

$$X + H - Y \longrightarrow X\cdots\cdots H\cdots\cdots Y \longrightarrow X - H + Y$$
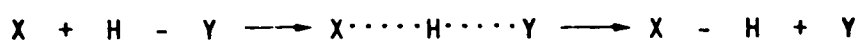
the total energy can be expressed as

$$V = E_{s_1} - E_{s_1} n^p - E_{s_2}(1-n)^q$$

$$= E_{s_1}(1-n^p) - E_{s_2}(1-n)^q$$

However a term has to be introduced to account for the repulsion between atoms X and Y since the electrons on the end atoms must have opposite spins and repel each other with a triplet interaction.

The spins must be oriented either

$$\alpha\cdots\cdots\beta\cdots\cdots\alpha \qquad \text{or} \qquad \beta\cdots\cdots\alpha\cdots\cdots\beta$$

thus the fractional bonds $X\cdots\cdots H$ and $H\cdots\cdots Y$ are bonding while the $X\cdots\cdots Y$ bond is anti-bonding.

This triplet repulsion may be estimated by a modified anti-Morse function[220]

$$V_{triplet} = 0.25 \, D_e \, (e^{-2\beta\Delta R} + 2e^{-\beta\Delta R})$$

where 0.25 is an arbitrary factor used by Johnston to approach more

closely the theoretical potential energy curve for the triplet hydrogen molecule. D_e is the X-Y bond dissociation energy, ΔR is the change in the X-Y bond length

$$\Delta R_{XY} = R - R_s$$

and β is an empirical factor given by

$$\beta = 1.2177 \times 10^7 \, \omega_e \sqrt{\frac{\mu}{De}}$$

where ω_e is the X-Y stretching frequency in cm^{-1}, μ is the reduced mass of X-Y in atomic mass units and D_e is the X-Y bond dissociation energy.

Thus the total energy is given by

$$V = E_{s_1}(1-n^P) - E_{s_2}(1-n)^q + V_{tr}$$

The function V can be evaluated from n=o to 1 and the maximum value of V gives directly the activation energy of the transfer reaction.

APPENDIX III

CALCULATION OF SILICON-HYDROGEN BOND ENERGIES

BY THE ELECTROSTATIC INTERACTION METHOD.

This approach by Benson and Luria[185-187] to resolving the cause of the differences in carbon-hydrogen bond energies in hydrocarbons begins with the assumption that each hydrogen atom bears a formal positive charge (+y) and each carbon atom a neutralizing negative charge. Thus the ethane molecule would have the following charge distribution:
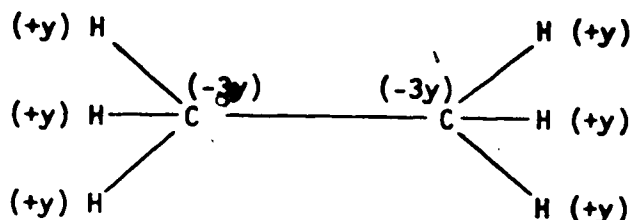
The electrostatic energy, E_{el}, arises from the interaction of all the formal charges, thus

$$E_{el} = \sum_{i<j} \frac{q_i q_j}{r_{i,j}}$$

where $r_{i,j}$ is the distance between the charges q_i and q_j.

For the alkanes this reduces to·

$$E_{el} = y^2 \sum_{i<j} \frac{n_i n_j}{r_{i,j}}$$

where n is the number of H atoms bonded on C atoms. The term in brackets is then dependent only on the geometry of the molecule. The electrostatic energy can be calculated in terms of y^2, using standard tetra-

hedral geometry with coplanar C atoms and staggered configurations. It is found that E_{el} is relatively insensitive to small changes in geometry.
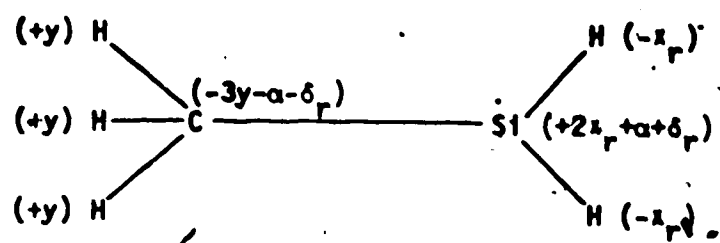
An absolute value of y^2 can be obtained by examining the enthalpies of formation of different isomers where the number of C-C and C-H bonds is constant. The heats of isomerization can be equated with the difference in electrostatic energies to give an absolute value for y. An average value from three different sets of isomers gives $|y| = 0.278 \times 10^{-10}$ esu.

A similar type of calculation can be carried out for alkyl free radicals but here the atoms around the radical site have a different formal charge:
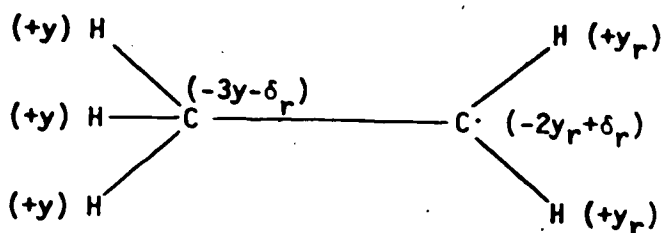
The radical centre is assumed to have sp^2 configuration. The parameters y_r and δ_r were then obtained by using different pairs of values to calculate the observed heats of formation of the alkyl radicals. The best values obtained were $|y_r| = 0.12 \times 10^{-10}$ esu and $|\delta_r| = 0.04 \times 10^{-10}$ esu.

For silicon radicals and molecules we can attempt similar calculations but in this case the situation is a little more complex since we must introduce different parameters which cannot be calculated from known bond enthalpies. For a silicon radical the charge distribution would be

$$(+y)\ H \diagdown \qquad (-3y-\alpha-\delta_r) \qquad \qquad H\ (-x_r)$$

(+y) H——C————————————Si (+2x_r+α+δ_r) ,

$$(+y)\ H \diagup \qquad \qquad \qquad \qquad H\ (-x_r)$$

The electrostatic energies of the silanes were calculated assuming tetrahedral geometry with $|x|$ = 0.24 x 10^{-10} esu and $|\alpha|$= 0.40 x 10^{-10} esu, while for the silyl radical $|x_r|$ = 0.12 x 10^{-10} esu and $|\alpha_r|$ = $|\alpha|$ with the radicals retaining pyramidal configuration. The charges on the methyl groups on the silanes were taken to be the same as in the alkanes. $|x|$ was estimated to be slightly lower than the $|y|$ value of 0.28 x 10^{-10} since the electronegativity difference between silicon and hydrogen is somewhat less than that between carbon and hydrogen. The charge separation between Si and C, $|\alpha|$, was estimated at 0.40 x 10^{-10} again from the electronegativity difference. δ_r was neglected since changes in this parameter made little difference to the final result.

The electrostatic energies in terms of the parameters are shown in Table AIII-1.

Since bond dissociation energies are given by

$$D(RH) \ = \ \Delta H_f(RH) - \Delta H_f(\dot{R}) - \Delta H_f(\dot{H})$$

the difference between two silicon-hydrogen bond energies cancels out the $\Delta H_f(\dot{H})$ term

$$D(R_1H) - D(R_2H) = \Delta H_f(R_1H) - \Delta H_f(\dot{R}) - \Delta H_f(R_2H) + \Delta H_f(\dot{R}_2)$$

This reduces to differences in electrostatic energy

TABLE AIII-1

Electrostatic Energy of Silicon Free Radicals and Parent Molecules
in Terms of the Formal Charge Parameters

Compound	Electrostatic Energy (E_{el}) esu^{2}Å^{-1}
SiH_4	$-8.33x^2$
SiH_3	$-4.84x_r^2$
Si_2H_6	$-9.17x^2$
Si_2H_5	$-4.84x^2 - 2.29x_r^2 + 0.34xx_r$
CH_3SiH_3	$-6.55y^2 - 4.84x^2 - 0.69xy - 3.12\alpha y - 2.54\alpha x$ $-0.53\alpha^2$
CH_3SiH_2	$-6.55y^2 - 2.29x_r^2 - 0.46x_r y - 3.12\alpha y - 1.69\alpha x_r$ $-0.53\alpha^2$
$(CH_3)_2SiH_2$	$-13.0y^2 - 2.29x^2 - 0.93xy - 6.80\alpha y - 3.38\alpha x$ $-1.81\alpha^2$
$(CH_3)_2SiH$	$-13.0y^2 - 0.68x_r^2 - 0.46x_r y - 6.80\alpha y - 1.69\alpha x_r$ $-1.81\alpha^2$
$(CH_3)_3SiH$	$-19.54y^2 - 0.68x^2 - 0.69xy - 11.0\alpha y - 2.54\alpha x$ $-3.83\alpha^2$
$(CH_3)_3Si$	$-19.54y^2 - 11.00\alpha y - 3.83\alpha^2$

$$D(R_1H) - D(R_2H) = \Delta E_{el}(R_1H\text{-}\dot{R}_1) - \Delta E_{el}(R_2H\text{-}\dot{R}_2)$$

The electrostatic energies of the molecules and radicals were calculated, the differences measured and then the increments between these differences show how the bond energies decrease. Results are shown in Table AIII-2.

TABLE AIII-2

Derivation of Silicon-Hydrogen Bond Strengths from the Difference
in Electrostatic Energy of Radical and Parent Molecule

Molecule	Radical	ΔE_{el} kcal.mole^{-1}	$\Delta(\Delta E_{el})$ kcal.mole^{-1}	D(Si-H) kcal.mole^{-1}
SiH_4	SiH_3	-5.9		94[a]
			0.2	
CH_3SiH_3	CH_3SiH_2	-5.7		93.8
			0.5	
$(CH_3)_2SiH_2$	$(CH_3)_2SiH$	-5.2		93.3
			1.3	
$(CH_3)_3SiH$	$(CH_3)_3Si$	-3.9		92.0
			1.2	
Si_2H_6	Si_2H_5	-2.7		90.8

[a] assuming $D(H-SiH_3) = 94$ kcal.mole^{-1}.